CZECH ACADEMY OF AGRICULTURAL SCIENCES

JOURNAL OF FOREST SCIENCE

VOLUME 69
ISSUE 7

Prague 2023

(On-line) ISSN 1805-935X
(Print) ISSN 1212-4834

Journal of Forest Science

continuation of the journal Lesnictví-Forestry

An international peer-reviewed journal published by the Czech Academy of Agricultural Sciences and supported by the Ministry of Agriculture of the Czech Republic

Aims and scope: The journal publishes original results of basic and applied research from all fields of forestry related to European forest ecosystems. Papers are published in English.

The journal is indexed in:
- AGRICOLA
- Agrindex of AGRIS/FAO database
- CAB Abstracts
- CNKI (China National Knowledge Infrastructure)
- CrossRef
- Czech Agricultural and Food Bibliography
- DOAJ (Directory of Open Access Journals)
- EBSCO Academic Search
- Elsevier Sciences Bibliographic Database
- Emerging Sources Citation Index (Web of Science)
- Google Scholar
- J-Gate
- Scopus
- TOXLINE PLUS
- Web of Science (ESCI, BIOSIS Citation Index)

Periodicity: 12 issues per year, volume 69 appearing in 2023.

Electronic open access

Full papers from Vol. 49 (2003), instructions for authors and information on all journals edited by the Czech Academy of Agricultural Sciences are available on the website: https://www.jfs.agriculturejournals.cz

Online manuscript submission

Manuscripts must be written in English. All manuscripts must be submitted to the journal website (https://www.jfs.agriculturejournals.cz). Authors are requested to submit the text, tables, and artwork in electronic form to this web address. It is to note that an editable file is required for production purposes, so please upload your text files as MS Word (.docx) files. Submissions are requested to include a cover letter (save as a separate file for upload), manuscript, tables (all as MS Word files – .docx), and photos with high (min 300 dpi) resolution (.jpeg, .tiff and), and charts as MS Excel files (with data), as well as any ancillary materials.

The day the manuscript reaches the editor for the first time is given upon publication as the date of receipt.

Editorial office

Journal of Forest Science, Czech Academy of Agricultural Sciences,
Slezská 7, 120 00 Prague 2, Czech Republic
phone: + 420 227 010 355, e-mail: jfs@cazv.cz

Subscription

Subscription orders can be entered only by calendar year and should be sent to email: redakce@cazv.cz.
The subscription prices are available on the journal website.

Licence terms

The articles are licensed under the Creative Commons Attribution-NonCommercial 4.0 International (CC BY-NC 4.0).

© 2023 Czech Academy of Agricultural Sciences

MK ČR E 1329

Journal of Forest Science

Volume 69, No. 7 **2023**

CONTENT

For information about Journal of Forest Science visit the website:

https://jfs.agriculturejournals.cz

Journal of Forest Science

Volume 69, No. 7 **2023**

Editor-in-Chief

Vilém V. Podrázský
Prague, Czech Republic

Co-editors

Vladimír Gryc
Brno, Czech Republic

Radek Pokorný
Brno, Czech Republic

Executive Editor

Ilona Procházková
Prague, Czech Republic

Editorial Board

Isabella Børja
Ås, Norway

Thomas Cech
Vienna, Austria

Jan Cukor
Jíloviště, Czech Republic

Ignacio J. Diaz-Maroto
Santiago de Compostela, Spain

Stanislav Drozdowski
Warsaw, Poland

Roger-Dirk Eisenhauer
Pirna, Germany

Michael Englisch
Vienna, Austria

Marek Fabrika
Zvolen, Slovak Republic

Paola Gatto
Legnaro, Italy

Petra Hlaváčková
Brno, Czech Republic

Petr Horáček
Brno, Czech Republic

Libor Jankovský
Brno, Czech Republic

Vilém Jarský
Prague, Czech Republic

Dušan Kacálek
Opočno, Czech Republic

Jiří Korecký
Prague, Czech Republic

Emanuel Kula
Brno, Czech Republic

Ivan Kuneš
Prague, Czech Republic

Carsten Lorz
Freising, Germany

W. Keith Moser
Flagstaff, Arizona, U.S.A.

Jindřich Neruda
Brno, Czech Republic

Valeriu-Norocel Nicolescu
Brasov, Romania

Sasa Orlovic
Novi Sad, Serbia

Hans Pretzsch
Freising, Germany

Peter Rademacher
Eberswalde, Germany

Jiří Remeš
Prague, Czech Republic

Petr Surový
Prague, Czech Republic

Vít Šrámek
Prague, Czech Republic

Igor Štefančík
Zvolen, Slovak Republic

Paweł Tylek
Kraków, Poland

Zdeněk Vacek
Prague, Czech Republic

Marcela Van Loo
Vienna, Austria

Klaus-Hermann von Wilpert
Freiburg, Germany

Aleš Zeidler
Prague, Czech Republic

https://doi.org/10.17221/10/2023-JFS

Pathogenicity of the entomopathogenic fungi against *Myllocerus fotedari* Ahmad, 1974 (Coleoptera: *Curculionidae*) under laboratory conditions in India

Shaziya Gull[1], *Tariq Ahmad*[1*], *Abdul Lateef Khanday*[2], *Pavittu Meethal Sureshan*[3], *Gowhar Rashid*[2]

[1]*Section of Entomology, Department of Zoology, Faculty of Biological Sciences, University of Kashmir, Srinagar, India*

[2]*Department of Zoology, Government Degree College Kulgam, Jammu and Kashmir, India*

[3]*Zoological Survey of India, Western Ghat Regional Centre, Kozhikode, Calicut, Kerala, India*

**Corresponding author: drtariqento@kashmiruniversity.ac.in*

Citation: Gull S., Ahmad T., Khanday A.L., Sureshan P.M., Rashid G. (2023): Pathogenicity of the entomopathogenic fungi against *Myllocerus fotedari* Ahmad, 1974 (Coleoptera: *Curculionidae*) under laboratory conditions in India. J. For. Sci., 69: 277–286.

Abstract: The weevil, *Myllocerus fotedari* Ahmad, 1974 (Coleoptera: *Curculionidae*) is widely recognised as one of the major walnut pests. Fungal pathogens have shown great potential for the management of some pest species. In the present study, the efficacy of three entomopathogenic fungi, namely *Beauveria bassiana* (Balsamo) Vuillemin, *Metarhizium anisopliae sensu lato* (Metchnikoff) Sorokin and *Lecanicillium lecanii* (Zimmerman) Zare and Gams were evaluated against the weevil, *M. fotedari,* under laboratory conditions. Each fungal suspension contained 1.0×10^9 spores of fungi in 1 mL. The experiment comprised of five treatments along with control (distilled water) and three replicates. An insecticide – chloropyrifos 20% emulsifiable concentrate (EC), was also used as positive control in the experiment. The experimental results revealed that the weevil, *M. fotedari,* showed mortality due to both virulence of entomopathogens and insecticide. The mortality caused by fungi varied from two days after treatment to eight days after treatment. However, the highest mortality of 100% was recorded for *B. bassiana*, followed by 85.1% for *M. anisopliae* after eight days of treatment. The efficacy of *L. lecani* was the lowest, leading to only 51.8% mortality, and was found significantly less virulent compared to the other two used entomopathogens. The present study is an attempt to use entomopathogens to control *M. fotedari* over conventional chemical insecticides.

Keywords: *Beauveria bassiana*; biological control; *Juglans regia; Metarhizium anisopliae*; *Lecanicillium lecanii*

The crops are usually infested with various pests and diseases making fruit crops and ornamental plants highly susceptible to pest attacks (Hill 1987; Oerke et al. 1994). Among different insect groups, coleopteran pests feed on the foliage and reduce the surface area of leaf that results in reduction of tree vigour, and thus host trees become prone to other diseases and insect attacks. *Myllocerus* spp. are economical pests feeding on numerous agricultural and horticultural crops with 4 144 genera, more than around 85 000 species with worldwide distribution (O'Brien, Wimber 1979). The occurrence of *Myllocerus* pests was first reported in Florida, feeding on numerous ornamental and fruit plants causing huge losses every year (O'Brien et al. 2006). In the Indian subcontinent, thirty-three species of this

© The authors. This work is licensed under a Creative Commons Attribution-NonCommercial 4.0 International (CC BY-NC 4.0).

https://doi.org/10.17221/10/2023-JFS

genus are recorded from diverse host plant species (Ramamurthy, Ghai 1988). Incidences of *Myllocerus* spp. are reported from various states of India with very scarce information on their bioecology and management (Ramamurthy, Ghai 1988; Azam 2007; Tara et al. 2010). These leaf pests are generally plant defoliators feeding on the foliage by nibbling irregular holes on the leaf surface, leaving behind midrib (Butani 1979). Their feeding activity lasts from April to November and remains indolent under the plant debris during winter (Atwal 1963). They are categorized as polyphagous pest because of their ability to feed on various host plants (Hill 1987). They can act as major pest when feeding on almond and walnut while as minor pest on apple trees (Butani 1979). The beetle has been documented to be a damaging foliage pest since adult *Myllocerus* spp. feed on leaf lamina, decreasing the quality and quantity of the fruit output by reducing the photosynthetic area of the leaf (Arévalo, Stansly 2009).

M. fotedari attacks walnut (*Juglans regia*), which is one of the main fruit crops of Jammu and Kashmir (India) and occupies almost 90% share of walnut industry in India. From an area of 61 723 ha, the state produces about 86 263 tons of walnut. *Myllocerus* sp. is a serious pest acting as an aerial and subterranean feeder which attacks each part of the plant, while its larvae are concealed feeders attacking roots inside the soil (Davidson 1966). Ahmad and Dar (1974) reported *M. fotedari* infesting apple, pear, plum and walnut. The adults are defoliators while larvae mainly infest the *Leguminacae* family. *Myllocerus* sp. attacking walnut trees cause blackening of leaf tips (Mir, Wani 2005; Gull et al. 2019). Many researchers have contributed to finding the lethal effects of the insecticides effective against *Myllocerus* sp. (Budhraja et al. 1984; Singh et al. 1991; Sinha, Marwaha 1995). Use of traditional chemical insecticides to control insect pests leads to an accumulation of persistent residues and as such an eco-friendly alternative is necessary. Introduction of biological control method as an essential part of integrated pest management (IPM) proved to be a more effective and rapidly developing alternative to chemical insecticide pest management. Thus, the primary focus is to find eco-friendly methods like the use of fungi to control various insect pests. The use of microbes in IPM strategies has been applied in both developing as well as developed countries and has been successfully used in South America and Asia (Fuxa 1984). Entomopathogens are highly eco-friendly with high persistence in the environment and mostly least harmless to non-target species. Thus, they can play an important role in controlling the population dynamics of pests. They are known to cause affliction in insects of nearly all orders, *viz. Diptera*, *Lepidoptera*, *Coleoptera*, *Hymenoptera*, *Hemiptera*, and *Orthoptera* (Ramanujam et al. 2014). These produce conidiospores which germinate on the cuticle breaching with the help of enzymes (like chitinase, proteinase and lipase) and mechanical pressure, developed hyphal tubes pierce integument, and hyphal bodies move towards haemolymph, where tremendous budding occurs to produce more spores leading to death of the host (Ferron 1978). Although various species are practically applied to control pests due to mycoinsecticidal activity, compared to other methods it is still in its infancy. In the present study, an attempt was made to know the bio-efficacy and comparative effects of some entomopathogenic fungi, *viz. Beauveria bassiana* (Balsamo), *Lecanicillium lecanii* (Zimmerman) and *Metarhizium anisopliae* (Metchnikoff) fungus against *M. fotedari* infesting walnut trees of Kashmir under laboratory conditions.

MATERIAL AND METHODS

Insect rearing. The specimens of the weevil, *M. fotedari,* were collected from the walnut trees of the Khimber (34.1898°N, 74.8609°E, elevation 1 682.80 m a.s.l.) in Srinagar, Jammu and Kashmir district. Thereafter, they were transferred to collection jars covered with muslin cloth to confirm air circulation, and were brought to Entomological Laboratory, University of Kashmir for evaluating the pathogenicity caused by various fungal treatments. Insect specimens were placed inside the rearing jars and were provided with fresh walnut leaves. GPS location of the sample site was taken from Google Earth Pro (7.3.2.5776, 2019).

Entomopathogenic fungi. Three commercial formulation of enthomopathogenic fungi with spore concentration 1.0×10^9 spores·mL^{-1}, namely *B. bassiana*, *L. lecanii*, and *M. anisopliae,* were obtained from Green Life Biotech Laboratory, Somanur, Coimbatore, India. For the evaluation of each entomopathogenic fungi treatment, three replicates were maintained. A total of 15 replicates were maintained including control comprising of distilled water and insecticidal treatment. The used insecticide was chloropyrifos 20% EC.

https://doi.org/10.17221/10/2023-JFS

Table 1. Treatment against *M. fotedari* using a Petri dish assay under laboratory conditions (29.85 °C ± 1.34 °C temperature and 77.57% ± 8.67% relative humidity)

Sample No.	Group*	No. of Petri dishes in each treatment/beetle	Preparation	Used quantity (mL per Petri dish)
1	G1		*Beauveria bassiana*	
2	G2		*Lecanicillium lecanii*	
3	G3	3/30	*Metarhizium anisopliae*	1.0
4	G4		insecticide	
5	G5		distilled water	

* Each group represents 3 Petri dishes with 10 *M. fotedari* adults subjected to 5 treatments

Bioassay. Each bio-preparation was diluted with distilled water forming 1 mL bio-preparation 1 000 mL^{-1} water to which a few drops of detergent were added as a wetting agent. 1 mL of each fungal suspension contained 1×10^9 spores·mL^{-1}. Each treatment was replicated three times. In each replicate 10 adult beetles were transferred using a camel hairbrush on walnut leaves into Petri dishes (11 cm diameter). In total, 30 beetles were used for each Petri dish assay (Table 1). Entomopathogenic fungal bioassay was conducted by using rapid jetting sprays two times, which was standardized at 1.0 mL for each replicate. For this purpose, a small calibrated hand spray with a one-litre capacity was used, which was fortified with a nozzle suited to low-volume spray applications on insect body as topical application method (Batta 2007; Khanday, Buhroo 2018; Khanday et al. 2018). All the treatments were sprayed with the same volumes (1 mL·$replicate^{-1}$) while for control, adult beetles were treated with distilled water. The mortality percentage data was recorded over a period of eight days and was evaluated 2, 4, 6, and 8 days after treatment. Fresh leaves were used each day for feeding the beetles. Mortality was assessed by observing beetles continuously for five minutes and if no movement occurred, they were treated as dead. Effected beetles developed mat-like mycelial growth on the body when kept under humid conditions (29.85 °C ± 1.34 °C and 77.57% ± 8.67%) for about one week due to germination of conidiospores which develop on superficial area cuticle and result in the development of long hyphal tubes penetrating directly into the insect's integument. Photographs were taken during the experiment by using a Leica DFC295 (Leica Microsystems, Gmbh, Germany) camera with an automontage software (4.10, 2017).

Statistical analyses. Experimental data was analysed by using Origin Pro software (Version 15, 2015). The collected data of mortality percentage and corrected mortality of *M. fotedari* adults in different treatments were analysed by means of the analysis of variance (ANOVA) at a 0.05% level of significance. Tukey's Honest Square Difference test was used to separate means of treatment. Abbott's formula (Abbott 1925) was used for mortality data correction with that in control [Equation (1)].

$$CM\ (\%) = \frac{T\ (\%) - C\ (\%)}{100 - C\ (\%)} \tag{1}$$

where:

CM (%) – corrected mortality;

T – mortality in treatment;

C – mortality in control.

RESULTS

In the present experiment, the results showing the mortality caused by fungal pathogens were recorded in treated replicates. The data shown in Table 2 indicate the corrected mortality of all the treatments used in the experiment, and it was observed (Table 2) that mortality in each treatment augmented with increasing time interval [Table S1 in the Electronic Supplementary Material (ESM)]. All the fungal treatments showed different mortality rates against *M. fotedari* in eight days after treatment. After two days of treatment at spore concentration 1×10^9 conidia·mL^{-1}, the mortality was 40 ± 10% for *B. bassiana*, 30 ± 10% for *M. anisopliae*, 10 ± 10% for *L. lecanii*, and 50 ± 10% for insecticide (positive control). Further, it was observed that insecticide showed a slightly higher mortality rate than other used treatments. On comparing the mean mortality percent of *B. bassiana, M. anisopliae, L. lecanii* and insecticide, it was recorded that *B. bassiana, M. anisopliae* and insecticide treat-

https://doi.org/10.17221/10/2023-JFS

Table 2. Effect of different treatments on the mortality rate of adults *Myllocerus fotedari* at different time interval

Treatment	Corrected mortality (%) (± SD)			
	2 DAT	4 DAT	6 DAT	8 DAT
Beauveria bassiana	40.0 (± 10)[a]	58.5 (± 10.33)[ad]	85.5 (± 17.14)[ad]	100.0 (± 0.00)[a]
Metarhizium anisopliae	30.0 (± 10)[a]	44.8 (± 5.01)[ac]	64.4 (± 11.73)[ac]	85.1 (± 16.99)[a]
Lecanicillium lecanii	10.0 (± 10)[b]	24.0 (± 5.25)[bc]	39.2 (± 5.58)[bc]	51.8 (± 16.95)[b]
Insecticide (chloropyrifos 20% EC)	50.0 (± 10)[a]	78.8 (± 11.74)[d]	100.0 (± 0.00)[d]	100.0 (± 0.00)[a]
Control (distilled water)	0.0 (± 0.00)[b]	3.3 (± 0.57)[e]	6.6 (± 0.57)[e]	10.0 (± 0.00)[c]

[a–e] mean values with different superscripts are significantly different ($P < 0.05$, Tukey's HSD); significant $P < 0.05$, non-significant $P > 0.05$; SD – standard deviation; DAT – day after treatment; EC – emulsifiable concentrate

ments were insignificant among themselves while *L. lecanii* showed a significant difference (one-way ANOVA; $P \leq 0.05$).

Four days after treatment, the maximum mortality was recorded for insecticide (78.8 ± 11.74%), followed by *B. bassiana* (58.5 ± 10.33%), *M. anisopliae* (44.8 ± 5.01%) and *L. lecanii* (24 ± 5.25%). One-way ANOVA revealed that treatment with *B. bassiana, M. anisopliae* and insecticide led to significantly higher mortality rates than other treatments ($P \leq 0.05$) while insignificant differences were observed between *B. bassiana* and insecticide. However, a significant difference ($P \leq 0.05$) was observed between insecticide and *M. anisopliae*, and also between *M. anisopliae* and *L. lecanii* (Figure 1).

After six days of treatment, an appreciable reduction in the number of beetles occurred, with a peak of 100% mortality in the case of insecticide, followed by *B. bassiana* (85.5 ± 17.14%), *M. anisopliae* (64.4 ± 11.73%), and *L. lecanii* (39.2 ± 5.58%). On analyzing the results with one-way ANOVA, an insignificant difference was found between insecticide and *B. bassiana*, while a significant difference was observed between insecticide and

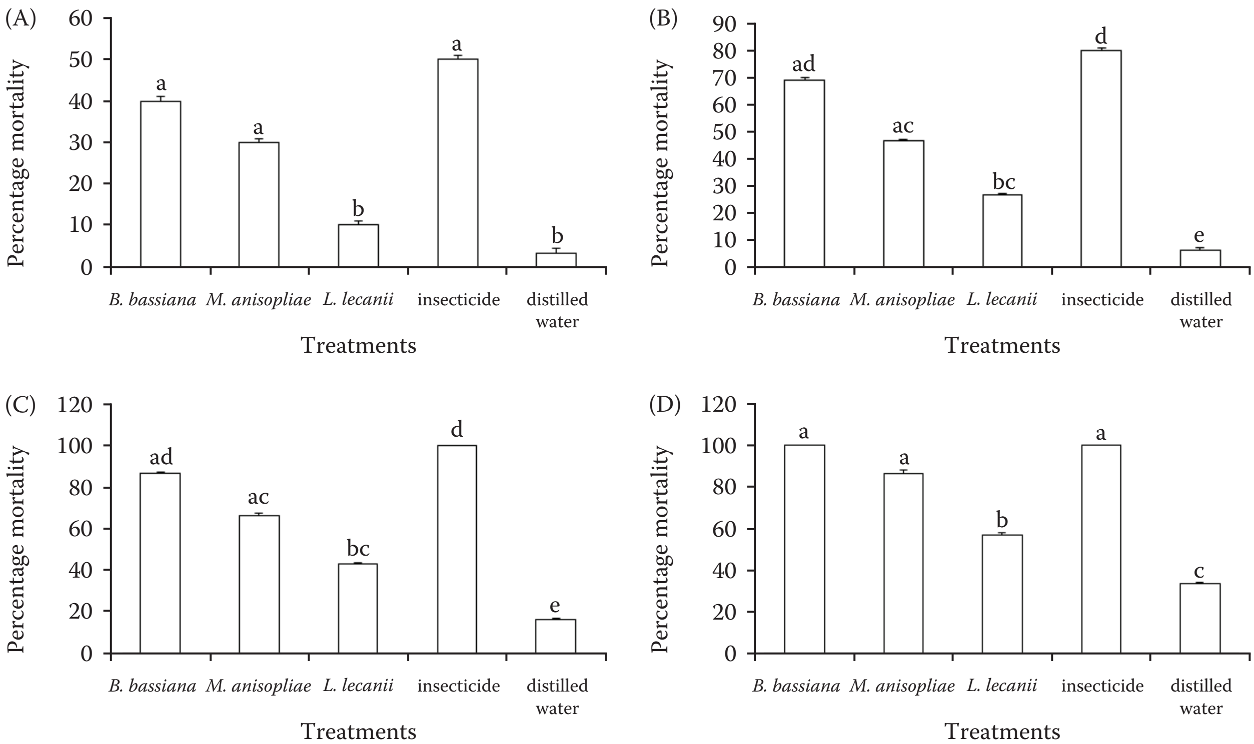

Figure 1. Mean percentage of corrected mortality of *Myllocerus fotedari* adults using Petri dish assays (A) 2 days after treatment; (B) 4 days after treatment; (C) 6 days after treatment; (D) 8 days after treatment

a–e – standard deviation is added on bars and the bars that do not share the same superscript are significantly different at $P < 0.05$ as indicated by Tukey's Honest Square Difference test

https://doi.org/10.17221/10/2023-JFS

other treatments ($P \leq 0.05$). Furthermore, *M. anisopliae* and *B. bassiana* were statistically the same at $P \leq 0.05$. Out of all the treated entomopathogenic fungi, *L. lecanii* showed significantly lower mortality rates in beetles (Figure 1).

Eight days after treatment, a marked increase in the mortality percent rate occurred, ranging from 51.8% to 100%. Among five treatments, 100% mortality occurred in the case of insecticide and *B. bassiana*, followed by *M. anisopliae* (85.1 ± 16.99%) and least by *L. lecanii* (51.8 ± 16.95%). On comparing the means with one-way ANOVA, *B. bassiana, M. anisopliae* and insecticide were insignificant to each other but significant to *L. lecanii* at $P \leq 0.05$. Among the three entomopathogens used, *B. bassiana* and *M. anisopliae* at spore concentration 1.0×10^9 resulted in the highest mortality rates, as compared to *L. lecanii* (Figure 1 and Table 2). The order of efficacy caused by five treatments in the present experiment can be ranked as: insecticide > *B. bassiana* > *M. anisopliae* > *L. lecanii* > control.

The regression equation for *B. bassiana* was calculated as $y = 10.35x + 19.25$, having a regression coefficient (R^2) value of 0.988 (Figure 2A).

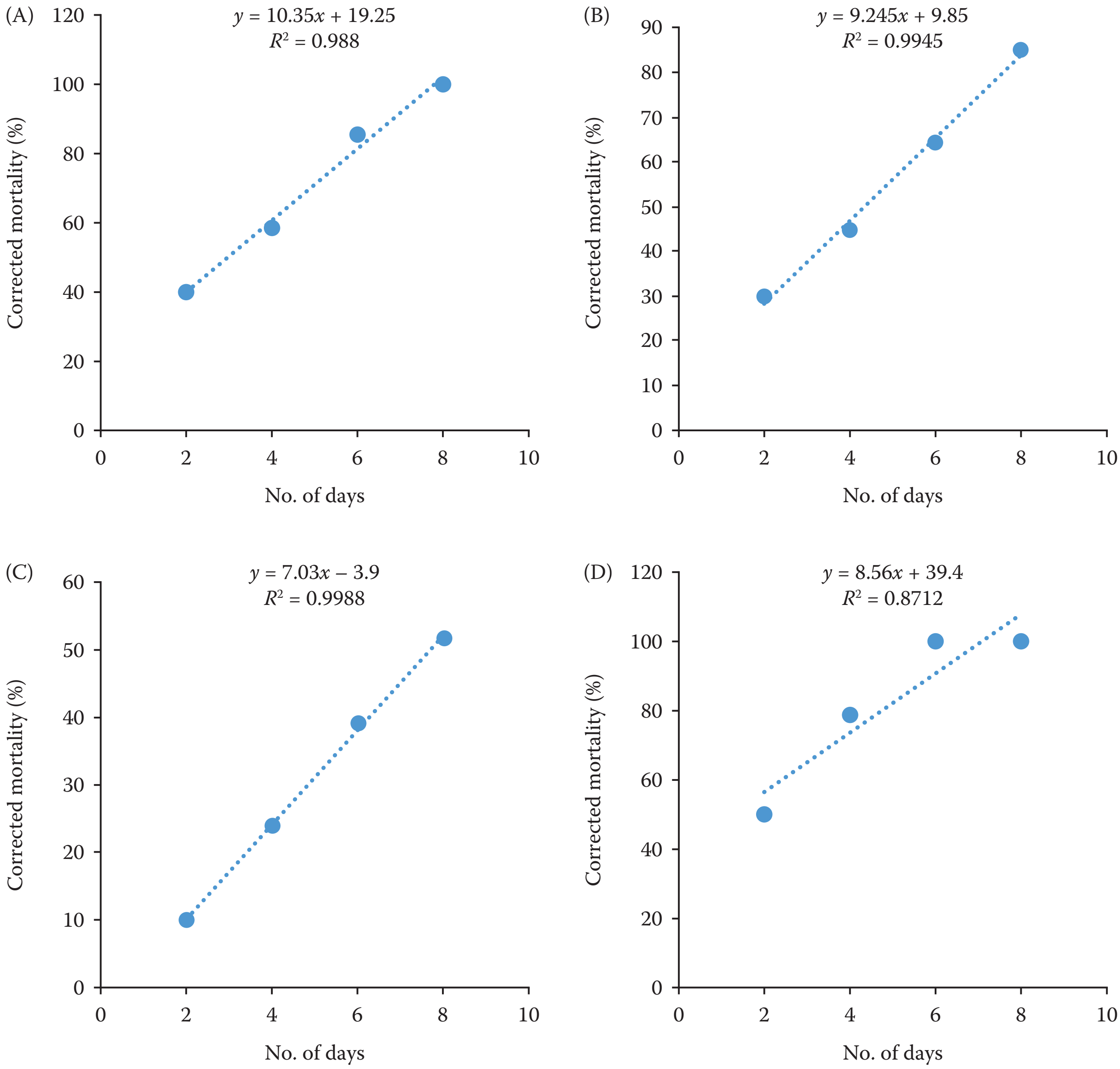

Figure 2. Graphs showing regression equation for mortality of *Myllocerus fotedari* by (A) *Beauveria bassiana*; (B) *Metarhizium anisopliae*; (C) *Lecanicillium lecanii*; (D) insecticide (chloropyrifos 20% EC)

EC – emulsifiable concentrate

https://doi.org/10.17221/10/2023-JFS

Positive correlation is exhibited between two variables *x* (No. of days) and *y* (mortality of beetles) as R^2 value tends to be less than 1. Regression equations for other treatments *viz. M. anisopliae* were $y = 9.245x + 9.85$ with R^2 value of 0.9945 (Figure 2B), *L. lecanii* had $y = 7.03x - 3.9$ along with R^2 of 0.9988 (Figure 2C) and for insecticide, the regression equation was $y = 8.56x + 39.4$, having R^2 value of 0.8712 (Figure 2D). Thus, it was concluded that an increasing number of days escalated the mortality rates of the beetles.

After 8 days of study, white mycelium mat growth was observed under a Leica M 205C stereo zoom trinocular microscope (Leica Microsystems, Gmbh, Germany) camera with an automontage software (4.10, 2017) on dead cadavers and fungal hyphae were observed protruding outside the body.

DISCUSSION

The efficacy of different entomopathogenic fungi was evaluated at 1.0×10^9 conidial spores·mL^{-1} against adults of *M. fotedari*, comprising of 5 treatments along with control and each treatment had three replicates. It was revealed from the results that there was a variation in pathogenicity of the entomopathogens used. *B. bassiana* (Figure 3C) and *M. anisopliae* (Figure 3A) showed high efficacy against *M. fotedari* in *in vitro* conditions leading to the highest mortality of 58.5% and 44.8%, respectively, after four days (96 h) of treatment, and 100% and 85.1% after eight days (192 h) of treatment, respectively. Further, dead cadavers developed white and green mat when treated with *B. bassiana* and *M. anisopliae*, respectively, due to hyphae penetration inside the cuticle consuming nutritional reserves of the body that leads to death of insects due to toxin production (Gabarty et al. 2014). Among the different known entomopathogens, *B. bassiana* and *M. anisopliae* gained attention for controlling weevils as they have a high potential to control long-lasting management, especially when used in combination with chemical insecticides (Mayer, Mannion 2011), and our results demonstrate that high mortality was observed on treating weevils with them. *B. bassiana* is well known for its insecticidal activities, having a high potential to kill a huge range of pests (Eken et al. 2006; Sabbour, E-Abd-El-Aziz 2007; Keyhani 2015), although, its efficacy varies on treating it with different Coleopteran species like in *Sitophilus zeamais* (Motschulsky 1855) (Coleoptera: *Curculionidae*) where 88% mortality occurred, when 10^4 conidial spores·mL^{-1} concentration was applied on 8th day of treatment (Adane et al. 1996). Conversely, 100% mortality was observed after 4.4 days on the larvae of *Saperda populnea* (Linnaeus 1758) (Coleoptera: *Cerambycidae*) under laboratory conditions (Eken et al. 2006). Similarly, our findings are in line with Yanar et al. (2015) who carried out an experiment on various isolates of *B. bassiana* and found 91.7% mortality rate on treating *Syrista parreyssii* (Spinola 1843) with them. Wu et al. (1995) also found 80% mortality caused in field trials, when *B. bassiana* was sprayed with spore concentration of 1.2×10^8 spores·mL^{-1} to control *Myllocerus* sp. Likewise, *B. bassiana* (Strain 871) was sprayed on tea crops with a spore suspension of 100–200 million spores·ha^{-1} leading to 95% mortality in brown weevil, *Mylloceus aurolineatus* (Voss 1959) after 10 days of treatment (Wu, Sun 1994).

It is also evident from our current findings that *B. bassiana* had more pathogenicity against the weevil *M. fotedari*, compared to other treated entomopathogens. Similar results were drawn by Mishra (1993) who found that among different entomopathogens, *B. bassiana* is the most promising and potential bio-control agent of *Hypsiphylla robusta* (Moore 1886). Our result also revealed that *B. bassiana* caused the highest mortality of 100% at 1.0×10^9 spores·mL^{-1} which is in line with the earlier findings of Logan et al. (1999) who reported 93.7% mortality at the same spore concentration in contrary to least mortality caused by *M. anisopliae* on the grey back cane grub, *Demolepida albohirtumn* (Waterhouse 1875) (Coleoptera: *Scarabidae*). Similarly, present results are in support of Senthilkumar and Murugesan (2010) who indicated that the highest concentration (1.0×10^9 spores·mL^{-1}) leads to the highest mortality in controlling the population of *Calopepla leayana* (Latreille 1807). The present inferences are in line with the findings of Sankaran et al. (1989) who carried out the management of *Myllocerus viridans* (Boheman 1840) with *B. bassiana* at spore concentration of 1.0×10^5 spores·mL^{-1}. Other workers have also studied pathogenicity caused due to *B. bassiana* on various curculionid beetles like banana weevil, *Cosmopolites sordidus* (Germar) (Godonou et al. 2000); pecan weevil, *Curcu-*

https://doi.org/10.17221/10/2023-JFS

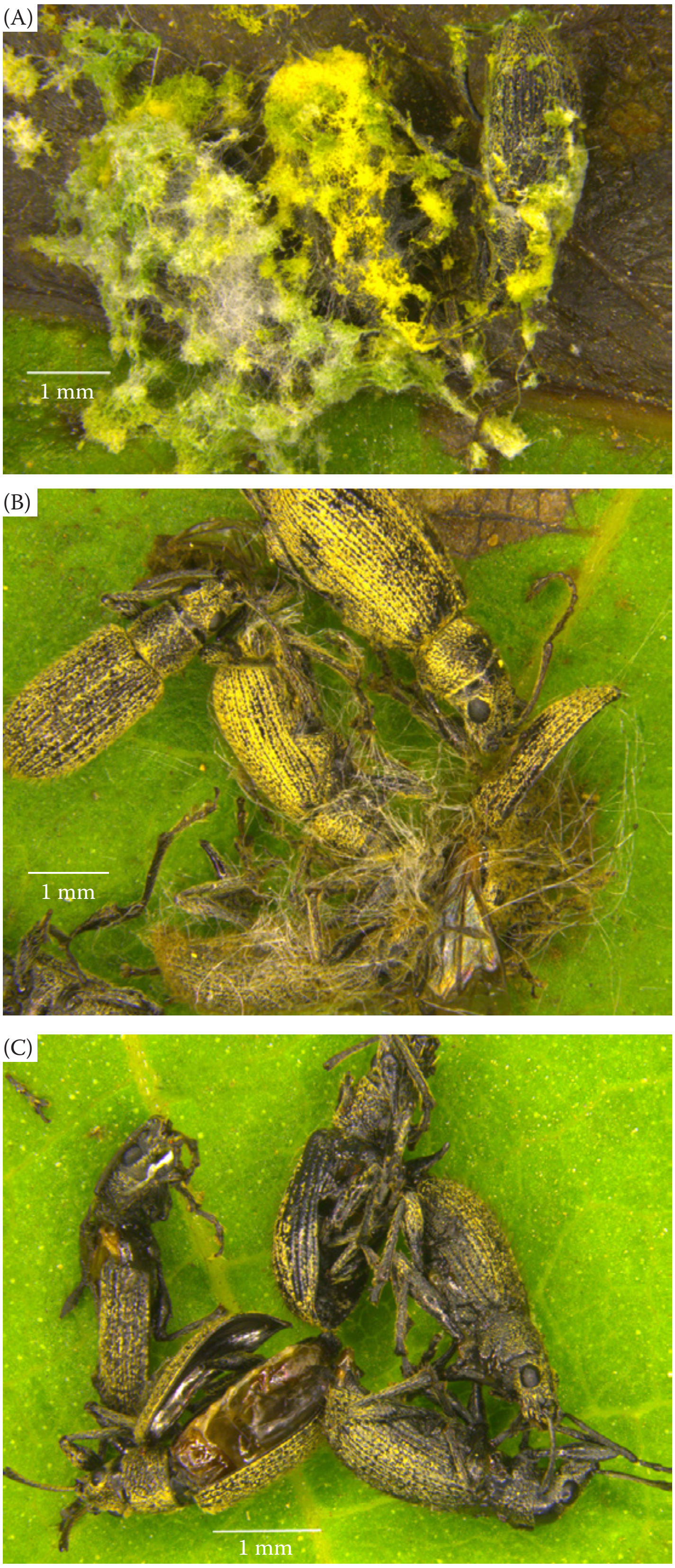

Figure 3. Entomopathogenic fungi *Metarhizium anisopliae, Lecanicillium lecanii*, and *Beauveria bassiana* infesting the weevil*, Myllocerus fotedari* infestation by (A) *Metarhizium anisopliae*; (B) *Lecanicillium lecanii*; (C) *Beauveria bassiana*

https://doi.org/10.17221/10/2023-JFS

lio caryae (Horn 1873) (Shapiro-Ilan et al. 2003) and pine weevil, *Hylobius abietis* (Linnaeus 1758) (Turchinskaya, Sherlyngina 1974).

In a Petri plate bioassay, 88–100% mortality occurred in *Ips typographus* (Linnaeus 1758) when treated with *B. bassiana*, which is in close proximity to our results (Vaupel, Zimmermann 1996; Kunca et al. 2009). Gopalakrishnan and Narayanan (1988) treated adults of *Mylloceus subfaciatus* (Guerin 1958) with *B. bassiana* where it was found that virulence in 5–8 days at a temperature of 25–27 °C and 80–90% relative humidity was 100%, which was in consonance with our findings where *B. bassiana* caused 100% mortality on the 8th day after application and is attributed to the fact that *B. bassiana* and *M. anisopliae* can cause virulence in insects at low ambient humidity as long as host cuticle contains ample moisture (Hallsworth, Mangan 1999). Further, the conclusion drawn by Batta (2007) was also the same, reporting high pathogenicity of *B. bassiana* against adults of almond bark beetle, *Scolytus amygdali* (Geoffroy 1792).

In the present study, a spore concentration of 1.0×10^9 spores·mL^{-1} was used to evaluate the mortality which was in line with various researchers who found that a higher concentration of spore suspension is likely to cause more virulence and infection of host (Ahmed, Elkatatny 2007; Steinwender et al. 2010). Further, *L. lecanii* (Figure 3) caused the lowest mortality compared to the other two entomopathogens, which is attributed to the fact that it is the potential biocontrol agent of aphids, thrips and whiteflies that is used mostly for the management of ornamental and salad crops (Chandler et al. 1993). Kreutz (2004) used entomopathogenic fungi, *B. bassiana,* and insecticide to control the insect population of *Ips typographus* (Linnaeus 1758) and achieved 100% and 93% mortality on treatment with insecticide and fungal isolate, respectively. Our results were similar and in covenant to their observations as within the first few days, the mortality caused by insecticide (positive control) was high but later mortality after 8 days of treatment reached 100% in both cases of insecticide and *B. bassiana*, and 85.1% with *M. anisopliae* and least with *L. lecanii* (51.8%). Similarly, the same conclusion is drawn by Kavallieratos et al. (2014) who carried out the work on *Sitophilus oryzae* (Linnaeus 1763) by controlling its population using *B. bassiana, Isaria furmosorea* and *M. anisopliae.* Observed mortality ranged from 0 to 100% and high efficacy, i.e. speed of killing, was shown by *B. bassiana* and *M. anisopliae*, which was in total agreement with our experimental findings. In the present investigation, it was further found that insecticide used in Petri plate assay caused higher mortality soon after the first day of treatment but widespread use of chemical pesticides caused a change in the ecosystem leading to death of non-target species (Aktar et al. 2009). Nevertheless, research has been carried out showing that entomopathogens can act as good biological control agents and are target specific with high virulence and various researchers are working to know the synergetic effect of entomopathogens with chemical insecticides (Rossetti et al. 2015).

CONCLUSION

Insects are highly susceptible to various fungal pathogens, having potent killing prowess against a wide range of hosts. This study discusses the use of various entomopathogenic fungi and a chemical insecticide on *M. fotedari* which caused significant mortality. Among the three entomopathogens, *B. bassiana* was found to be an apposite and more promising pesticide due to its high virulence. Thus, it can be used as a safe method to control insect pest instead of using chemical insecticides. However, field trials are indispensable to validate the virulence caused by these entomopathogens which led to high mortality in laboratory conditions, and further, field studies are a prerequisite to making them a major component of integrated pest management for *M. fotedari*.

REFERENCES

Abbott W.S. (1925): A method of computing the effectiveness of an insecticide. Journal of Economic Entomology, 18: 265–267.

Adane K., Moore D., Archer S.A. (1996): Preliminary studies on the use of *Beauveria bassiana* to Control *Sitophilus zeamais* (Coleoptera: *Curculionidae*) in the laboratory. Journal of Stored Product Research, 32: 105–113.

Ahmad D., Dar H.U. (1974): A new species of weevil (Curculionidae: *Coleoptera*) from Kashmir Valley. Kashmir Journal of Science, 2: 91–94.

Ahmed A.M., El-Katatny M.H. (2007): Entomopathogenic fungi as biopesticides against the Egyptian cotton leaf

https://doi.org/10.17221/10/2023-JFS

worm, *Spodoptera littoralis* between biocontrol promise and immune-limitation. Journal of Egyptian Society of Toxicology, 37: 39–51.

Aktar W., Sengupta D., Chowdhury A. (2009): Impact of pesticides use in agriculture: Their benefits and hazards. Interdisciplinary Toxicology, 2: 1–12.

Arévalo H.A., Stansly P.A. (2009): Suppression of *Myllocerus undatus* (Coleoptera: *Curculionidae*) in Valencia Orange with chlorpyrifos spray directed at ground and foliage. Florida Entomologist, 92: 150–152.

Atwal A.S. (1963): Insect pests of mango and their control. Punjab Horticultural Journal, 3: 235–258.

Azam M. (2007): Diversity, distribution and abundance of weevil (Coleoptera: *Curculiondidae*) of district Poonch and Rajouri (Jammu). [Ph.D. Thesis.] Jammu, University of Jammu.

Batta Y.A. (2007): Biocontrol of almond bark beetle (*Scolytus amygdali* Guerin-Meneville, Coleoptera: *Scolytidae*) using *Beauveria bassiana* (Bals.) Vuill (Deuteromycotina: *Hyphomycetes*). Journal of Applied Microbiology, 103: 1406–1414.

Budhraja K., Singh O.P., Misra U.S., Dhamdhere S.V., Deole J.Y. (1984): Seasonal incidence, host plants, and efficacy of some insecticides against *Mycllocerus maculosus* infesting hybrid sorghum. Indian Journal of Agricultural Sciences, 54: 418–421.

Butani D.K. (1979): Insect and Fruits. New Delhi, Periodical Expert Book Agency: 415.

Chandler D., Heale J.B., Gillespie A.T. (1993): Germination of the entomopathogenic fungus *Verticillium lecanii* on scales of the glasshouse whitefly *Trialeurodes vaporariorum*. Biocontrol Science and Technology, 3: 161–164.

Davidson R.H., Peairs L.M. (1966): Insect Pests of Farm, Garden, and Orchard. 6th Ed. New York, John Wiley and Sons, Inc.: 675.

Eken C., Tozlu G., Dane E., Çoruh S., Demirci E. (2006): Pathogenicity of *Beauveria bassiana* (Deuteromycotina: *Hypomycetes*) to larvae of the small poplar longhorn beetle, *Saperda populnea* (Coleoptera: *Cerambycidae*). Mycopathologia, 162: 69–71.

Ferron P. (1978): Biological control of insect pests by entomogenous fungi. Annual Review of Entomology, 23: 409–442.

Fuxa J.R. (1984): Dispersion and spread of entomopathogemic fungus *Nomuraea rileyi* (Moniliales: *Moniliaceae*) in a soybean field. Environmental Entomology, 13: 252–258.

Gabarty A., Salem H.M., Fouda M.A., Abas A.A., Ibrahim A.A. (2014): Pathogenicity induced by the entomopathogenic fungi *Beauveria bassiana* and *Metarhizium anisopliae* in *Agrotis ipsilon* (Hufn). Journal of Radiation Research and Applied Science, 7: 95–100.

Godonou I., Green K.R., Oduro K.A., Lomer C.J., Afreh-Nuamah K. (2000): Field evaluation of selected formulations of *Beauveria bassiana* for the management of the banana weevil (*Cosmopolites sordidus*) on plantain (*Musa* spp., AAB group). Biocontrol Science Technology, 10: 779–788.

Gopalakrishnan M., Narayanan K. (1988): Occurrence of the entomopathogenic fungi *Nomuraea rileyi* (Farlow) Samson on *Acontia graellsii* F. (Noctuidae: *Lepidoptera*) and *Beauveria bassiana* (Balsamo) Vuill. on *Myllocerus subfaciatus* G. (Curculionidae: *Coleoptera*). Journal Biological Control, 2: 58–59.

Gull S., Ahmad T., Rasool A. (2019): Studies on diversity indices and insect pest damage of walnuts in Kashmir, India. Acta Agriculturae Slovenica, 113: 121–135.

Hallsworth J.E., Magan N. (1999). Water and temperature relations of growth of the entomogenous fungi *Beauveria bassiana*, *Metarhizium anisopliae* and *Paecilomyces farinosus*. Journal of Invertebrate Pathology, 74: 261–266.

Hill D.S. (1987): Agricultural Insect Pests of the Tropics and their Control. 2nd Ed. Cambridge, Cambridge University Press: 516.

Kavallieratos N.G., Athanassiou C.G., Aountala M.M., Kontodimas D.C. (2014): Evaluation of the entomopathogenic fungi *Beauveria bassiana, Metarhizium anisopliae* and *Isaria fumosorosea* for control of *Sitophilus oryzae*. Journal of Food Protection, 77: 87–93.

Keyhani N.M. (2015): A beetle versus a fungus: *Tribolium castaneum*, a pest of stored grains and insect pathogenic fungus *Beauveria bassiana*. In: 5th Entomopathogens and Microbial Control Congress, Ankara, Sept 9–11, 2015: 9–11.

Khanday A.L., Buhroo A.A. (2018): An assessment of biological control of *Polygraphus major* Stebbing, 1903 (Coleoptera: *Curculionidae*) by entomopathogenic fungi. Journal of Forest Science, 64: 178–186.

Khanday A.L., Buhroo A.A., Ranjith A.P., Kerchev I.A. (2018): Evaluating the efficacy of entomopathogenic fungi against the bark beetles, *Ips stebbingi* Strohmeyer (Coleoptera, *Curculionidae: Scolytinae*) in India. Entomological Review, 98: 985–994.

Kunca A. Vakula J., Galko J., Gubka A. (2009): Výskum využitia entomopatogénnej huby *Beauveria bassiana* pri ochrane smrečín pred podkôrnymi druhmi hmyzu. In: Hudec K., Roháčik T. (eds.): Tretie rastlinolekárske dni Slovenskej rastlinolekárskej spoločnosti, Nitra, Nov 8–19, 2009: 95–99. (in Slovak)

Kreutz J., Vaupe O., Zimmermann G. (2004): Efficacy of *Beauveria bassiana* (Bals.) Vuill. against the spruce bark beetle, *Ips typographus* L., in the laboratory under various conditions. Journal of Applied Entomology, 128: 384–389.

Logan D.P., Robertson L.N., Milner R.J. (1999): Review of the development of *Metarhizium anisopliae* as a microbial insecticide, BioCane™, for the Control of greyback cane grub *Dermolepida albohirtumn* (Waterhouse) (Coleoptera: *Scarabidae*) in Queensland sugarcane. Bulletion OILB/SROP 2000, 23: 131–137.

Mayer H., Mannion C. (2011): Weevil problems in the landscape with emphasis on *Myllocerus undatus* (Sri Lanka Weevil). Proceedings of the Florida State Horticultural Society, 124: 301–302.

Mir G.M., Wani M.A. (2005): Severity of infestation and damage to walnut plantation by important insect pests in Kashmir. Indian Journal of Plant Protection, 33: 188–193.

Mishra R.M. (1993): *Beauveria bassiana* (Balsamo) Vuillemin a fungal pathogen of *Hypsiphyla robust* Moore (*Lepidoptera: Pyralidae*). Indian Journal of Forestry, 16: 236–238.

O'Brien C.W., Wibmer G.J. (1979). The use of trend curves of rates of species descriptions: examples from the *Curculionidae* (*Coleoptera*). The Coleopterists' Bulletin, 33: 151–166.

O'Brien C.W., Haseeb M., Thomas M.C. (2006): *Myllocerus undecimpustulatus undatus* Marshall (Coleoptera: *Curculionidae*), a recently discovered pest weevil from the Indian subcontinent. Entomology Circular, 412: 1–4.

Oerke E.C., Dehne H.W., Schönbeck F., Weber A. (1994): Crop Production and Crop Protection: Estimated Losses in Major Food and Cash Crops. Amsterdam, Elsevier Science B.V.: 808.

Ramamurthy V.V., Ghai S. (1988): A study on the genus *Myllocerus* (Coleoptera: *Curculionidae*). Oriental Insects, 22: 377–500.

Ramanujam B., Rangeshwaran R., Sivakmar G., Mohan M., Yandiger M. (2014): Management of insect pests by microorganisms. Proceeding Indian National Science Academy, 80: 455–471.

Sabbour M.M., E-Abd-El-Aziz S. (2007): Efficiency of some bio-insecticides against broad bean beetle, *Bruchus rufimanus* (Coleoptera: *Bruchidae*). Research Journal of Agriculture and Biological Sciences, 3: 67–72.

Sankaran K.V., Mohanadas K., Ali M.I.M. (1989): *Beauveria bassiana* (Bals.) Vuill, a possible biocontrol agent against *Myllocerus viridanus* Fabr. and *Calopepla leayana* Latreille in South India. Current Science, 58: 467–469.

Senthilkumar N., Murugesan S. (2010). Entomopathogenic fungi for the management of *Calopepla leayana* on *Gmelina arborea*. Journal of Ecobiotechnology, 2: 1–6.

Shapiro-Ilan D.I., Gardner W.A, Fuxa J.R, Wood B.W., Nguyen K.B., Adams B.J., Humber R.A., Hall M.J. (2003): Survey of entomopathogenic nematodes and fungi endemic to pecan orchards of the southeastern United States and their virulence to the pecan weevil (Coleoptera: *Curculionidae*). Environment Entomology, 32: 187–195.

Singh U.C., Dhamdhere S.V., Misra U.S., Bhadauria N.S. (1991): Seasonal incidence and toxicity of some newer insecticides against *Myllocerus undecimpustulatus*. Indian Journal of Agricultural Research, 25: 119–124.

Sinha R.B.P., Marwaha K.K. (1995): Persistent and residual toxicity of certain insecticides against the adult of grey weevil, *Myllocerus undecimpustulatus* Var. *maculosus*. Journal of Applied Biology, 5: 53–57.

Steinwender B.M., Krenn H.W., Wegensteiner R. (2010): Different effects of the insect pathogenic fungus *Beauveria bassiana* (Deuteromycota) on the bark beetle *Ips sexdentatus* (Coleoptera: *Curculionidae*) and on its predator *Thanasimus formicarius* (Coleoptera: *Cleridae*). Journal of Plant Diseases and Protection, 117: 33–38.

Tara J.S., Sharma S., Kour R. (2010): A record of weevil (Coleoptera: *Curculionoidea*) diversity from District Samba (J&K). The Bioscan, 5: 391–394.

Turchinskaya I.A., Sherlyngina A.N. (1974): The use of white muscardine fungus *Beauveria bassiana* (Bals.) Vuill. for the control of the pine weevil. Proceedings Forest Research (Leningrad Institute of Forestry), 21: 106–113.

Vaupel O., Zimmermann G. (1996): Orientierende Versuche zur Kombination von Pheromonfallen mitdem insektenpathogenen Pilz *B. bassiana* (Bals.) Vuill. gegen die Borkenkäferart *Ips typographus* L. (*Col*eoptera, *Scolytidae*). Anzeiger Schädlingskde, 69: 175–179. (in German)

Wu G.Y., Sun J.D. (1994): A study and application of *Beauveria bassiana* (Bals.) Vuill in the control of the tea brown weevil. China Tea, 16: 30–31.

Wu J.F., Sun J.D., Zeng M.S., Lin A.X., Xu D.Y., Wang Q.S. (1995): Application of *Beauveria bassiana* strain 871 in controlling tea weevil (*Myllocrinus aurolineatus*). Journal of Fujian Academy of Agricultural Science, 10: 39–43.

Yanar D., Soy B., Yanar Y., Yalçın M. (2015): Effective entomopathogenic fungi *Beauveria bassiana* on *Syrista parreysii* Spin. (*Cephidae*) under laboratory conditions. In: VI. International Scientific Symposium for PhD Students and Students of Agricultural College, Bydgoszcz-Ciechocinek, Sept 17–19, 2015: 145.

Received: January 25, 2023
Accepted: May 17, 2023
Published online: July 1, 2023

https://doi.org/10.17221/125/2022-JFS

Assessment of aboveground biomass and carbon stock of subtropical pine forest of Pakistan

Nizar Ali[1], Muhammad Saad[1], Anwar Ali[2], Naveed Ahmad[3], Ishfaq Ahmad Khan[4], Habib Ullah[5], Areeba Binte Imran[3]*

[1]Department of Forestry and Wildlife Management, University of Haripur, Haripur, Pakistan
[2]Pakistan Forest Institute Peshawar, Peshawar, Pakistan
[3]Department of Forestry and Range Management, University of Arid Agriculture Rawalpindi, Rawalpindi, Pakistan
[4]Department of Forest Science & Biodiversity, Faculty of Forestry and Environment, University Putra Malaysia (UPM), Serdang, Malaysia
[5]School of Forestry, North-East Forestry University, Herbin, China

**Corresponding author: ishfaqahmad860@gmail.com*

Citation: Ali N., Saad M., Ali A., Ahmad N., Khan I.A., Ullah H., Imran A.B. (2023): Assessment of aboveground biomass and carbon stock of subtropical pine forest of Pakistan. J. For. Sci., 69: 287–304.

Abstract: The presented study estimated the aboveground biomass (*AGB*) of *Pinus roxburghii* (chir pine) natural forests and plantations, and created biomass maps using a relationship (regression model) between *AGB* and Sentinel-2 spectral indices. The mean *AGB* and *BGB* (belowground biomass) of natural forests were 79.54 $Mg \cdot ha^{-1}$ and 20.68 $Mg \cdot ha^{-1}$, respectively, whereas the mean *AGB* and *BGB* of plantations were 94.48 $Mg \cdot ha^{-1}$ and 24.56 $Mg \cdot ha^{-1}$, respectively. Correlation showed that mean diameter at breast height (*DBH*) and mean height have weak relationships with *AGB*, and *BGB* has shown correlation coefficients (R^2 = 0.46) and (R^2 = 0.56) for polynomial models. Regression models between *AGB* ($Mg \cdot ha^{-1}$) of *Pinus roxburghii* natural forest and Sentinel-2 spectral indices showed a strong relationship with Ratio Vegetation Index (*RVI*) with R^2 = 0.72 followed by Normalized Difference Vegetation Index (*NDVI*) and Atmospherically Resistant Vegetation Index (*ARVI*) with R^2 = 0.70. In contrast, the lower performance of spectral indices has been shown in regression with plantation *AGB*. Correlation coefficients (R^2) were 0.41, 0.41, and 0.40 for *RVI*, *NDVI*, and *ARVI*, respectively. All indices showed that the distribution of *AGB* data was not the best fit with the linear regression model. Therefore, non-linear exponential and power models were considered the best fit for *NDVI*, *RVI*, and *ARVI*. A biomass map was developed from *RVI* for both natural forests and plantation because RVI has the highest R^2 and lowest *P*-value.

Keywords: natural forest; *Pinus roxburghii*; plantations; regression analysis; Sentinel-2; vegetation index

The world forest has spread around 4.06 billion ha, which accounts for 31% of the total area and has been showing a decreasing trend for the last three decades (FAO 2020). The world's forest land is believed to have declined from 31.6% to 31.0% of the total area (Jallat et al. 2021). Human intervention on a large scale is the main factor in reducing the world's forests (FAO 2020; Kyere-Boateng, Marek 2021). Deforestation and forest degradation contribute to global climate change (GCC) by releasing carbon into the atmosphere, which has detrimental effects on the environment. In this context, world forests are crucial since they function as a carbon sinker and carbon source (Raihan et al. 2019; Huang et al. 2020; Babbar et al. 2021).

© The authors. This work is licensed under a Creative Commons Attribution-NonCommercial 4.0 International (CC BY-NC 4.0).

https://doi.org/10.17221/125/2022-JFS

The forest's role in removing carbon from the atmosphere and GCC mitigation has been fully acknowledged (Houghton et al. 2015). Reducing or reversing forest degradation in (sub)tropical regions will contribute to GCC mitigation, given the significant impacts of forest degradation on global biodiversity and ecosystem services, including carbon sequestration (Nyamari et al. 2021; Thammanu et al. 2021). The extent of forest biomass determines ecosystem productivity. It is used to evaluate the function of vegetation in the carbon cycle, its energy production capacity, and the carbon stock assessment for climate change modelling (Siddiq et al. 2021). Due to the high potential of carbon dioxide (CO_2) storage, the forest's role as a carbon sink has long been recognised as the most significant one, as forests hold most of the above- and belowground terrestrial regenerative carbon (Zhang et al. 2013). Nevertheless, at the global level, the soil is considered the largest carbon pool compared to other major terrestrial ecosystems such as forests (Zhang et al. 2021). Aboveground biomass (*AGB*) comprises stems, stumps, branches, bark, seeds, and leaves; belowground biomass (*BGB*) contains all active roots with a diameter greater than 2 mm; and the dead mass of coarse and fine aggregate attached to the soil. The more easily measured *AGB* can be used to estimate the other terrestrial carbon pools. As a result, *AGB* has typically been the focus of biomass estimation research (Goetz, Dubayah 2011). Hereafter, the term 'forest biomass' is used to indicate forest *AGB*.

Forest biomass can be estimated through destructive or non-destructive methods (Khan et al. 2021a). The destructive method is generally not favoured as it is costly, laborious, limited in spatial and temporal samplings, and may have a negative effect on forest health (Qureshi et al. 2012). The non-destructive method comprises physiological-based models, carbon flux measurements, forest yield models, forest inventory-based approaches, and remote-sensing methods (Qureshi et al. 2012). Furthermore, remote sensing products such as Sentinel-2 can provide spatially clearly defined and precisely combined information about forest biomass quantity at the broad level of spatial and temporal resolutions by frequent revisit time of 10 days for a single Sentinel-2 satellite and 5 days for constellation and usage of historical data archives (Nhangumbe et al. 2023). The assessment of forest biomass can be greatly improved by using satellite data such as Sentinel-2 images, which offer superior spectral coverage, spatial resolution, and temporal frequency compared to other platforms (Shoko, Mutanga 2017). The Sentinel-2 platform boasts a multispectral instrument (MSI) sensor that captures images with a wider range of spectral coverage, including red-edge and shortwave infrared bands, as well as higher spatial resolution (10 m, 20 m, 60 m) and more frequent temporal coverage than Landsat (Sun et al. 2019; Isbaex, Coelho 2021; Ahmad et al. 2023). Sentinel-2 imagery is open-source data that can be acquired freely from the European Space Agency (ESA) hub. Its use has improved the integration of biomass modelling with vegetation indices, spectral bands, and biophysical variables based on field-measured data (Castillo et al. 2017; Zhang et al. 2017). The red-edge band present in Sentinel-2 product is particularly well-suited for mapping and assessing vegetation characteristics (Shoko, Mutanga 2017; Pertille et al. 2019; Ahmad et al. 2023). Among remote sensing technologies, Synthetic Aperture Radar (SAR) has proven to be the most sensitive in retrieving forest biophysical parameters such as canopy height and aboveground biomass (Khati et al. 2017; Musthafa et al. 2020), with SAR backscatter being the most commonly used parameter for biomass retrieval. In recent years, Light Detection and Ranging (LiDAR) has gained significant traction as a complementary remote sensing tool for forest biophysical parameter retrieval, as it provides highly accurate three-dimensional forest structures (Musthafa, Singh 2022).

Although remote sensing is unlikely to provide more precise biomass estimates at the plot or stand level in the mid-term, it is equally unlikely that field-based inventories can effectively address the systematic, wall-to-wall mapping at regional or larger scales. Nonetheless, field-based biomass assessments are crucial for remote-sensing methodologies for calibrating models and validating results (Ahmad et al. 2023).

Pakistan has a low forest cover of about 5% of the total land area, with most of the forest in the country's northern region (Bukhari et al. 2012; Khan et al. 2021a). Various evergreen trees of the *Pinaceae* family, including the *Pinus roxburghii*, are present in the Himalayas and can be found in Pakistan, India, Nepal, and Bhutan. There are approximately 105 *Pinus* species present in the world (Satyal et al. 2013); out of these, six species occur in Pakistan: *Abies pindrow, Cedrus deodara, Picea smithi-*

https://doi.org/10.17221/125/2022-JFS

ana, *Pinus gerardiana*, *Pinus roxburghii*, and *Pinus wallichiana*. *Pinus roxburghii* is a coniferous tree that may grow to a height of up to 55 m with a stem diameter reaching up to 2 m (Satyal et al. 2013). *Pinus roxburghii* has a long rotational age and a high carbon sequestration potential. In Kashmir Himalaya, Pakistan, the *AGB* of a mature Chirpine forest was estimated to be 191.8 $Mg \cdot ha^{-1}$ (Shaheen et al. 2016). Another study in Azad Jammu and Kashmir (AJK) reported the average carbon stock potential of chir pine to be 5.93 $Mg \cdot ha^{-1}$ (Khan et al. 2021b). *Pinus roxburghii* is the most dominant *Pinus* species in Buner district. The main objectives of this study were (*i*) to evaluate aboveground dry biomass (*AGB*) of *Pinus roxburghii* natural forests and plantations in the study area, and (*ii*) to develop a relationship (regression model) between aboveground biomass and Sentinel-2 spectral indices to generate biomass maps.

MATERIAL AND METHODS

The study area – Buner Forest Division. Buner Forest Division is the study area of the current research. It is located at the coordinates of 34°10'N and 34°43'N, and 72°11'E and 72°49'E (Figure 1). Different types of forests can be found in the area, including dry subtropical broadleaved, pure chir pine, dry oak (*Quercus baloot*), and mixed chir and kail forests. The forest inventory for the present study was conducted mainly in chirpine forests that fall in submature category i.e. 40 years. These forests extend from 1 000 m a.s.l. to 1 500 m a.s.l. and occupy a vast majority of the Gadazai, Malik Pur, Batai, Karakar, Daggar, Chamla, Nagri, Mohaban, and Malka areas. The broadleaved species that exist in these forests are Kao (*Olea cuspidata*), *Ficus* spp., batangi, white oak, sanatha (*Dodonaea viscose*), *Celtis australis*, *Rubus* spp., gurgura (*Monotheca buxifolia*), and bhekar (*Adhatoda vassica*) etc. The mean annual temperature, mean annual precipitation and relative humidity of the study area are recorded as 19 °C, 1 068 mm, and 60–65% respectively (Rahman et al. 2022). The plot-wise coordinates, elevation (m), slope (degrees), and aspect (degrees) are summarised in Table S1 in the Electronic Supplementary Material (ESM). Regarding natural forests, the elevation ranges from 795 to 1 885 m, while the slope ranges from 10.45 to 48.57 degrees. Similarly, aspects range from 1.64 to 359.37 degrees. Likewise, mean elevation, aspect, and slope were 1 180.10 ± 63.27 m a.s.l., 28.15 ± 23.43 degrees, and 173.53 ± 2.03 degrees, respectively. On the other hand, in the case of plantations, the highest elevation, slope, and aspect for natural forests were 1 707 m a.s.l., 42.51 degrees, and 349.05 degrees, respectively. The lowest elevation, slope and aspect were 699 m, 4.39 degrees, and 15.85 degrees, respectively. At the same time, the mean elevation, slope, and aspect were 923.32 m ± 53.20, 23.29 ± 2.25 degrees, and 243.39 ± 21.4 degrees, respectively.

Forest inventory. Table 1 below shows various instruments used for field sampling for *AGB*, including satellite images.

Field data were collected from 57 sample plots during January 2020 for biomass and carbon stock estimation. The random sampling design was adopted during inventory. 29 plots were from the natural forest of *Pinus roxburghii*, and 28 plots were from the plantation of *Pinus roxburghii*, re-

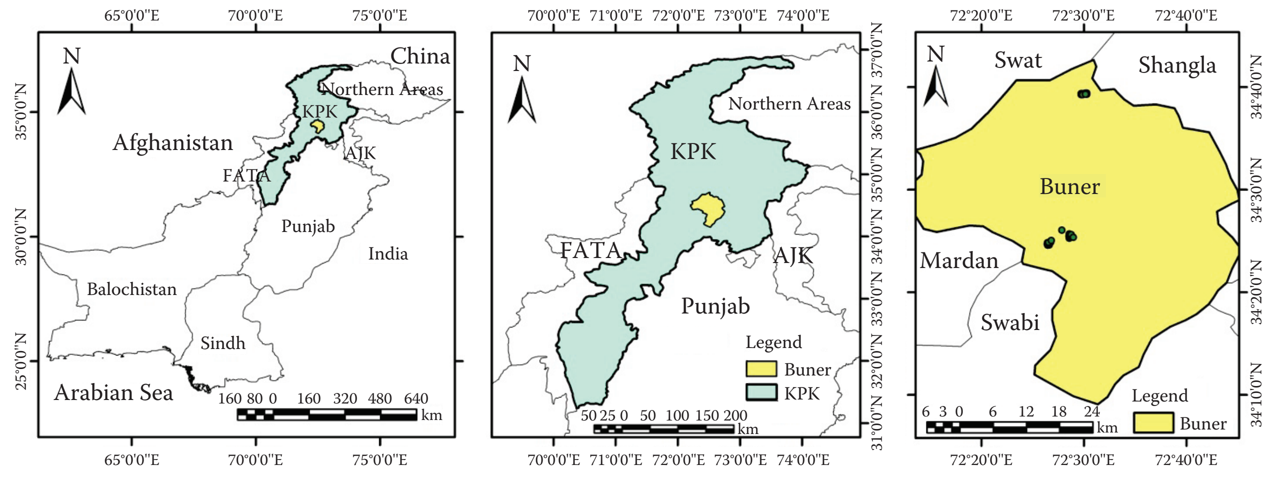

Figure 1. Study area map

https://doi.org/10.17221/125/2022-JFS

Table 1. Tools used in field sampling

Materials	Purpose	Unit
Diameter caliper (120 cm)	diameter measurement	cm
Haga altimeter	height measurement	m
Sunnto clinometer	slope and height measurement	degrees and m
Measuring tape (100 m)	measuring distance	m
Ranging rods	plot centre and other location	–
Garmin GPS	navigation	degree, minute, second
Sentinel-2 image	computation of vegetation indices and biomass	ratio

spectively. Each plot was circular with a radius of 17.84 m and an area of 0.1 ha, all of them being distributed in the Buner Forest Division. Tree height and diameter at breast height (*DBH*) were measured in all plots to calculate aboveground biomass (Afzal, Akhter 2011; Nizami 2012). All trees with a *DBH* of ≥ 5 cm were measured. Diameter caliper of 120 cm length was used to measure *DBH*. As per UNFCCC guidelines (Nizami 2012; Ahmad et al. 2023) regarding tree measurement, forked and defective trees were also subjected to measurement as they are believed to have a quantity of biomass (Ali et al. 2018). Haga Altimeter used for height measurement is a gravity-oriented pointer device for height measurement within a fixed range of distances (20 m, 25 m, and 30 m). As height measurement is difficult and time-consuming for variable distances and viewpoints, it was only measured for dominant trees in the plots. Suunto Clinometer (Finland) was used for slope estimation, the distance was measured with the help of a measuring tape (100 m), and GPS (Garmin, USA) was used for location identification or navigation purposes. Compass was used for the proper direction of plot selection in the area for aspect identification. During the field survey, selected samples included maximum variability of available *DBH* and height groups in homogeneous forest regions for each species.

For tree height estimation, the following Equation (1) was used:

$$H = \tan\theta \times b + a \quad (1)$$

where:
H – total height of a tree (m);
θ – angle of a tree to the top of the tree from observers' eyes;
b – distance between the tree base and the observer (m);
a – observer eye height (m).

Full enumeration and direct measurement of *AGB* through destructive sampling is considered the most accurate; however, such methods are costly and laborious (Kumar, Mutanga 2017). Regression models (allometric equations) provide effective alternatives to destructive sampling (Seidel et al. 2011). These equations convert inventory data into an estimate of aboveground biomass. A literature survey was conducted for the selection of species-specific as well as general allometric models. Biomass carbon contents of each species differ from others due to specific wood density and properties (Lamlom, Savidge 2003).

Biomass estimation. Pool 1: Aboveground biomass (*AGB*).

Method 1: Using *BEF* (biomass expansion factor) (Ali et al. 2020b) [Equation (2)]:

$$AGB = V \times WD \times BEF \quad (2)$$

where:
AGB – aboveground biomass;
V – volume;
WD – wood density [available from literature (Ali et al. 2018)];
BEF – biomass expansion factor [available from literature (Ali et al. 2018)].

Method 2: Using allometric equation.

Aboveground biomass (*AGB*) was estimated by allometric equation in two steps (Ali et al. 2020a) [Equations (3–4)]:

$$H = 0.0044 \times DBH^2 + 0.686\, DBH - 0.7196 \quad (3)$$

$$AGB = 0.0224\, (DBH^2 \times H)^{0.9767} \quad (4)$$

where:
AGB – aboveground biomass (kg);
DBH – diameter at breast height (cm);
H – height (m).

https://doi.org/10.17221/125/2022-JFS

Pool 2: Belowground biomass (*BGB*) (Ali et al. 2020b) [Equation (5)]:

$$BGB = AGB \times R/S \quad (5)$$

where:

BGB – belowground biomass;

R/S – root-shoot ratio [available from literature (Ali et al. 2017)].

The species-wise aboveground and belowground biomass were estimated by summing up the tree biomass values (kg) calculated for each plot. According to a plot size of 1 000 m^2, the plot-based *AGB* (Mg) were converted to standard *AGB* units per hectare by multiplying by a scaling factor of 10. The plot-based *AGB* and *BGB* values were given in kg, then converted to Mg by dividing by 1 000.

The Intergovernmental Panel on Climate Change (IPCC) explains how to calculate changes in carbon stocks, greenhouse gas emissions, and biomass content in forest areas using various methodologies. Typically, carbon accounts for around half of the dry biomass (Malhi et al. 2004). Thus, the carbon stock can be estimated by multiplying the dry biomass by 0.47 (Ali et al. 2020b). Belowground biomass was calculated by multiplying the *AGB* by 0.26 according to IPCC guidelines (Ravindranath, Ostwald 2008). Aboveground carbon stocks (*AGC*) and belowground carbon stocks (*BGC*) were calculated by multiplying the dry biomass (aboveground and belowground) by 0.47 (Afzal, Akhter 2011). After that, the carbon stock was multiplied by 44/12 (the carbon atom ratio in the molecular weight of CO_2) to get the CO_2 equivalent value (Pearson et al. 2007).

Remote sensing. The current study used a Sentinel-2 image for *AGB* estimation; the Sentinel-2 image was acquired from Copernicus Sentinel Scientific Data Hub (https://scihub.copernicus.eu/) on Jan 13, 2020. Pre-processing of Sentinel-2 image was the first step before using it for biomass estimation purposes. The aim was to avoid the effects of atmospheric scattering or cloud cover shadows, visual aid interpretation, and extract plenty of information from remotely sensed images. Pre-processing included radiometric, geometric, and terrain corrections. Sentinel Application Platform (SNAP 5.0, 2016) is a toolbox used for analysis and processing of Sentinel-2 images. Sen2Cor is a third-party plugin in SNAP 5.0, used for pre-processing of Sentinel-2 Level-1C raw image into Level-2A rectified image. Atmospheric correction comprised of bottom-of-the atmosphere (BoA) reflectance and top-of-the-atmosphere (ToA) reflectance. Sentinel-2 Level-1C was processed by Sen2Cor plugin, starting with cloud correction and classification, followed by aerosol particle thickness and retrieval of water vapours; ultimately the process ended with Level-2A output. The subsetting of rectified images has been done up to the extent of the research area where forest inventory was carried out. In order to calculate the average value for the plot, mean filter of 3 × 3 matrixes has been run on Sentinel-2 image to resample it as per field sample plot size. Further, different vegetation indices were computed using SNAP for Sentinel-2 images, respectively (Table 2). These indices indicate biomass potential and the health of the vegetation. *AGB* shapefile created via ArcGIS 10.3 (2014) was overlaid on corresponding vegetation indices of both the acquired images. The values of masked pixels (where field data was overlaid) were extracted for all the indices, and mean values were calculated.

Statistical analysis. Different explanatory variables explain total carbon sequestered and carbon in other pools (above- and belowground). These variables and their analysis include *DBH* versus height, *AGB* versus *DBH*, and *AGB* versus height. Moreover, scatter plots were also created to examine the association between biomass and individ-

Table 2. Sentinel-2 vegetation indices

Indices	Sentinel-2 bands	Reference
Normalized Difference Vegetation Index (*NDVI*)	(Band 8 – Band 4) / (Band 8 + Band 4)	Rouse et al. (1973)
Atmospherically Resistant Vegetation Index (*ARVI*)	((Band 8–Band 4 – (Band 2 – Band 4)) / (Band 8 + + Band4 – (Band 2 – Band 4))	Kaufman, Tanre (1992)
Ratio Vegetation Index (*RVI*)	(Band 8) / (Band 4)	Tucker (1979)

https://doi.org/10.17221/125/2022-JFS

ual indices. The coefficient of determination (R^2), *RMSE* (root mean square error), and *P*-value were calculated for each model in SPSS 16.0 (2007). As a result, the model fulfilling the conditions of high R^2, low *RMSE*, and ($P < 0.05$) was selected for effective biomass estimation and generation of biomass map in ArcGIS (Version 10.3, 2014).

RESULTS

Tree attributes of natural forests. Mean *DBH* and mean height was determined for each natural forest plot, and the mean values of these attributes are shown in Table S2 in the ESM. These values were determined by taking an average of the trees' *DBH* and height within the given plot. The highest number of stems was recorded at 610 trees·ha^{-1} from plot 11, and the highest mean *DBH* (56.6 cm) and height (26.9 m) were recorded in plot 13, with the smallest number of stems being 90 trees·ha^{-1}. The lowest mean *DBH* and mean height were recorded at 18.38 cm, with the lowest mean height of 11.19 m.

Aboveground biomass and carbon stock estimation from inventory data of natural forest. The biomass estimation of natural forests includes aboveground biomass and carbon (Mg·ha^{-1}), belowground biomass (Mg·ha^{-1}), total biomass,

Table 3. Biomass and carbon stocks estimation of plot data in natural forest

Plot No.	*AGB*	*AGC*	*BGB*	*BGC*	Total biomass	Total C	CO_2e
	(Mg·ha^{-1})						
1	77.44	36.40	20.14	9.46	97.58	45.86	167.85
2	35.15	16.52	9.14	4.30	44.29	20.82	76.19
3	18.91	8.89	4.92	2.31	23.83	11.20	40.99
4	41.87	19.68	10.89	5.12	52.75	24.79	90.75
5	62.63	29.43	16.28	7.65	78.91	37.09	135.74
6	77.26	36.31	20.09	9.44	97.35	45.76	167.46
7	42.24	19.85	10.98	5.16	53.22	25.02	91.56
8	39.63	18.63	10.30	4.84	49.94	23.47	85.90
9	56.76	26.68	14.76	6.94	71.52	33.61	123.03
10	57.95	27.23	15.07	7.08	73.01	34.32	125.60
11	102.40	48.13	26.62	12.51	129.03	60.64	221.95
12	137.06	64.42	35.63	16.75	172.69	81.16	297.06
13	140.79	66.17	36.61	17.20	177.40	83.38	305.16
14	106.73	50.16	27.75	13.04	134.48	63.21	231.34
15	70.11	32.95	18.23	8.57	88.34	41.52	151.96
16	25.32	11.90	6.58	3.09	31.90	14.99	54.88
17	174.74	82.13	45.43	21.35	220.18	103.48	378.75
18	106.82	50.21	27.77	13.05	134.60	63.26	231.53
19	10.12	4.75	2.63	1.24	12.74	5.99	21.92
20	129.68	60.95	33.72	15.85	163.40	76.80	281.07
21	96.06	45.15	24.98	11.74	121.04	56.89	208.21
22	68.82	32.34	17.89	8.41	86.71	40.75	149.16
23	32.67	15.36	8.49	3.99	41.17	19.35	70.81
24	77.41	36.38	20.13	9.46	97.54	45.84	167.79
25	74.51	35.02	19.37	9.10	93.88	44.12	161.49
26	110.70	52.03	28.78	13.53	139.48	65.55	239.93
27	144.69	68.00	37.62	17.68	182.31	85.68	313.61
28	117.47	55.21	30.54	14.35	148.01	69.56	254.60
29	70.72	33.24	18.39	8.64	89.11	41.88	153.29

AGB – aboveground biomass; *BGB* – belowground biomass; *AGC* – aboveground carbon; *BGC* – belowground carbon

https://doi.org/10.17221/125/2022-JFS

and carbon stocks, as summarised in Table 3. The highest total biomass was 220.18 Mg·ha^{-1} with *AGB* and *BGB* of 174.74 Mg·ha^{-1} and 45.43 Mg·ha^{-1} in plot 17, whereas the lowest total biomass was 12.74 Mg·ha^{-1} in plot 19 with *AGB* and *BGB* 10.12 Mg·ha^{-1} and 2.63 Mg·ha^{-1}, respectively. The mean *AGB* and *BGB* were estimated as 79.54 Mg·ha^{-1} and 20.68 Mg·ha^{-1}, respectively, while the mean biomass for both *AGB* and *BGB* was 100.22 Mg·ha^{-1}, as presented in Table 3. Similarly, the highest total carbon stocks, *AGC* and *BGC*, were 103.48 Mg·ha^{-1}, 82.13 Mg·ha^{-1}, and 21.35 Mg·ha^{-1}, respectively, whereas the lowest total carbon stocks, *AGC,* and *BGC* were calculated as 5.99 Mg·ha^{-1}, 4.75 Mg·ha^{-1}, and 1.24 Mg·ha^{-1}, respectively. Regarding CO_2 equivalent, the highest (378.75 CO_2e) was found in plot 17, while the lowest 21.92 CO_2e was in plot 19. The mean *AGC* and *BGC* were 37.38 Mg·ha^{-1} and 9.72 Mg·ha^{-1}, respectively, whereas mean carbon stocks (including both *AGC* and *BGC*) were 47.10 Mg·ha^{-1}, as shown in Table 3.

Relationship between tree attributes and *AGB* of inventory data in natural forests. A simple linear regression model was developed between *AGB* (Mg·ha^{-1}) and plot-wise attributes (mean *DBH* and height). Results showed that mean *DBH* has a weak relationship with *AGB* and a correlation coefficient (R^2 = 0.46) with a polynomial model, which explained only 46% of data and 56% of *AGB* data remained unexplained (Figure 2A). The lower correlation of *DBH* versus *AGB* may be explained by the fact that plot-wise mean values were regressed against each other; if single tree measurements are correlated, the correlation coefficient would be better. Similarly, the mean height of each plot was regressed against plot-wise mean *AGB*, and the scatter plot showed that the correlation was lower (R^2 = 0.56) with the polynomial model (Figure 2B). This model explained only 56% of the *AGB*, whereas 44% of *AGB* data was left unexplained. However, its correlation was higher than the *DBH* polynomial model.

Sentinel-2 spectral indices for natural forests. Results of regression models between *AGB* (Mg·ha^{-1}) of *Pinus roxburghii* natural forest and Sentinel-2 spectral indices have been summarised in Table 4. All vegetation indices showed a strong relationship with field *AGB* data; Ratio Vegetation Index (*RVI*) showed the best performance with correlation (R^2 = 0.72), which means that the *RVI* polynomial model explained 72% of forest inventory data while the remaining 28% of *AGB* data remained unexplained (Figure 3C). Similarly, Normalized Difference Vegetation Index (*NDVI*) and Atmospherically Resistant Vegetation Index (*ARVI*) showed good performance, and the coefficient of correlation (R^2) was 0.70 for both indices (Figure 3A–B). It means that 70% of *AGB* was explained by *NDVI* and *ARVI* models, and the rest of the 30% data was not explained. *NDVI* has shown the highest correlation in the polynomial model, whereas *ARVI* achieved the highest correlation in the power model. Likewise, all indices showed that the distribution of *AGB* data was not the best fit with the linear regression model. Therefore, non-linear polynomial and power were best for *NDVI*, *RVI*, and *ARVI*, respectively (Table 4).

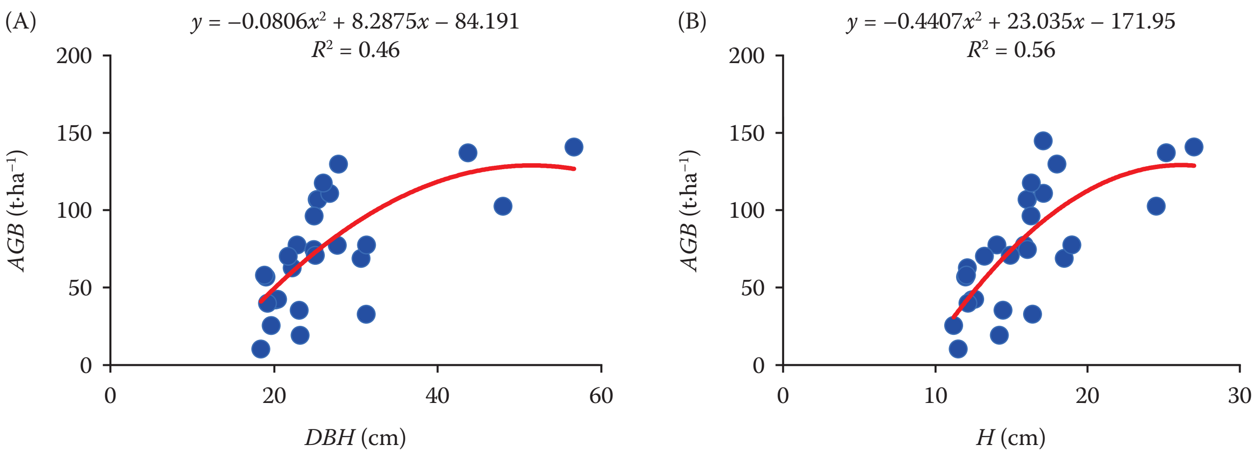

Figure 2. (A) *AGB* vs *DBH*; (B) *AGB* vs *H*

AGB – aboveground biomass; *DBH* – diameter at breast height; *H* – height

https://doi.org/10.17221/125/2022-JFS

Table 4. Summary of regression models between *AGB* and Sentinel-2 spectral indices

Index	Equation	Model	R^2
Natural forests			
NDVI	$y = -244.7x^2 + 614.48x - 154.23$	polynomial	0.70
ARVI	$y = 264.15x^{2.2769}$	power	0.70
RVI	$y = -11.452x^2 + 128.35x - 187.65$	polynomial	0.72
Plantations			
NDVI	$y = 5.7006e^{5.6445x}$	exponential	0.41
ARVI	$y = 13.029e^{3.1633x}$	exponential	0.40
RVI	$y = 8.7573x^{2.1666}$	power	0.41

AGB – aboveground biomass; *NDVI* – Normalized Difference Vegetation Index; *ARVI* – Atmospherically Resistant Vegetation Index; *RVI* – Ratio Vegetation Index

Hence, the polynomial model was used to minimise error and ensure best fit along the curvature of *AGB* data. The polynomial models of *NDVI* and *RVI* have shown a high correlation compared to linear models. However, their performance was affected by the data's outliers (Figures 3B–C). Similarly, in the case of *ARVI*, the correlation was increased using a power model, which means that

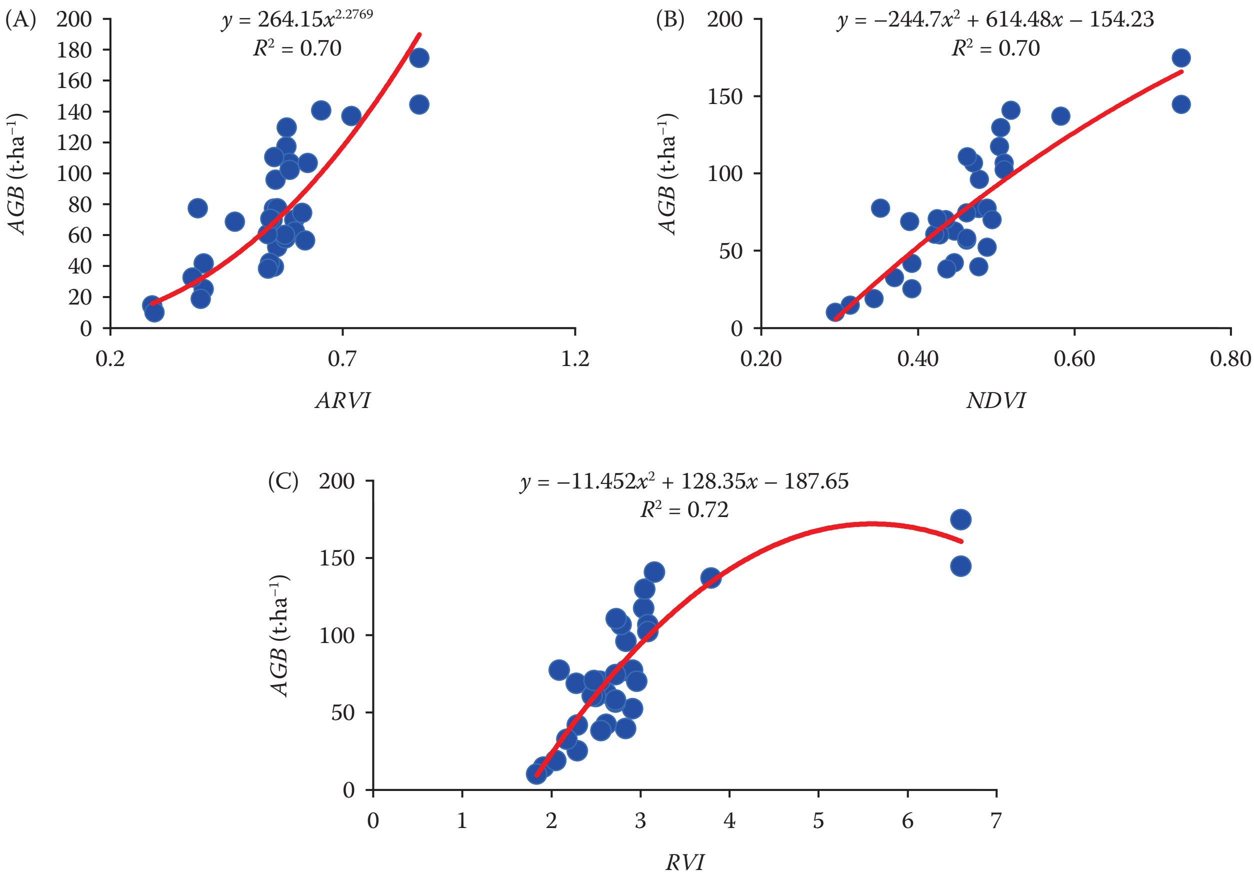

Figure 3. Relationships of Sentinel-2 vegetation indices and natural forest *AGB*; (A) *AGB* vs *ARVI*; (B) *AGB* vs *NDVI*; (C) *AGB* vs *RVI*

AGB – aboveground biomass; *ARVI* – Atmospherically Resistant Vegetation Index; *NDVI* – Normalized Difference Vegetation Index; *RVI* – Ratio Vegetation Index

https://doi.org/10.17221/125/2022-JFS

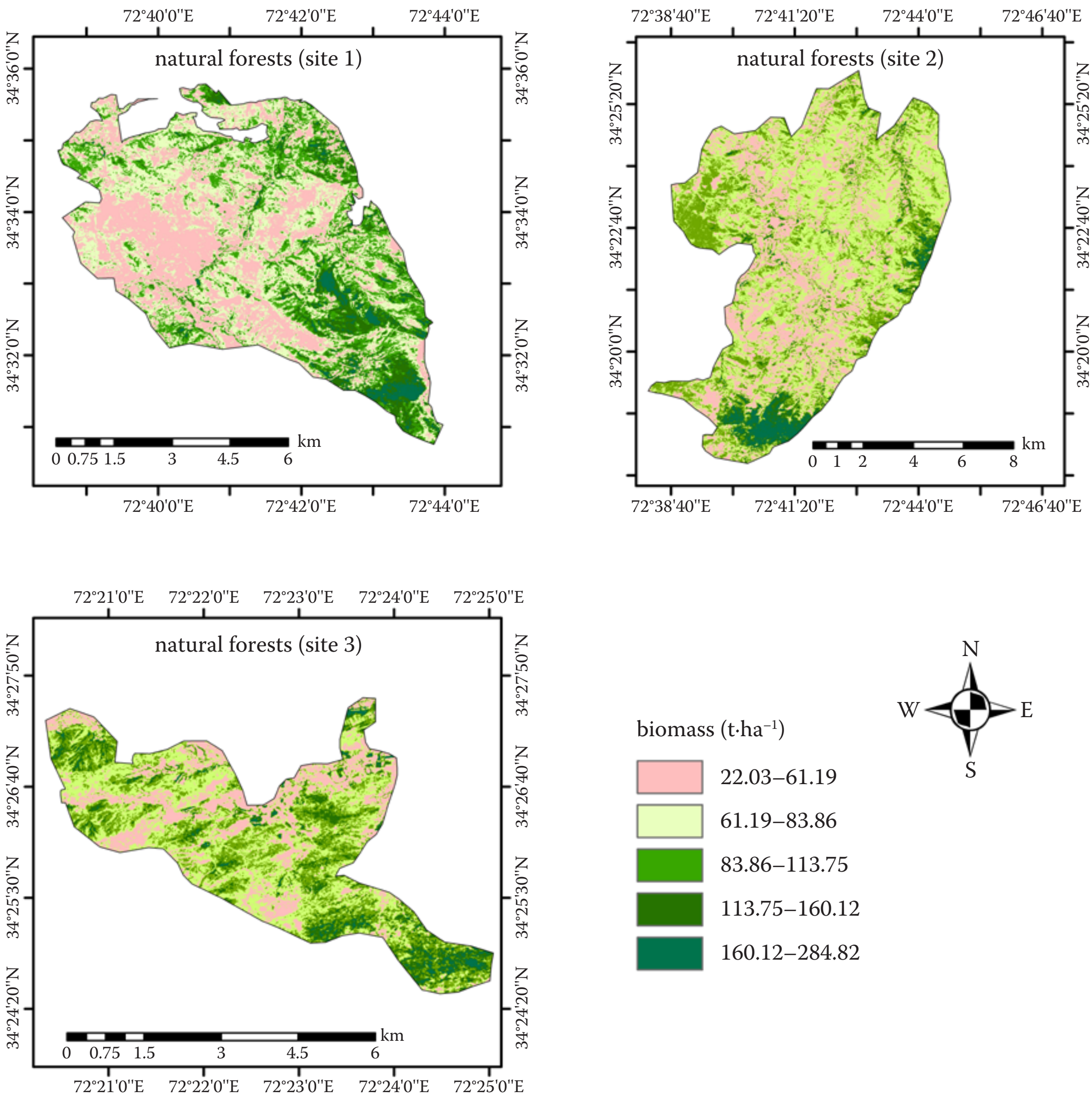

Figure 4. Biomass maps of different sites of natural forest in the study area

AGB data was proportional to *ARVI* values raised to a power. Comparatively, *RVI* was selected as the best index for *AGB* mapping of natural forests in the study area (Figure 4).

Tree attributes of plantation. The mean *DBH* and mean height of each plantation plot were determined, and the mean values of these attributes are shown in Table S3 in the ESM. The *DBH* and height mean values were calculated by averaging the *DBH* and height of the trees within the plot. The highest number of stems was recorded at 630 trees·ha^{-1} in plot 9. The highest mean *DBH* and height were 46 cm and 26.21 m, recorded in plot 17 with stem number (360 trees·ha^{-1}). The lowest mean *DBH* and mean height were recorded at 16 cm, with the lowest mean height of 10.43 m. Comparison of mean *DBH*, mean height and total biomass of natural forest and plantation have been represented in Figure 5.

Aboveground biomass and carbon stock estimation from inventory data of plantation. Plantation carbon stocks, aboveground biomass, belowground biomass (t·ha^{-1}), and total biomass and carbon stocks assessment is summarised in Table 5. According to Table 5, the highest total biomass was 360.05 Mg·ha^{-1} with *AGB* and *BGB* of 285.75 Mg·ha^{-1} and 74.30 Mg·ha^{-1} in plot 17. Likewise, the lowest total biomass is 28.26 Mg·ha^{-1}, with *AGB* and *BGB* 22.43 Mg·ha^{-1} and 5.83 Mg·ha^{-1} in plot 8, respectively. The mean *AGB* and *BGB* were

https://doi.org/10.17221/125/2022-JFS

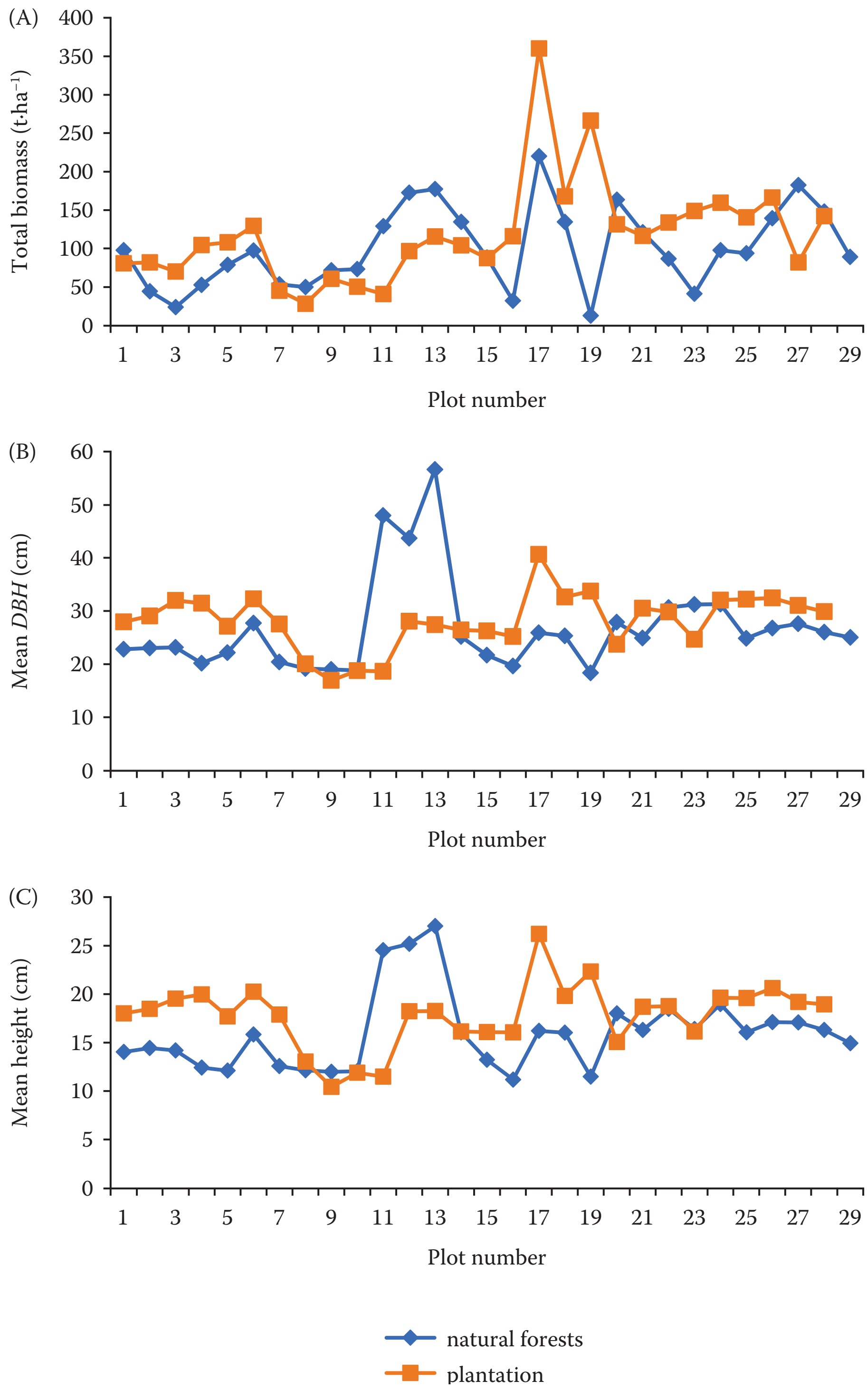

Figure 5. Comparison of mean *DBH*, mean height, and total biomass of natural forest and plantation
DBH – diameter at breast height

94.48 Mg·ha^{-1} and 24.56 Mg·ha^{-1}, respectively, whereas the mean biomass for both *AGB* and *BGB* was 119.04 Mg·ha^{-1}, as shown in Table 5. Concerning carbon stocks, the maximum total carbon stocks, *AGC* and *BGC*, were 169.22 Mg·ha^{-1}, 134.30 Mg·ha^{-1}, and 34.92 Mg·ha^{-1}, respectively, while the lowest total carbon stocks, *AGC* and *BGC*, were calculated as 13.28 Mg·ha^{-1}, 10.54 Mg·ha^{-1} and 2.74 Mg·ha^{-1}, respectively. Similarly, the highest CO_2 equivalent was 619.35 CO_2e

https://doi.org/10.17221/125/2022-JFS

Table 5. Biomass and carbon stock estimation of plot data in plantation

Plot No.	*AGB*	*AGC*	*BGB*	*BGC*	*TB*	*TC*	CO_2e
				(Mg·ha^{-1})			
1	63.93	30.05	16.62	7.81	80.55	37.86	138.57
2	65.14	30.62	16.94	7.96	82.08	38.58	141.20
3	55.46	26.06	14.42	6.78	69.88	32.84	120.19
4	82.80	38.92	21.53	10.12	104.33	49.03	179.45
5	85.82	40.34	22.31	10.49	108.14	50.82	186.00
6	102.63	48.24	26.68	12.54	129.32	60.78	222.45
7	35.82	16.83	9.31	4.38	45.13	21.21	77.63
8	22.43	10.54	5.83	2.74	28.26	13.28	48.60
9	48.04	22.58	12.49	5.87	60.53	28.45	104.13
10	39.78	18.70	10.34	4.86	50.13	23.56	86.23
11	32.38	15.22	8.42	3.96	40.80	19.18	70.20
12	76.50	35.95	19.89	9.35	96.39	45.30	165.80
13	91.56	43.03	23.81	11.19	115.37	54.22	198.45
14	82.70	38.87	21.50	10.11	104.20	48.98	179.27
15	69.33	32.58	18.02	8.47	87.35	41.05	150.24
16	92.16	43.32	23.96	11.26	116.12	54.58	199.76
17	285.75	134.30	74.30	34.92	360.05	169.22	619.35
18	133.30	62.65	34.66	16.29	167.95	78.94	288.92
19	211.23	99.28	54.92	25.81	266.15	125.09	457.83
20	104.25	49.00	27.10	12.74	131.35	61.73	225.93
21	92.30	43.38	24.00	11.28	116.29	54.66	200.06
22	106.05	49.84	27.57	12.96	133.62	62.80	229.85
23	118.23	55.57	30.74	14.45	148.96	70.01	256.24
24	126.46	59.44	32.88	15.45	159.34	74.89	274.10
25	111.62	52.46	29.02	13.64	140.64	66.10	241.93
26	131.93	62.01	34.30	16.12	166.23	78.13	285.96
27	64.94	30.52	16.88	7.94	81.82	38.46	140.76
28	112.88	53.05	29.35	13.79	142.23	66.85	244.67
Mean	94.48	44.41	24.56	11.55	119.04	55.95	204.78

AGB – aboveground biomass; *AGC* – aboveground carbon; *BGB* – belowground biomass; *BGC* – belowground carbon; *TB* – total biomass; *TC* – total carbon

in plot 17, while the lowest 48.60 CO_2e was in plot 8. As shown in Table 5, the mean *AGC* and *BGC* were 44.41 Mg·ha^{-1} and 11.55 Mg·ha^{-1}, respectively, but the mean carbon stocks (containing both *AGC* and *BGC*) were 55.95 Mg·ha^{-1}.

Sentinel-2 spectral indices for plantation. Results of regression models between *AGB* (Mg·ha^{-1}) of *Pinus roxburghii* plantation and Sentinel-2 spectral indices have been summarised in Table 4. All vegetation indices were good with field *AGB* data. However, *RVI* represents the strongest correlation (R^2 = 0.41). The *RVI* power model represented 41% of the forest inventory data model, while the other 59% of *AGB* data remained unexplained (Figure 6B). Similarly, *NDVI* also showed good performance with the correlation coefficient (R^2 = 0.41), as shown in Figure 6A. *ARVI* performed the lowest correlation with an R^2 of 0.40, which means that the *ARVI* model explained only 40% of *AGB*, and the remaining 60% of the data was not

https://doi.org/10.17221/125/2022-JFS

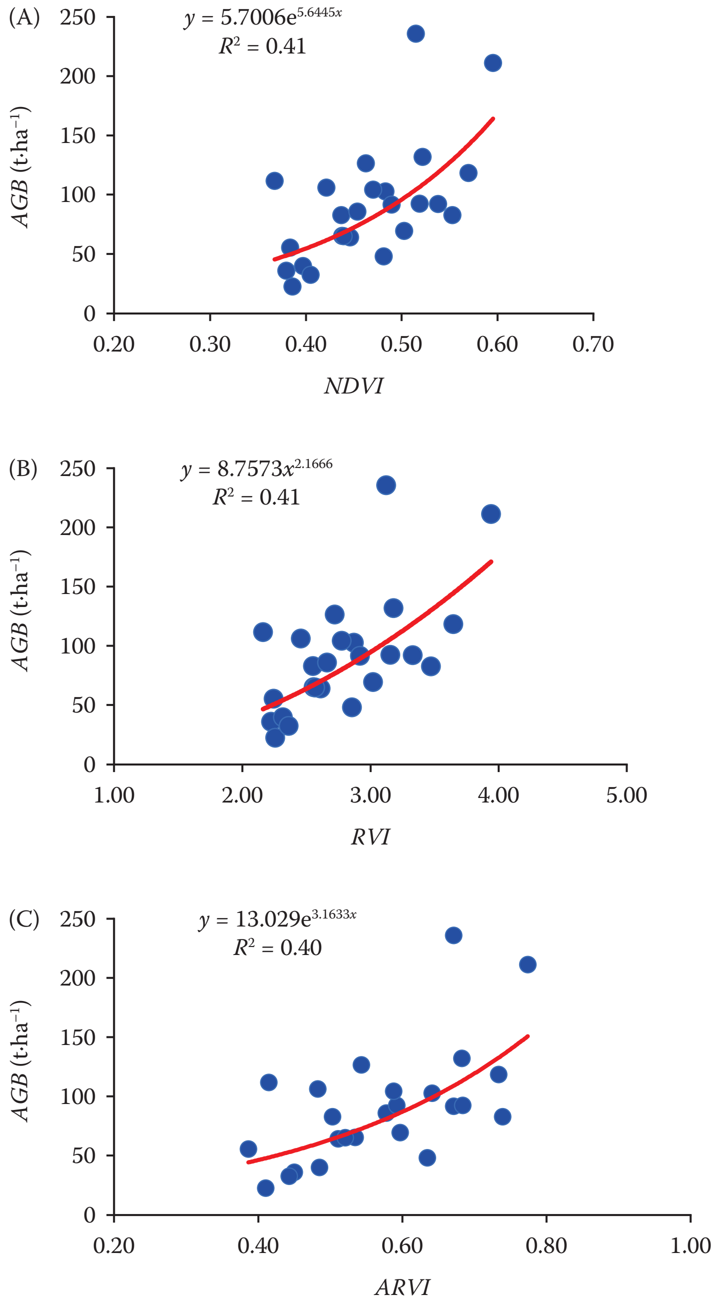

Figure 6. Scatterplots of Sentinel-2 vegetation indices and plantation *AGB*; (A) *AGB* vs *NDVI*; (B) *AGB* vs *RVI*; (C) *AGB* vs *ARVI*

AGB – aboveground biomass; *NDVI* – Normalized Difference Vegetation Index; *RVI* – Ratio Vegetation Index; *ARVI* – Atmospherically Resistant Vegetation Index

defined (Figure 6C). All indices showed that the distribution of *AGB* data was not the best fit with the linear regression model. Therefore, non-linear exponential and power were best for *NDVI*, *RVI*, and *ARVI*, respectively (Table 4). Linear regression showed less correlation and high error or cost function. Therefore, non-linear models (exponential and power) were used to minimise error and ensure best fit along the curvature of *AGB* data. Similarly, *RVI* correlation was increased using the power model, which means that *AGB* data was proportional to *RVI* values raised to a power. On the other hand, the exponential models of *NDVI* and *ARVI* have shown a high correlation compared to linear models. *RVI*-based model was used for *AGB* mapping in plantation sites of the study area (Figure 7).

https://doi.org/10.17221/125/2022-JFS

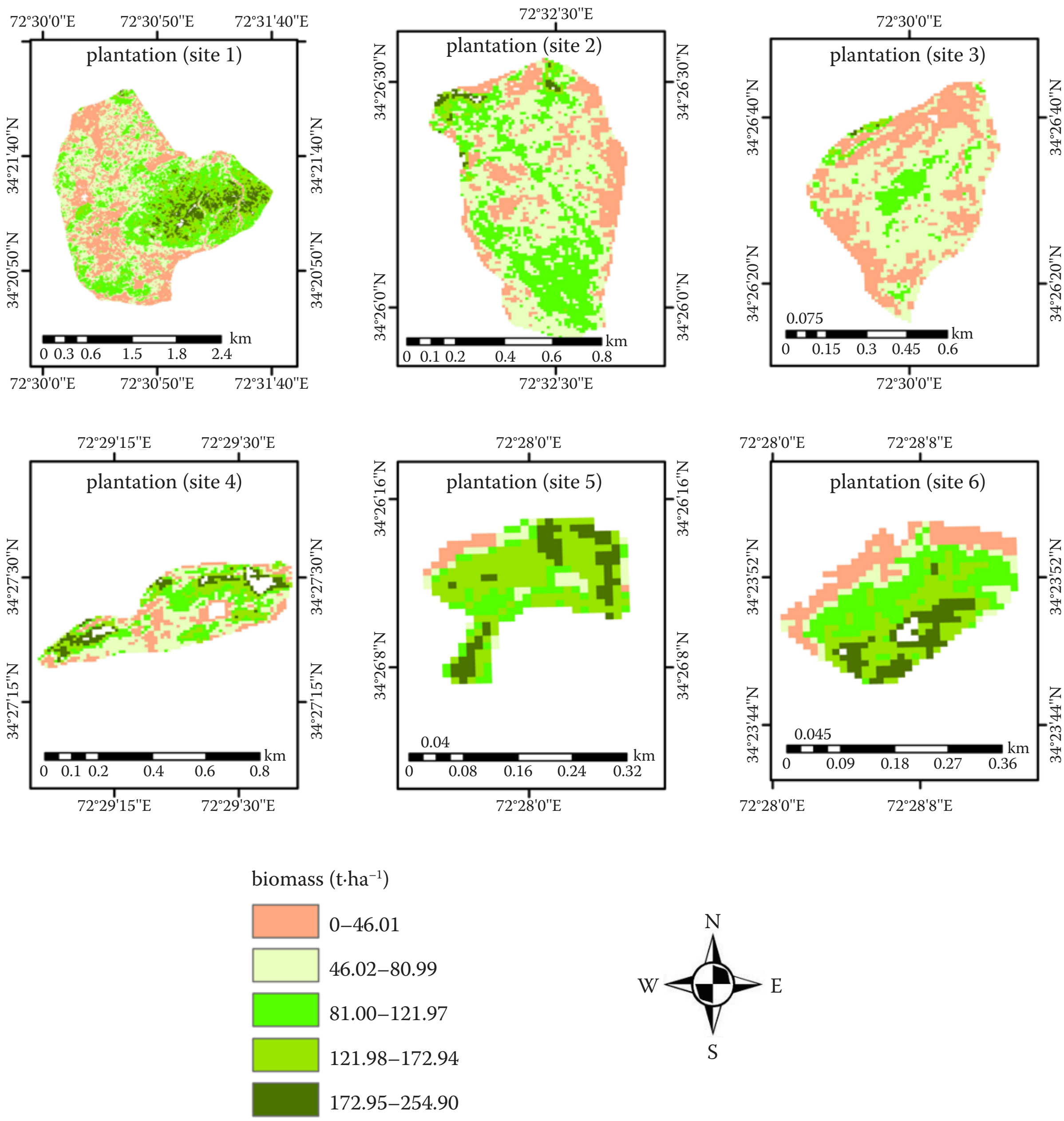

Figure 7. Biomass maps of different sites of plantation in the study area

DISCUSSION

***AGB* and carbon stock estimation.** In the present research, the average number was 302 trees·ha^{-1} in the natural forest. In comparison, in artificial plantations, the average number was 326 trees·ha^{-1}, similar to 332 trees·ha^{-1} for conifer forests of Mansehra, Pakistan (Ali et al. 2017). At the same time, Nizami et al. (2009) reported an average of 211 chir pine trees·ha^{-1} having greater than 21 cm diameter in Ghoragali. In another area, however, a smaller number of trees per hectare (149 trees·ha^{-1}) with the same stem diameter (21 cm) was found (Lehterar). Likewise, the over-matured chir pine stand has less density (147 trees·ha^{-1}) compared to the young pine stand (with 636 trees·ha^{-1}) in the Ghoragali forest managed under the shelterwood silvicultural system (Amir et al. 2018). Ali et al. (2020a) reported that the *DBH* and height of the sampled trees ranged from 12 cm to 93 cm and 9.50 m to 40.10 m, respectively. Sheikh et al. (2012) estimated that the average *DBH* was 34.80 cm and the average height was 17.24 m, with a stand density of 275 trees·ha^{-1}. Nizami et al. (2009)

https://doi.org/10.17221/125/2022-JFS

reported maximum height (31 m) and maximum *DBH* (64 cm) in a natural forest of *Pinus roxburghii*. According to Shaheen et al. (2016), tree density was 492 trees·ha^{-1}, with an average *DBH* of 87.27 cm and a tree height of 13.3 m. However, the current study tree density is lower than the reported tree density of the Indian chir pine forest (Pant, Tewari 2020), possibly due to age difference and other external disturbances because the local community depends on these forests for fuel and construction wood collection, resulting in forest degradation.

The presented study compared different tree attributes such as diameter at breast height and height of chir pine plantation and natural forest. Furthermore, the study comparatively examined the aboveground biomass of planted and natural chir pine forests. The results showed that plantations store more carbon than natural forests because the mean *DBH* and height of plantations were greater than those of natural forests. Several studies found a high link between *DBH* and biomass, height and biomass (Banday et al. 2018), and no relationship between tree density and carbon stock (Sharma et al. 2020). In the present study, the aboveground biomass is comparatively lower than that of the chir pine plantation in India, reported as 154.33 Mg·ha^{-1} (Bandy et al. 2018). Another study in the Indian chir pine forest reported that aboveground biomass ranged from 97 Mg·ha^{-1} to 145 Mg·ha^{-1} (Pant, Tewari 2020). Amir et al. (2018) estimated tree biomass and carbon stocks of young, mature, and over-matured chir pine trees, and the results showed that the highest biomass was 529 Mg·ha^{-1} for over-matured trees, followed by the 343 Mg·ha^{-1} for mature stands and 80 Mg·ha^{-1} for young trees. Similarly, carbon contents were 264 Mg·ha^{-1}, 172 Mg·ha^{-1}, and 40 Mg·ha^{-1} for over-matured, mature, and young chir pine trees, respectively. Ali et al. (2018) reported that *AGB* in the mixed forest was 149 Mg·ha^{-1} with 39 Mg·ha^{-1} of biomass in the underground parts of vegetation. The study reported total carbon contents (88 Mg·ha^{-1}), in which 70 Mg·ha^{-1} carbon contents in aboveground vegetation and 18 Mg·ha^{-1} in belowground parts in subtropical scrub forests in Haripur, Pakistan. To accurately estimate biomass, local developed allometric equation is used. However, the literature review indicated that there is no allometric equation available for chir pine of our study area. A recent review also stated that there is a lack of local developed allometric equation for major species (Khan et al. 2021a).

Chir pine species is one of the notable coniferous species in the study area and has the potential to sequester more carbon, keeping in view the protection and conservation of chirpine forests (Ali et al. 2020b). The chirpine forests are of great significance in the context of GCC as these species have a long rotation period and can fix a huge amount of carbon from the atmosphere.

Vegetation indices and *AGB* estimation. The research results were also consistent with Pandit et al. (2018), who estimated the *AGB* of forests and reported *NDVI* with correlation (R^2 = 0.70). However, this study also computed red-edge band-based *NDVI*, which showed an R^2 of 0.80 (Pandit et al. 2018). Similarly, Imran and Ahmed (2018) also estimated *AGB* in subtropical pine forests using spectral indices (*NDVI* and *ARVI*). This study reported that *NDVI* performed better with the correlation (R^2 = 0.67), whereas *ARVI* performance was not impressed with correlation (R^2 = 0.23). In another study, Imran et al. (2020) explored various broadband and narrowband indices computed from Sentinel-2 and reported *NDVI* and *ARVI* to estimate *AGB*. This study also said that *NDVI* performed better than *ARVI* and showed a correlation coefficient of 0.53 and 0.31, respectively. Many other recent studies reported a high correlation for *NDVI*, such as Shaheen et al. (2016), which showed an R^2 of 0.80, and Adan (2017), which showed an R^2 of 0.60. Like *NDVI*, *RVI* was also reported to be an efficient vegetation index for *AGB* and carbon stock estimation (Das, Singh 2012; Kumar, Shekhar 2015). Similarly, recent research also used Sentinel-2 spectral indices to estimate *AGB* in moist temperate forests and reported a lower correlation (R^2 = 0.28) for *NDVI* (Khan et al. 2020). Das and Singh (2012) assessed the relationship of vegetation indices against *AGB* and concluded that *RVI* showed the best performance with an R^2 of 0.78, followed by *NDVI* with an R^2 of 0.75. Nuthammachot et al. (2018) used Sentinel-2 indices to estimate *AGB* in private forests and reported 0.80 and 0.85 correlations for *NDVI* and simple ratio, respectively. Therefore, a simple ratio may outperform *NDVI* in predicting the biophysical properties of vegetation (Frampton et al. 2013). Furthermore, many kinds of research showed that broadband vegetation indices experienced saturation issues in high forest density, resulting in a lower correlation of *NDVI* with biomass (Imran et al. 2020; Khan et al. 2020). Similarly, Steininger (2000) and

https://doi.org/10.17221/125/2022-JFS

Kasischke et al. (2014) reported that the accuracy of predicated *AGB* is significantly affected by vegetation indices saturation in dense forests (stocking density from 80 to 100). This may be caused by the fact that the reflectance might diffuse within dense canopy cover, thus distorting the actual signal. Vafaei et al. (2018) explored Sentinel-2 images combined with PALSAR-2 to estimate biomass and indicated that integrating optical and radar images significantly improved biomass prediction. The study used *NDVI* and *RVI* to model biomass. However, Sentinel-2 performed better (high correlation) than PALSAR-2. Vegetation mapping and modelling from local or regional to large continental scales was performed with vegetation indices (Wang et al. 2004; Wessels et al. 2004; Amiri, Tabatabaie 2009). In the context of temporal changes in vegetation, such as seasonal or annual variations and comparison, NDVI provides meaningful derived information to identify vegetation health and stress conditions (Chen et al. 2006; Zoran, Stefan 2006).

CONCLUSION

This research study investigated carbon stock in two pools, *AGB* and *BGB*, in the chir pine natural forests and in chir pine plantations of Buner District. Results showed that the highest mean *DBH* and height in natural forests were 56.6 cm and 26.9 m, while the lowest mean *DBH* and mean height were recorded at 18.38 cm, with the lowest mean height of 11.19 m. Similarly, the highest total biomass was 220.18 Mg·ha^{-1} with *AGB* and *BGB* of 174.74 Mg·ha^{-1} and 45.43 Mg·ha^{-1} in plot 17, whereas the lowest total biomass was 12.74 Mg·ha^{-1} in plot 19 with *AGB* and *BGB* 10.12 Mg·ha^{-1} and 2.63 Mg·ha^{-1}, respectively. On the other hand, concerning the plantation, the highest mean *DBH* and height were 46 cm and 26.21 m, whereas the lowest mean *DBH* and mean height were recorded at 16 cm with the lowest mean height, 10.43 m. Similarly, the plantation's highest total biomass was 360.05 Mg·ha^{-1}, with *AGB* and *BGB* of 285.75 Mg·ha^{-1} and 74.30 Mg·ha^{-1}, respectively. The plantation's lowest total biomass was 28.26 Mg·ha^{-1}, with *AGB* and *BGB* at 22.43 Mg·ha^{-1} and 5.83 Mg·ha^{-1}, respectively. It would be beneficial to implement this study's results in forest management practices. Also, the development of this study would be helpful in the debate on carbon storage in managed and natural forests.

Furthermore, the present study could also be helpful in forest management to increase carbon sequestration. Exploring Sentinel-2 in Pakistan, specifically in the study area, will provide a pilot study for future research and contribute to regional carbon stocks and emission accounting. LiDAR canopy height, combined with other remote sensing techniques, has proved to be successful at demonstrating estimates of aboveground biomass (*AGB*) with high accuracy levels. Nandy et al. (2021) used a random forest algorithm to interpolate canopy height from a combination of spectral variables obtained from Sentinel-2 and ICESat-2 data, resulting in improved estimates of forest height and *AGB* in subtropical forests. Modelling accurate *AGB* in mountainous regions with diverse topography is always a challenging task. The present study utilised Sentinel-2 spectral indices to model *AGB*, but the accuracy of this approach can be further improved by incorporating LiDAR data (Narine et al. 2019; Chen et al. 2022). The fusion of pixel-sized LiDAR data and *AGB* spectral predictors can significantly reduce landscape heterogeneity and *AGB* saturation. However, acquiring ubiquitous coverage of LiDAR data for large-scale *AGB* estimation can be costly and commercially challenging (Su et al. 2020). In Pakistan, the use of LiDAR systems is currently limited to smaller areas, and thus a LiDAR-based analysis for *AGB* modelling was not considered due to its high cost and limited acquisition scope. The present study has several limitations that may affect the accuracy of *AGB* estimation. One of the limitations is the use of third-party allometric equations, which may not account for local variations within the stand. Developing locally-based standard allometric equations is crucial for accurately estimating *AGB*. Additionally, variations of biomass in dense canopies in subtropical forests may not be accurately quantified by Sentinel-2 images with a spatial resolution of 10 metres. The research concluded that forests of the study area have a great potential for conservation projects such as Reducing Emissions from Deforestation and Forest Degradation (REDD+). If the REDD+ project and forest management under REDD+ are implemented in the study area, it will positively impact the forest cover, local communities, and other stakeholders. Moreover, the study suggests that the accuracy of carbon stock estimates can be enhanced by using locally developed allometric equations and high-resolution remote sensing data.

https://doi.org/10.17221/125/2022-JFS

REFERENCES

Adan M.S. (2017): Integrating Sentinel-2 derived vegetation indices and terrestrial laser scanner to estimate above-ground biomass/carbon in Ayer Hitam tropical forest Malaysia. [MSc. Thesis.] Enschede, University of Twente.

Afzal M., Akhtar A.M. (2011): Estimation of biomass and carbon stock: Chichawatni Irrigated Plantation in Punjab, Pakistan. In: SDPI's 14th Sustainable Development Conference, Islamabad, Dec 13–15, 2011.

Ahmad N., Ullah S., Zhao N., Mumtaz F., Ali A., Ali A., Shakir M. (2023): Comparative analysis of remote sensing and geo-statistical techniques to quantify forest biomass. Forests, 14: 379.

Ali A., Ayaz M., Muhammad S. (2017): A study of stand structure of temperate forests of Kaghan valley, Mansehra, Khyber Pakhtunkhwa. The Pakistan Journal of Forestry, 67: 20171.

Ali A., Saleem U., Shaiza B., Naveed A., Asad A., Khan M.A. (2018): Quantifying forest carbon stocks by integrating satellite images and forest inventory data. Austrian Journal of Forest Science/Centralblatt für das gesamte Forstwesen, 135: 93–117.

Ali A., Ashraf M.I., Gulzar S., Akmal M. (2020a): Development of an allometric model for biomass estimation of *Pinus roxburghii*, growing in subtropical pine forests of Khyber Pakhtunkhwa, Pakistan. Sarhad Journal of Agriculture, 36: 236–244.

Ali A., Ashraf M.I., Gulzar S., Akmal M. (2020b): Estimation of forest carbon stocks in temperate and subtropical mountain systems of Pakistan: implications for REDD+ and climate change mitigation. Environmental Monitoring and Assessment, 192: 1–13.

Amir M., Liu X., Ahmad A., Saeed S., Mannan A., Muneer M.A. (2018): Patterns of biomass and carbon allocation across chronosequence of chir pine (*Pinus roxburghii*) forest in Pakistan: Inventory-based estimate. Advances in Meteorology, 2018: 1–8.

Amiri F., Tabatabaie T. (2009): Operational monitoring of vegetative cover by remote sensing in semi-arid lands of Iran. In: Proceedings of the 7th FIG Regional Conference, Spatial Data Serving People: Land Governance and the Environment-Building the Capacity, Hanoi, Oct 19–22, 2009: 1–18.

Babbar D., Areendran G., Sahana M., Sarma K., Raj K., Sivadas A. (2021): Assessment and prediction of carbon sequestration using Markov chain and InVEST model in Sariska Tiger Reserve, India. Journal of Cleaner Production, 278: 123333.

Banday M., Bhardwaj D.R., Pala N.A. (2018): Variation of stem density and vegetation carbon pool in subtropical forests of Northwestern Himalaya. Journal of Sustainable Forestry, 37: 389–402.

Bukhari B.S.S., Haider A., Laeeq M.T. (2012): LAND Cover Atlas of Pakistan. Peshawar, Pakistan Forest Institute: 140.

Castillo J.A.A., Apan A.A., Maraseni T.N.., Salmo S.G. (2017): Estimation and mapping of above-ground biomass of mangrove forests and their replacement land uses in the Philippines using Sentinel imagery. ISPRS Journal of Photo and Remote Sensing, 134: 75–85.

Chen P.Y., Fedosejevs G., Tiscareño-López M., Arnold J.G. (2006): Assessment of MODIS-EVI, MODIS-NDVI and VEGETATION-NDVI composite data using agricultural measurements: An example at corn fields in western Mexico. Environmental Monitoring and Assessment, 119: 69–82.

Chen L., Ren C., Bao G., Zhang B., Wang Z., Liu M., Liu J. (2022): Improved object-based estimation of forest above-ground biomass by integrating LiDAR data from GEDI and ICESat-2 with multi-sensor images in a heterogeneous mountainous region. Remote Sensing, 14: 2743.

Das S., Singh T.P. (2012): Correlation analysis between biomass and spectral vegetation indices of forest ecosystem. International Journal of Engineering Research & Technology, 1: 1–13.

FAO (2020): Global Forest Resources Assessment 2020 – Key Findings. Rome, FAO: 16.

Frampton W.J., Dash J., Watmough G., Milton E.J. (2013): Evaluating the capabilities of Sentinel-2 for quantitative estimation of biophysical variables in vegetation. ISPRS Journal of Photogrammetry and Remote Sensing, 82: 83–92.

Goetz S., Dubayah R. (2011): Advances in remote sensing technology and implications for measuring and monitoring forest carbon stocks and change. Carbon Management, 2: 231–244.

Houghton R.A., Byers B., Nassikas A.A. (2015). A role for tropical forests in stabilizing atmospheric CO_2. Nature Climate Change, 5: 1022–1023.

Huang L., Zhou M., Lv J., Chen K. (2020): Trends in global research in forest carbon sequestration: A bibliometric analysis. Journal of Cleaner Production, 252: 119908.

Imran A.B., Ahmed S. (2018): Potential of Landsat-8 spectral indices to estimate forest biomass. International Journal of Human Capital in Urban Management, 3: 303–314.

Imran A.B., Khan K., Ali N., Ahmad N., Ali A., Shah K. (2020): Narrow band based and broadband derived vegetation indices using Sentinel-2 Imagery to estimate vegetation biomass. Global Journal of Environmental Science and Management, 6: 97–108.

Isbaex C., Coelho A.M. (2021): The potential of Sentinel-2 satellite images for land-cover/land-use and forest biomass estimation: A review. In: Forest Biomass: From Trees to Energy. London, IntechOpen: 1–24.

https://doi.org/10.17221/125/2022-JFS

Jallat H., Khokhar M.F., Kudus K.A., Nazre M., Saqib N.U., Tahir U., Khan W.R. (2021): Monitoring carbon stock and land-use change in 5000-year-old juniper forest stand of ziarat, Balochistan, through a synergistic approach. Forests, 12: 1–15.

Kasischke E.S., Kane E.S., Genet H., Turetsky M.R., O'Donnell J.A., Hoy E., Barrett K., Baltzer J.L. (2014): A geographic perspective on factors controlling post-fire succession in boreal black spruce forests in Western North America. In: AGU Fall Meeting Abstracts, San Francisco, Dec 15–19, 2014: B31D-0038.

Kaufman Y.J., Tanre D. (1992): Atmospherically resistant vegetation index (ARVI) for EOS-MODIS. IEEE Transactions on Geoscience and Remote Sensing, 30: 261–270.

Khan K., Iqbal J., Ali A., Khan S.N. (2020): Assessment of Sentinel-2-derived vegetation indices for the estimation of aboveground biomass/carbon stock, temporal deforestation and carbon emissions estimation in the moist temperate forests of Pakistan. Applied Ecology and Environmental Research, 18: 783–815.

Khan I.A., Khan W.R., Ali A., Nazre M. (2021a): Assessment of above-ground biomass in Pakistan forest ecosystem's carbon pool: A review. Forests, 12: 586.

Khan R.W.A., Shaheen H., Awan S.N. (2021b): Biomass and soil carbon stocks in relation to the structure and composition of chir Pine dominated forests in the lesser Himalayan foothills of Kashmir. Carbon Management, 12: 429–437.

Khati U., Singh G., Ferro-Famil L. (2017): Analysis of seasonal effects on forest parameter estimation of Indian deciduous forest using TerraSAR-X PolInSAR acquisitions. Remote Sensing Environment, 199: 265–276.

Kumar D., Shekhar S. (2015): Statistical analysis of land surface temperature–vegetation indexes relationship through thermal remote sensing. Ecotoxicology and Environmental Safety, 121: 39–44.

Kumar L., Mutanga O. (2017): Remote sensing of aboveground biomass. Remote Sensing, 9: 935.

Kyere-Boateng R., Marek M.V. (2021): Analysis of the social-ecological causes of deforestation and forest degradation in Ghana: Application of the DPSIR framework. Forests, 12: 409.

Lamlom S., Savidge R. (2003): A reassessment of carbon content in wood: variation within and between 41 North American species. Biomass and Bioenergy, 25: 381–388.

Malhi Y., Baker T.R., Phillips O.L., Almeida S., Alvarez E., Arroyo L., Chave J., Czimczik C.I., Di Fiore A., Higuchi N., Killeen T.J., Laurance S.G., Laurance W.F., Lewis S.L., Montoya L.M.M., Monteaguda A., Neill D.A., Vargas P.N., Patiño S., Pitman N.A.C., Quesada C.A., Salomão R., Silva J.N.M., Lezama A.T., Martínez R.V., Terborgh J., Vinceti B., Lloyd J. (2004): The aboveground coarse wood productivity of 104 Neotropical forest plots. Global Change Biology, 10: 563–591.

Musthafa M., Singh G. (2022): Improving forest aboveground biomass retrieval using multi-sensor L-and C-Band SAR data and multi-temporal spaceborne LiDAR data. Frontiers in Forests and Global Change, 5: 14.

Musthafa M., Khati U., Singh G. (2020): Sensitivity of PolSAR decomposition to forest disturbance and regrowth dynamics in a managed forest. Advances in Space Research, 66: 1863–1875.

Narine L.L., Popescu S., Neuenschwander A., Zhou T., Srinivasan S., Harbeck K. (2019): Estimating aboveground biomass and forest canopy cover with simulated ICESat-2 data. Remote Sensing of Environment, 224: 1–11.

Nhangumbe M., Nascetti A., Ban Y. (2023): Multi-Temporal Sentinel-1 SAR and Sentinel-2 MSI Data for Flood Mapping and Damage Assessment in Mozambique. ISPRS International Journal of Geo-Information, 12: 53.

Nizami S.M. (2012): The inventory of the carbon stocks in sub tropical forests of Pakistan for reporting under Kyoto Protocol. Journal of Forestry Research, 23: 377–384.

Nizami S.M., Mirza S.N., Livesley S., Arndt S., Fox J.C., Khan I.A., Mahmood T. (2009): Estimating carbon stocks in sub-tropical pine (*Pinus roxburghii*) forests of Pakistan. Pakistan Journal of Agricultural Sciences, 46: 266–270.

Nuthammachot N., Phairuang W., Wicaksono P., Sayektiningsih T. (2018): Estimating aboveground biomass on private forest using Sentinel-2 imagery. Journal of Sensors, 2018: 1–11.

Nyamari N., Cabral P. (2021): Impact of land cover changes on carbon stock trends in Kenya for spatial implementation of REDD+ policy. Applied Geography, 133: 102479.

Pandit S., Tsuyuki S., Dube T. (2018): Estimating aboveground biomass in sub-tropical buffer zone community forests, Nepal, using Sentinel 2 data. Remote Sensing, 10: 601.

Pant H., Tewari A. (2020): Green sequestration potential of chir pine forests located in Kumaun Himalaya. Forest Products Journal, 70: 64–71.

Pearson T.R.H., Brown S.L., Birdsey R.A. (2007): Measurement Guidelines for the Sequestration of Forest Carbon. Vol. 18. Newtown Square, US Department of Agriculture, Forest Service, Northern Research Station: 42.

Qureshi A., Badola R., Hussain S.A. (2012): A review of protocols used for assessment of carbon stock in forested landscapes. Environmental Science & Policy, 16: 81–89.

Rahman S.U., Ullah Z., Ali A., Ahmad M., Sher H., Shinwari Z.K., Nazir A. (2022): Ethnoecological knowledge of wild fodder plant resources of district buner Pakistan. Pakistan Journal of Botany, 54: 645–652.

Raihan A., Begum R.A., Mohd Said M.N., Abdullah S.M.S. (2019): A review of emission reduction potential and cost

https://doi.org/10.17221/125/2022-JFS

savings through forest carbon sequestration. Asian Journal of Water, Environment and Pollution, 16: 1–7.

Ravindranath N.H., Ostwald M. (2008): Methods for estimating aboveground biomass. In: Carbon Inventory Methods. Handbook for Greenhouse Gas Inventory, Carbon Mitigation and Roundwood Production Projects. Dordrecht, Springer: 113–147.

Rouse J.W., Haas R.H., Schell J.A., Deering D.W. (1973): Monitoring vegetation systems in the Great Plains with ERTS. Available at: https://ntrs.nasa.gov/api/citations/19740022614/downloads/19740022614.pdf.

Satyal P., Paudel P., Raut J., Deo A., Dosoky N.S., Setzer W.N. (2013): Volatile constituents of *Pinus roxburghii* from Nepal. Pharmacognosy Research, 5: 43–48.

Seidel D., Fleck S., Leuschner C., Hammett T. (2011): Review of ground-based methods to measure the distribution of biomass in forest canopies. Annals of Forest Science, 68: 225–244.

Shaheen H., Khan R.W.A., Hussain K., Ullah T.S., Nasir M., Mehmood A. (2016): Carbon stocks assessment in subtropical forest types of Kashmir Himalayas. Pakistan Journal of Botany, 48: 2351–2357.

Sharma K.P., Bhatta S.P., Khatri G.B., Pajiyar A., Joshi D.K. (2020): Estimation of carbon stock in the chir pine (*Pinus roxburghii Sarg.*) plantation forest of Kathmandu Valley, Central Nepal. Journal of Forest and Environmental Science, 36: 37–46.

Sheikh M.A., Kumar S., Kumar M. (2012): Above and below ground organic carbon stocks in a sub-tropical *Pinus roxburghii* Sargent forest of the Garhwal Himalayas. Forestry Studies in China, 14: 205–209.

Shoko C., Mutanga O. (2017): Examining the strength of the newly-launched Sentinel 2 MSI sensor in detecting and discriminating subtle differences between C3 and C4 grass species. ISPRS Journal of Photogrammetry and Remote Sensing, 129: 32–40.

Siddiq Z., Hayyat M.U., Khan A.U., Mahmood R., Shahzad L., Ghaffar R., Cao K.F. (2021): Models to estimate the above and below ground carbon stocks from a subtropical scrub forest of Pakistan. Global Ecology and Conservation, 27: e01539.

Steininger M. (2000): Satellite estimation of tropical secondary forest aboveground biomass: Data from Brazil and Bolivia. International Journal of Remote Sensing, 21: 1139–1157.

Su H., Shen W., Wang J., Ali A., Li M. (2020): Machine learning and geostatistical approaches for estimating aboveground biomass in Chinese subtropical forests. Forest Ecosystems, 7: 64.

Sun X., Guicai L., Meng W., Zemeng F. (2019): Analyzing the uncertainty of estimating forest aboveground biomass using optical imagery and space-borne LiDAR. Remote Sensing, 11: 722.

Thammanu S., Han H., Marod D., Srichaichana J., Chung J. (2021): Aboveground carbon stock and REDD+ opportunities of community-managed forests in northern Thailand. PLoS ONE, 16: e0256005.

Tucker C.J. (1979): Red and photographic infrared linear combinations for monitoring vegetation. Remote Sensing of Environment, 8: 127–150.

Vafaei S., Soosani J., Adeli K., Fadaei H., Naghavi H., Pham T.D., Tien Bui D. (2018): Improving accuracy estimation of Forest Aboveground Biomass based on incorporation of ALOS-2 PALSAR-2 and Sentinel-2A imagery and machine learning: A case study of the Hyrcanian forest area (Iran). Remote Sensing, 10: 172.

Wang Y., Woodcock C.E., Buermann W., Stenberg P., Voipio P., Smolander H., Häme T., Tian Y, Hu J., Knyazikhin Y., Myneni R.B. (2004): Evaluation of the MODIS LAI algorithm at a coniferous forest site in Finland. Remote Sensing of Environment, 91: 114–127.

Wang D., Wan B., Liu J., Su Y., Guo Q., Qiu P., Wu X. (2020): Estimating aboveground biomass of the mangrove forests on northeast Hainan Island in China using an upscaling method from field plots, UAV-LiDAR data and Sentinel-2 imagery. International Journal of Applied Earth Observation and Geoinformation, 85: 101986.

Wessels K.J., De Fries R.S., Dempewolf J., Anderson L.O., Hansen A.J., Powell S.L., Moran E.F. (2004): Mapping regional land cover with MODIS data for biological conservation: Examples from the Greater Yellowstone Ecosystem, USA and Pará State, Brazil. Remote Sensing of Environment, 92: 67–83.

Zhang Y., Gu F., Liu S., Liu Y., Li C. (2013): Variations of carbon stock with forest types in subalpine region of southwestern China. Forest Ecology and Management, 300: 88–95.

Zhang T., Su J., Liu C., Chen W.H., Liu H., Liu G. (2017): Band selection in Sentinel-2 satellite for agriculture applications. In: 23rd International Conference on Automation and Computing (ICAC). Huddersfield, Oct 26, 2017: 1–6.

Zhang Y., Ai J., Sun Q., Li Z., Hou L., Song L., Thang G., Li L., Shao G. (2021): Soil organic carbon and total nitrogen stocks as affected by vegetation types and altitude across the mountainous regions in the Yunnan Province, southwestern China. Catena, 196: 104872.

Zoran M., Stefan S. (2006): Atmospheric and spectral corrections for estimating surface albedo from satellite data. Journal of Optoelectronics and Advanced Materials, 8: 247–251.

Received: August 31, 2022
Accepted: May 11, 2023
Published online: July 10, 2023

https://doi.org/10.17221/133/2022-JFS

Assessment of the Ellenberg quotient as a practical tool for vertical vegetation zonation

Petr Dujka[1,2]*, *Antonín Kusbach*[1]

[1]*Department of Forest Botany, Dendrology and Geobiocenology, Faculty of Forestry and Wood Technology, Mendel University in Brno, Brno, Czech Republic*
[2]*Forest Management Institute Brandýs nad Labem, Branch Kroměříž, Kroměříž, Czech Republic*

**Corresponding author: dujka10@seznam.cz*

Citation: Dujka P., Kusbach A. (2023): Assessment of the Ellenberg quotient as a practical tool for vertical vegetation zonation. J. For. Sci., 69: 305–316.

Abstract: The Ellenberg quotient (*EQ*) is a climate index defined as a ratio of the hottest month's temperature and the average annual precipitation sum. The quotient indirectly expresses the relationship between climate and vegetation, and its application is related to the ecological niche of *Fagus* sp. Although the quotient was curated on the grounds of field research primarily on German vegetation, the possibilities of its utilisation are not limited to the Central European region. The objective of this study is (*i*) to compare the *EQ* values calculated for the forest vegetation zones in the Czech Republic with the published data using the ecological niche of *Fagus sylvatica*; and (*ii*) to compare the new *EQ*-based vertical model with field empirical mapping. The study area is the Czech Republic, Central Europe. We used climate data from 1970–2000 and the data of the National Forest Inventory, 2nd cycle (2011–2015), representing an objective data design. Geospatial analytic methods, machine learning (boosting), and verification through statistical testing were performed. The results indicate higher *EQ* values between the two most substantial spatial frames – the Hercynicum and Carpaticum regions. By comparing empirical mapped units to their climatic potential (in the *EQ*), a match was found only within the Carpaticum region. The study presents a concretisation of the general climate index for a specific region, adds to the knowledge about the *Fagus* ecological niche in context with the Central European vegetation, and also points to the *EQ*'s potential for evaluating the concept of vertical differentiation of forest communities, as well as a possible prediction tool for the vegetation migration in context with climate change.

Keywords: European beech; *Fagus sylvatica*; forest vegetation zones; national forest inventory; zonal concept

European beech (*Fagus sylvatica*) belongs to the ecologically and commercially most important and widespread broadleaved species in Central Europe (Houston Durrant et al. 2016), being also the subject of a whole series of both local and regional studies (Stojanović et al. 2013; Garamszegi, Kern 2014; Salamon-Albert et al. 2016). Many climate indices have been employed to evaluate the climate change impact on beech, e.g. the Forest Aridity Index – FAI (Führer et al. 2011) or Ellenberg quotient (Ellenberg 2009). For the evaluation of the current state and possible prediction of the impact of climate change on vegetation, the Ellenberg quotient appears as very promising (Mellert et al. 2016; Neniu, Vlăduț 2020).

The Ellenberg quotient is defined as a ratio of the average temperature in the hottest month of a year (July) and the average annual precipitation sum (Ellenberg, Leuschner 2010). In the Czech Republic (CZ), its use is first mentioned by Ambros (1993)

© The authors. This work is licensed under a Creative Commons Attribution-NonCommercial 4.0 International (CC BY-NC 4.0).

https://doi.org/10.17221/133/2022-JFS

as a potential tool for defining the dry (xeric) variant of vegetational zonation, within which forest communities of lower altitudes with a natural absence of beech can be found (Buček, Lacina 2007). Hruban (2010) evaluated macroclimate characteristics of the forest vegetation zones (FVZs) on the grounds of the Database of Czech Forest Classification System (DCFCS; Zouhar 2012) data, where the *EQ* value range was calculated for each FVZ. This calculation was then used by Mikeska and Prausová (2013) to characterise FVZs.

The Czech Forest Classification System (ÚHÚL 2023) used for the classification of forest sites in the Czech Republic uses FVZs as a frame for the vertical differentiation of tree vegetation (Zlatník 1976). The FVZs are labelled by their dominant tree species such as oaks (*Quercus* sp.), European beech (*Fagus sylvatica*), silver fir (*Abies alba*), Norway spruce (*Picea abies*) and mountain pine (*Pinus mugo*) (Zlatník 1961, 1963). European beech has a unique status in the system not only for its absence in the hottest (1st) and coldest (9th) FVZs but mostly for its presence from the 2nd (beech-oak) up to the 8th (spruce) FVZs (Plíva 1971). The most important environmental characteristics of FVZs are summarised in Table 1 (the characteristics of Hercynicum and Carpaticum separately were not calculated so far, as the current version of the Czech Forest Ecosystem Classification assumes a uniform unit for the entire study area). Besides the presence of the dominant species, the concept and practical mapping of FVZs have been following their growth/productivity, composition and structure of a tree community since the 1970s. However, the correctness of this approach has not yet been assessed more in-depth (Kusbach et al. 2017, 2018).

The *EQ* values of forest vegetation zones published to this day appear as problematic from a practical perspective: (*i*) intervals of the *EQ* values overlap (Table 1), (*ii*) the values stem merely from macroclimate characteristics with no links to the actual vegetation, (*iii*) more complex, critical assessment of the detected values is missing. For example, in the 4th FVZ of the Czech Forest Classification System (ÚHÚL 2023), where beech is dominant and creates monocenoses, Mikeska and Prausová (2013) established the *EQ* range of 18–27. According to Ellenberg (2009), however, an unmixed beech forest is defined by the *EQ* range of 10–20.

Ellenberg and Leuschner (2010) established value ranges of forest communities in Central Europe (Table 6–7, p. 339). Although the results of their work build mostly on research made in Germany, their concept can be used in other parts of Central Europe as well (Jensen et al. 2004; Mátyás et al. 2010). On the other hand, Stojanović et al. (2013) warned against strictly applying a regional approach for evaluating the *EQ*, as in the case of Serbian beech forests. These values differed widely from those stated in the Ellenberg (2009) model. Due to obvious site-climate-vegetation peculiarities and geographically related pitfalls, we examined the *EQ*'s potential to be a conceptual tool for vertical vegetation differentiation.

The objective of this study is (*i*) to compare the *EQ* values calculated for the forest vegetation zones in CZ with the published data using the ecological niche of *Fagus sylvatica*; and (*ii*) to compare the new *EQ*-based vertical model with field empirical mapping.

MATERIAL AND METHODS

Study area. The study area includes the territory of the CZ (48°33'–51°03'N, 12°05'–18°51'E). The Natural Forest Areas (NFAs) represent a more detailed division of the territory and are being used

Table 1. Characteristics of forest vegetation zones in the Czech Republic (Mikeska, Prausová 2013)

Forest vegetation zones (Plíva 1971)	Altitude (m a.s.l.)	Mean annual temperature (°C)	Mean annual precipitation (mm)	Ellenberg quotient
1st oak zone	175–400	7.7–9.2	493–665	26–39
2nd oak-beech zone	253–465	7.3–8.5	550–724	24–32
3rd beech-oak zone	280–535	6.8–8.2	585–803	20–30
4th beech zone	395–620	6.4–7.6	618–851	18–27
5th fir-beech zone	480–790	5.4–7.0	677–1 000	15–24
6th spruce-beech zone	600–994	4.3–6.3	736–1 126	12–21
7th beech-spruce zone	810–1 139	3.4–5.3	798–1 158	11–18
8th spruce zone	900–1 275	2.7–4.5	967–1 274	10–13

https://doi.org/10.17221/133/2022-JFS

in the forestry practice since the late 1980s. In the forestry legislation, NFAs are defined as continuous territories with similar growth conditions for forest growth. The CZ is divided into 41 NFAs (Plíva, Žlábek 1986; Annex 1 of the 298/2018 Decree of the Forest Act). For analytic purposes, we aggregated the NFAs into two spatial frames, resulting from the different geographic, geomorphologic (Bína, Demek 2012; Pánek, Kapustová 2016) and climate conditions: Hercynicum and Carpaticum. The Hercynicum spatial frame represents an area potentially more influenced by oceanic climate (Beck et al. 2018) and, for this study, is represented by NFAs 1–33. The Carpaticum spatial frame presumes a significant influence of continental climate (Hradecký, Brázdil 2016) and consists of the aggregated NFAs 34–41.

Data. The first input data was vector data with the information collected from the ground investigation of the National Forest Inventory, 2nd cycle (NFI II), 2011–2015, representing an objective data design (Kučera, Adolt 2019). The total number of inventory plots in the category 'FOREST' is 6 709. Each plot contains information about the FVZ, edaphic category (ÚHÚL 2023), and tree species present on the inventory site at the time of the investigation (actual vegetation during field survey 2011–2015).

The second input data consisted of raster data with climate characteristics: the average temperature in July (T07) and average annual precipitation sum in 1970–2000 extracted for the CZ (Fick, Hijmans 2017). The size of a raster layer pixel was interpolated from the original 500 m × 500 m to 250 m × 250 m.

Analysis. For the analysis, we considered the complete dataset of 6 709 inventory plots, from which the subset of representative and verification plots (NFI_II_V, Figure 1) labelled as 'zonal sites' was selected. A zonal site is defined by the presence of up to 50% of the rock fragment content (by volume), normal hydric regime, and amount of nutrients that does not radically impact the composition of vegetation communities (Dujka, Kusbach 2022). Additionally, a zonal site is where the prevailing influence of macroclimate is expected to affect the growth/succession of the vegetation. On the other hand, the effect of mesoclimate (topoedaphic conditions) and microclimate is minimal *sensu* Major (1951), regionally verified for the CZ by Macků (2014), or Kusbach et al. (2017, 2018).

For the complete NFI dataset, we calculated the *EQ* from raster climatic data according to the following Equation (1) (Ellenberg, Leuschner 2010, p. 339):

$$EQ = \frac{T07 \times 1\,000}{PREC} \qquad (1)$$

where:
EQ – the Ellenberg quotient;
T07 – average temperature in July (°C);
PREC – average annual rainfall (mm).

This calculation resulted in an inventory plots layer NFI_II_*EQ* (Figure 1). Considering that the actual vegetation composition is far from the original outlay due to intensive forest management in the past 200 years (Chytrý et al. 2013), we characterized the composition using a scale of naturalness of a forest stand (percentual naturalness index of 0–100; Macků 2012). From the NFI_II_*EQ* layer, representative plots (NFI_II_R) were chosen based on their degree of naturalness (4–6 was desirable), i.e. zonal sites with the naturalness index above 50%. These selected sites were close-to-natural tree species composition. The presence of European beech in the forest layers, according to Zlatník's classification (Randuška et al. 1986) in the 1st to the 8th FVZs was also crucial (ÚHÚL 2023) in the analysis.

The criteria of plot selection based on the degree of naturalness were met by 32 inventory plots from the 2nd to 6th FVZ range in the Carpaticum spatial frame and by 94 inventory plots from the 2nd to 7th FVZ range in the Hercynicum spatial frame. However, we needed the same foundation in the number of inventory plots.

The *EQ* values of the representative plots were used for the calculation of confidence intervals (Figure 1). In case of a low number of values (e.g. the 2nd or 7th FVZs) when it was not possible to transform data and reach a normal distribution, we increased the number of data artificially using the boosting method (Frey 2020). Having the same starting point in the amount of modelled *EQ* values for every interval allowed us to set down the confidence intervals more precisely, as the values were normally distributed and did not include extreme cases. The *EQ* confidence interval values were calculated for each FVZ of the Hercynicum and Carpaticum spatial frames using the RStudio software (Version R.4.1.2, 2020), package 'interpretCI', with the significance value $\alpha = 0.05$. Threshold interval values equalled 2.5% and 97.5% of the confidence interval. To create

https://doi.org/10.17221/133/2022-JFS

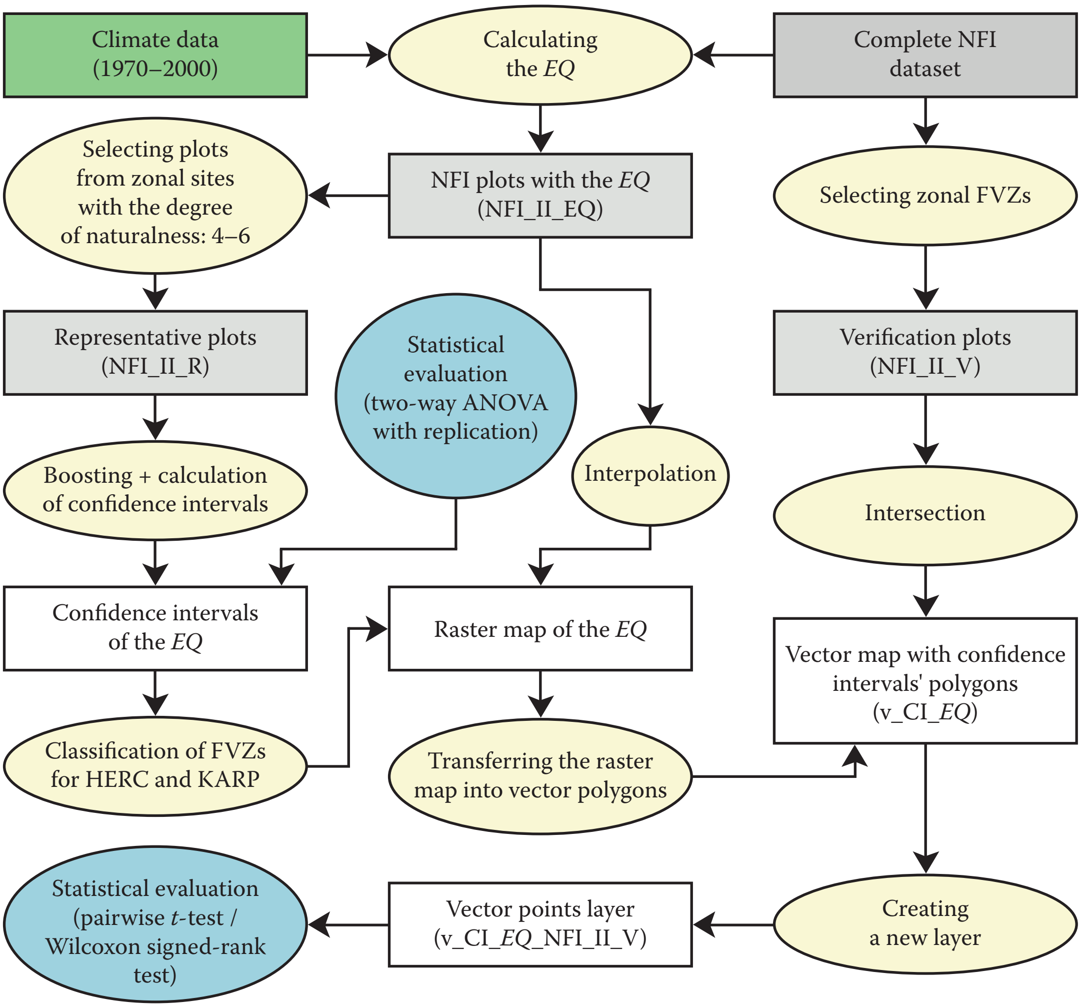

Figure 1. A scheme of the analytical process

Grey rectangles – NFI II input data; green rectangle – climate data; yellow ellipses – processes; white rectangles – outcomes of these processes; blue ellipses – statistical evaluations and methods; *EQ* – Ellenberg quotient; FVZ – forest vegetation zone

a continuous interval of the *EQ* values, which would not create duplex results in the spatial analyses, threshold values of neighbouring FVZs were linearly interpolated, and the resulting value was used for creating a polygon edge. The variability difference of the *EQ* values between the FVZs of the two spatial frames (incl. the differences inside both frames) was tested by a two-way analysis of variance (ANOVA) with replication (level of significance $P = 0.05$).

In the next step, the inventory plots of the NFI_II_*EQ* layer (in the form of vector points) were interpolated using the method of Inverse Distance Weighing into a grid with a pixel size of 100 m × 100 m and then transferred into a raster map.

The values of the raster map were then divided according to (*i*) their spatial frame (Hercynicum and Carpaticum) and (*ii*) the interpolated confidence intervals of each FVZ's *EQ*. It was not possible to include the 1st and 8th FVZs for the lack of relevant data. For better visual output, we calculated their proxy values as a sum of the corresponding *EQ* values, which were higher (in the case of the 1st FVZ) or lower (in the case of the 8th FVZ) than threshold values for the 2nd and 7th FVZ. For further geospatial analysis, the raster layer was transferred into a vector map (v_CI_*EQ*).

In the QGIS (QGIS Development Team 2023) software interface (Version 3.28.0, 2022), an intersection (using the *Intersection* command) of the v_CI_*EQ* layer with the verification layer NFI_II_V was made. A new vector layer (v_CI_*EQ*_NFI_II_V) was thus created, consisting of points with the attributes of FVZs according to *i*) confidence interval values of representative plots and *ii*) NFI field survey of the verification plots (Figure 1).

https://doi.org/10.17221/133/2022-JFS

Table 2. Forest community type and the corresponding *EQ* values (modified from Ellenberg and Leuschner, 2010, p. 339)

Forest community type	*EQ*
Oak forest (± no beech)	> 30
Beech forest with oaks	20–30
Beech forest	10–20
Beech-fir forest	~ 10
Subalpine beech forest	< 10

EQ – Ellenberg quotient

In the next step, a statistical evaluation was performed to see the match/difference rate between the confidence intervals of the *EQ* and the verification plots. The *EQ* confidence intervals of each FVZ represent the climatic potential for the succession of communities with the presence/absence of European beech according to potential natural spreading of climax tree species (Zlatník 1976). To verify the normality of the v_CI_*EQ*_NFI_II_V attribute table values, we used the Shapiro-Wilk normality test (level of significance P = 0.05). In case the normal distribution was detected, a paired t-test was performed. If normal distribution was not found, a non-parametric Wilcoxon signed-rank test (Wilcoxon 1945) was performed (level of significance P = 0.05). The calculations were done in the R Studio software using the 'tidyverse' package; the graphic output was made using the 'ggstatplot' package. To evaluate the power of the test's statistical significance, the package 'effectsize' was used. We employed a verbal scale to describe the *rank biserial* indicator (Funder and Ozer 2019). We used the 'qqwithinstats' function for displaying the results as it is capable of creating a user-friendly output based on the probability density function. This innovative approach (Patil 2021) uses box/violin plot methods of display (Hintze, Nelson 1998) which can help to easily interpret the results of the Wilcoxon signed-rank test and is more comprehensible than a long-winded text description.

The detected *EQ* interval values were compared to those stated in the literature (Ellenberg, Leuschner 2010, p. 339; or Table 2). The suitability of dividing the study area into spatial frames was then evaluated.

RESULTS

Revision of the *EQ* values. In the first step, *EQ* threshold values were calculated for those FVZs which can be compared with the so-far published values (Table 1), as the definition of an FVZ is identical in both cases.

The confidence intervals for the Hercynicum and Carpaticum FVZs are listed in Table 3 and graphically in Figure 2.

The *EQ* confidence intervals calculated for the individual FVZs in both spatial frames were more or less continuous and, after interpolating their threshold values, created mostly continuous polygons. For example, an interpolated confidence interval for the 2nd FVZ in the Carpaticum frame is shown: The newly interpolated confidence interval ranges between 31.1 and 26.4. The spatial distribution of values in the modelled FVZs (Figure 3) points out the diffusive character of the borders between neighbouring polygons (intervals). Higher *EQ* values (shades of red) represent a transition towards the 1st FVZ, which is warmer and drier. Meanwhile, lower values (shades of blue) point to a transition towards the colder and moister 3rd FVZ (Figure 3).

Two-way analysis of variance denied the null hypothesis of the *EQ* confidence intervals' match in both Hercynicum and Carpaticum, and their respective FVZs. A statistically significant difference was found between the two frames: $F(1,5)$ = 10 715; P < 0.05. The Tukey's HSD post-hoc test then revealed statistically significant differences between (*i*) confidence intervals in each spatial frame individually, and (*ii*) confidence intervals when comparing the two frames. An exception was found

Table 3. The calculated confidence intervals and mean values of the *EQ* for the Hercynicum and Carpaticum FVZs

FVZ (Plíva 1971)	Hercynicum			Carpaticum		
	2.5%	50.0%	97.5%	2.5%	50.0%	97.5%
2nd beech-oak zone	33.6	31.9	30.3	31.1	28.7	26.1
3rd oak-beech zone	29.7	28.9	28.0	26.6	25.6	24.5
4th beech zone	26.8	25.5	24.3	22.8	21.1	19.5
5th fir-beech zone	23.8	22.3	20.9	19.0	17.2	15.7
6th spruce-beech zone	18.7	16.8	15.1	13.3	12.6	12.0
7th beech-spruce zone	15.2	13.5	11.7	–	–	–

EQ – Ellenberg quotient; FVZ – forest vegetation zone

https://doi.org/10.17221/133/2022-JFS

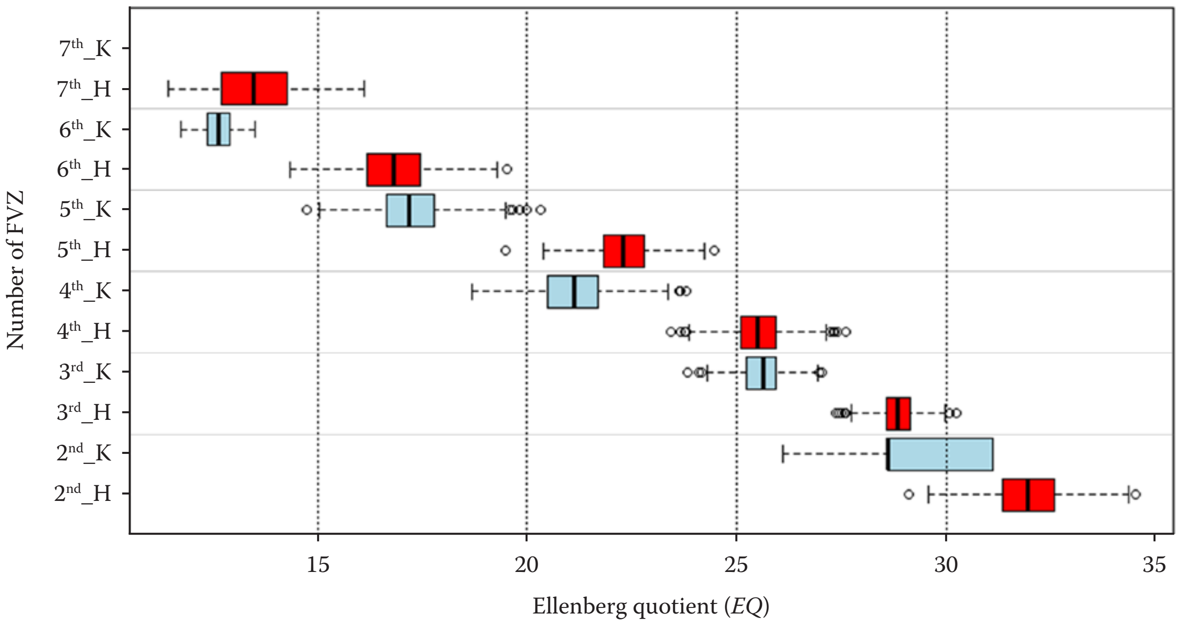

Figure 2. Diagram of the Ellenberg quotient (*EQ*) values distribution for each FVZ (2nd–7th) of Hercynicum (labelled with the letter H, boxplots in red) and Carpaticum (labelled with the letter K, boxplots in blue)

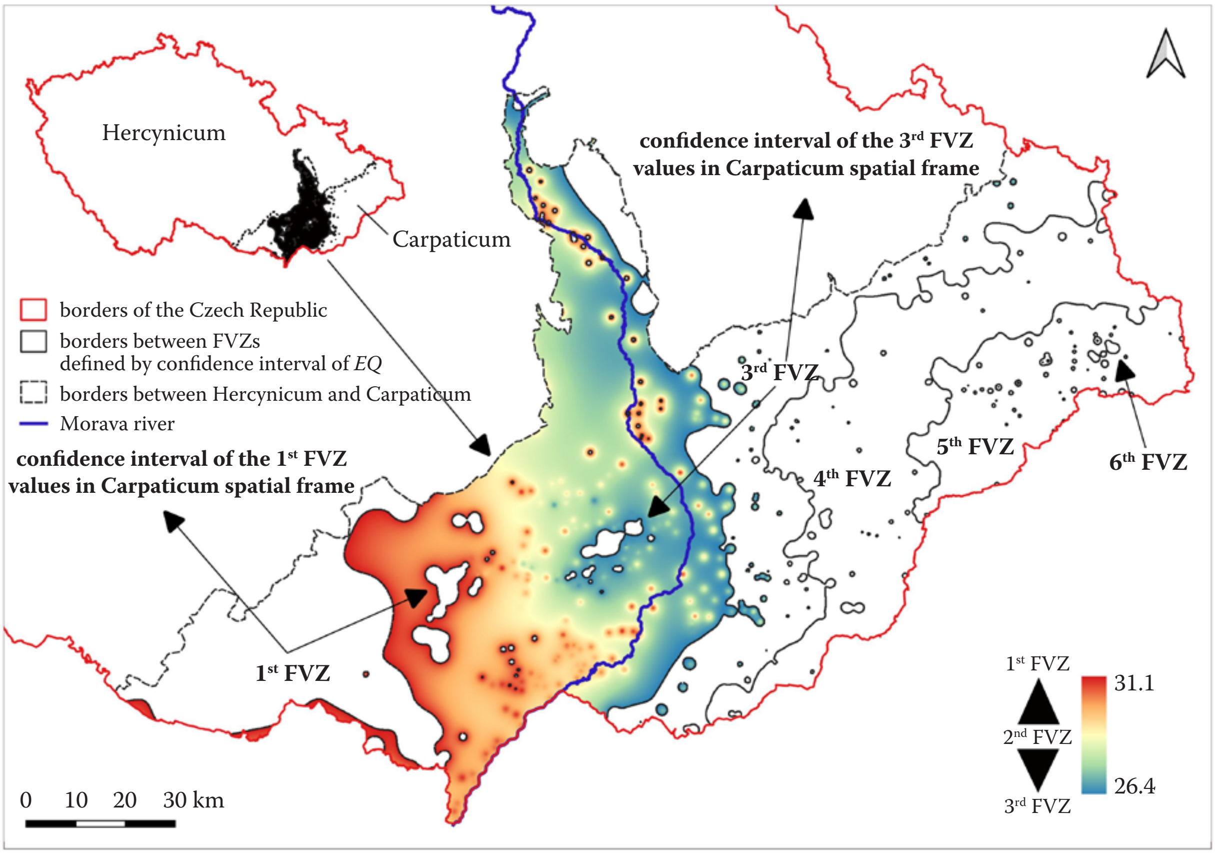

Figure 3. Schematic visualisation of *EQ* values distribution by confidence interval, calculated on the grounds of ecological *Fagus sylvatica* niche, defined by close-to-nature communities of the 2nd FVZ in the Carpaticum frame

Red shades – the highest values of the interval that can be found in the transition towards the lower (1st) FVZ; blue shades – transition to the higher (3rd) FVZ; *EQ* – Ellenberg quotient; FVZ – forest vegetation zone

https://doi.org/10.17221/133/2022-JFS

in the confidence interval of the 4th FVZ in Hercynicum and the 3rd FVZ in Carpaticum. In this one case only, the difference between the two FVZ values was found statistically insignificant (P = 0.63). The study area can be labelled, from the point of the *EQ*, as consisting of two heterogenous frames.

Evaluation of the FVZs. In Carpaticum, a statistical assessment of the FVZs was carried out based on the *EQ* confidence intervals and the NFI II field survey on 532 inventory plots that met the conditions of a zonal site (verification plots, Figure 1). In Hercynicum, the number of plots was notably higher – 3 046 in total. However, in both cases, the Shapiro-Wilk test did not prove the data file's distribution normality. Therefore, it was undesirable to use the paired t-test, and the non-parametric Wilcoxon signed-rank test was performed instead.

In the case of Carpaticum, the test did not deny the null hypothesis (Z = 11 336; P = 0.54), and the zonal FVZs of the NFI II survey do match the climate characteristics based on the calculated *EQ* confidence intervals. The rank biserial correlation = 0.04 [confidence interval $CI_{95\%}$ (–0.05; 0.14)], effect size verbally rated as 'tiny'. The positive effect points to a positive correlation between the two compared approaches (*EQ* and NFI II survey). The correlation between the FVZs modelled by using the *EQ* confidence intervals and the FVZs from the NFI II survey, although it may be 'tiny', points to the trend of either increase or decrease of density in both columns (*EQ*_K and NFI_II_K) respectively (Figure 4A). While the inventory zonal plots of the 1st–6th could have been used from the survey data, we needed to calculate the *EQ* interval even for the 7th FVZ. The graphic comparison points to a more balanced distribution trend of the *EQ*_K column, while the NFI_II_K column presents an uneven value distribution (Figure 4A). Most notably, the representation of values is higher in the 3rd FVZ and lower in the 2nd FVZ.

In the case of Hercynicum, the test did deny the null hypothesis (Z = 1 162 096; P = 0.02), and the zonal FVZs of the NFI II field survey mostly do not match the climate characteristics based on the calculated *EQ* confidence intervals. The rank biserial correlation = –0.05 [confidence in-

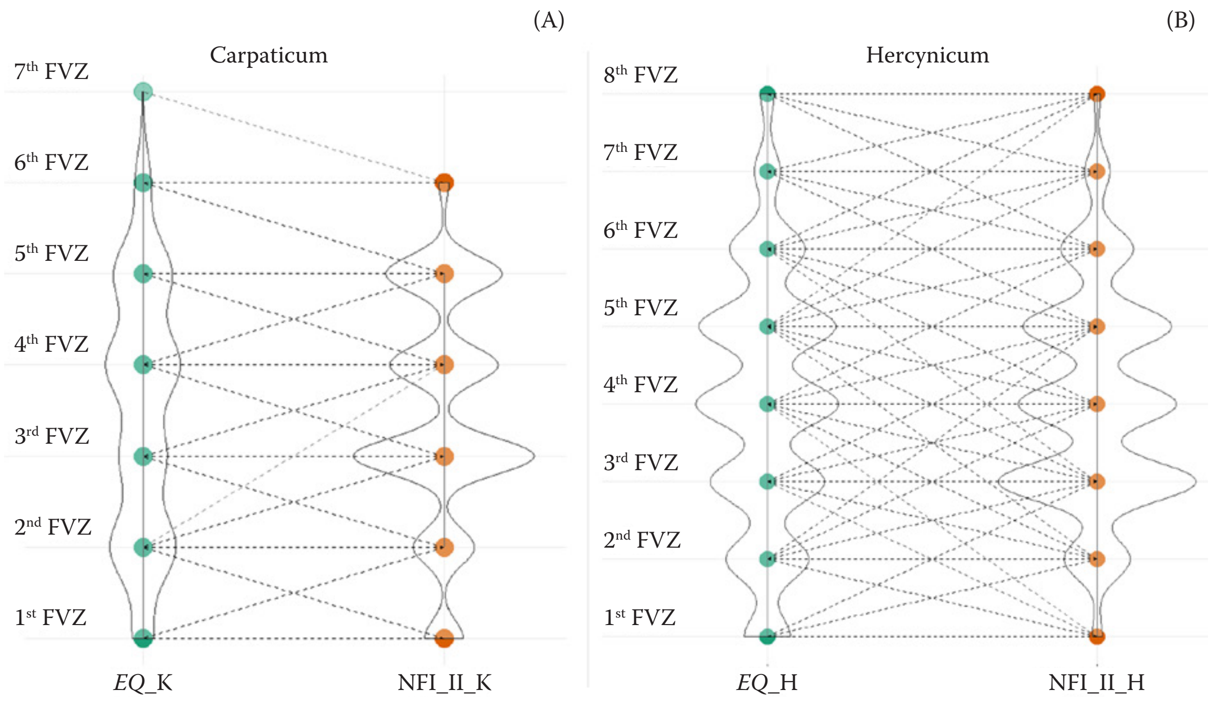

Figure 4. Diagram of the non-parametric Wilcoxon signed-rank test results for (A) Carpaticum and (B) Hercynicum

Green points – median value of the *EQ* confidence intervals of each FVZ (based on representative plots); orange points – median value of the zonal FVZs based on the NFI II field survey (verification plots); dashed black lines connect and compare the green and orange points (in an ideal case, a green point would correspond with an orange one on the same level; connection on different levels presents a misalliance); dashed grey lines depict isolated incidents; *EQ* – Ellenberg quotient; FVZ – forest vegetation zone; NFI – National Forest Inventory

https://doi.org/10.17221/133/2022-JFS

terval $CI_{95\%}$ (–0.09; –0.01)], effect size verbally rated as 'very small'. The difference between the FVZs modelled by using the *EQ* confidence intervals and the FVZs from the NFI II survey is very small, and the negative effect points to a negative correlation. The correlation between the FVZs modelled by using the *EQ* confidence intervals and the FVZs from the NFI II survey is very small, and the increase/decrease of density in both columns (*EQ*_H and NFI_II_H) respectively does not show a unified trend (a decreasein density of the *EQ* column can mean an increase in density for the NFI II column and vice versa). The comparison points to a more balanced density distribution of the (modelled) *EQ* column, while the NFI II column is unevenly distributed (Figure 4B).

DISCUSSION

Interval values of the *EQ*, defining natural forest communities with the presence/absence of beech, originate from studies performed on German and Alpine vegetation and can differ depending on geographic location and climatic data range, similarly to the widely used Ellenberg indicator value (Chytrý et al. 2018). The applicability of the *EQ*, however, exceeds the Central European region (Fang, Lechowicz 2006; Mátyás et al. 2010; Stojanović et al. 2013; Hohnwald et al. 2020). The *EQ*, in this study applied to the region of Central Europe, is purely a climate index/factor, and its assertion should have its regional limits, as is the case of the regional climate (Stojanović et al. 2013) or macroclimate (Major 1951). The modification of the *EQ* value intervals of the study area using the degree of naturalness of the sites (Macků 2012) appears as a promising approach, as the *EQ* values link with forest communities with relatively intact special composition. Those, when found on the zonal sites (Dujka, Kusbach 2022), in the long term reflect the effects of the macroclimate as the dominant environmental gradient (Kusbach et al. 2017, 2018). Boosting is a common method of ecological data analysis (De'ath 2007; Hastie et al. 2009), appropriate where the amount of data is limited. The compactness of the original dataset, combined with a carefully chosen algorithm for selecting sites that are 'typical' for each FVZ, proved to be sufficient for employing the boosting method, which is based on the principles of machine learning (Frey 2020).

For the 1st FVZ, the absence of beech is typical except for wetter locations (Průša 2001). This completely matches the Ellenberg and Leuschner's (2010) definition with a threshold value of *EQ* > 30. Ambros (1993) stated the possibility of defining the dry (xeric) plot variant with a natural absence of beech for the *EQ* > 30. Similar beech threshold values were defined by Czúcz et al. (2011) and Garamszegi and Kern (2014); in those cases, the threshold value of beech was even lower, the *EQ* = 29. Mellert et al. (2016) listed the *EQ* = 30 value as the 'maximal value of the intermediate' in which beech is consecutively present. However, the maximal value for its marginal occurrence equalled 40.4. Interestingly though, Miletić et al. (2021) listed the occurrence of beech even for the *EQ* = 38.26 in some locations in Serbia. Similarly, Stojanović et al. (2013) stated that the *EQ* values of the Serbian beech forests commonly surpass a threshold value of 30. It is, however, necessary to remind that Serbian *Fagus* forests grow upon a mostly basic substrate derived from limestone in contrast with generally acidic soils weathering from a crystalline parent material of Central Europe. High *EQ* values, which in Central Europe indicate a remarkable absence of European beech, do not necessarily indicate the same in Serbia – growth of the *Fagus* trees is controlled by different factors there, probably due to topoedaphic factors. The results of this study point to a divergence between the values stated by Ellenberg and Leuschner (2010) and Czúcz et al. (2011). Values for Hercynicum and Carpaticum hover slightly above the *EQ* > 30. The range of values published by Mikeska and Prausová (2013) seems to be significantly imprecise (*EQ* = 26–39), namely due to the lower interval boundary in the transition towards the 2nd FVZ. A lower elevation line of natural presence/absence of beech is difficult to identify in the field because of intensive human activities and the alteration of the natural special composition (Chytrý 2012).

In the 2nd FVZ, beech can be found as a minor species (Průša 2001), i.e. 10–30%. In the 3rd FVZ, beech is majorly represented, i.e. > 50%. Oak becomes a minor species, which finds its production optimum here contrary to its ecological optimum in the 1st FVZ (Vacek, Simon 2009). The division of mixed stands of beech and oak species into the two FVZ in the Czech Forest Classification System contrasts the concept of Central European

https://doi.org/10.17221/133/2022-JFS

vegetation (Ellenberg 2009). The difference in the division of both communities in the Czech system is justified by the different social status of *Fagus* and *Quercus* and the production demands of forest management. In anthropogenically influenced forests of mid-altitudinal locations, however, cannot be uncritically accepted because of (*i*) a lack of original natural communities (Culek et al. 2005), and (*ii*) past forest management influencing the composition and structure of forest stands (Maleki et al. 2020). Lower *EQ* values of both FVZs were detected in Carpaticum, where they fall into a range of 31.1–24.5 and do correspond more to the values by Ellenberg and Leuschner (2010). They also match the values for the 2nd FVZ (Mikeska, Prausová 2013). In Hercynicum, both zones' values are generally higher (33.6–28.0), here we can also find a parallel to the basic Serbian forests, e.g. in the Bohemian Karst region. Although the *EQ* values in this instance range from 29–33, the 2nd FVZ is prevalent in Hercynicum. However, due to the influence of mesoclimate, conditions for both the 1st and 3rd FVZ can emerge (Šamonil, Viewegh 2005; Šamonil et al. 2009).

The beech (4th) FVZ is characterized by Průša (2001) as an unmixed beech forest where a slight occurrence of sessile oak or silver fir is possible. While Ellenberg and Leuschner (2010) state the value range of *EQ* = 20–30 for beech communities, Mellert et al. (2016) listed values of 11.8–22.6 for optimal beech growth conditions. According to this, the beech FVZ would be above this interval's upper border (26.8–24.3) in Hercynicum. In Carpaticum, the values are lower (22.8–19.5). The *EQ* value range published by Mikeska and Prausová (2013) (18–27) is too wide, with the upper border too high. Matějka (2012) adds that around the turn of the 20th and 21st century, field survey of the 4th FVZ was either suppressed, or this zone was not recorded at all. Kubošová et al. (2011) also point out the need to revise the surface representation of the 3rd and 5th FVZs, as the mapped area of the 4th FVZ seems to be smaller than that of the 3rd and 5th FVZs. This problem is also noticeable in comparing the employed *EQ* method and the NFI II field survey in Hercynicum (Figure 4B). Inventory plots of the 4th FVZ correspond to up to four intervals of the *EQ* values, revealing the unequivocal delimitation of beech communities in relation to macroclimate.

Ellenberg and Leuschner (2011) list the occurrence of beech-fir stands in the *EQ* value range ~ 10. Průša (2001) characterizes the corresponding 5th FVZ as a community with the prevalence of either beech or silver fir with a potential addition of spruce and absence of oak. Mikeska and Prausová (2013) list the value range of *EQ* = 15–24, which would match the results of this study. However, the values differ substantially for Hercynicum, where the values' interval range is more expansive than that of Carpaticum, ranging from 19–24 from the average to the upper border of the interval. In Carpaticum, it is the opposite (15–19). The comparison of the *EQ* method and the NFI II field survey in Hercynicum seems considerably problematic, as the zonal 5th FVZ range corresponds to up to six confidence interval values, which suggests that the mapping of the 5th FVZ has been done in macroclimate conditions of the 2nd–6th FVZs. This can be due to overestimating the actual tree composition (Zlatník 1955), given the fact that the recent representation of silver fir in the actual tree composition (including zonal sites) is very low in comparison with the site's vegetation potential (Novák, Dušek 2021; Remeš 2022).

Evaluation of the Hercynicum and Carpaticum spatial frames is fully justified in case of higher altitudes, defined by forest communities of the 6th and 7th FVZs. The potential natural tree composition consists of a mixture of spruce, fir and beech, which on the transition to the 8th (spruce) FVZ recedes into the understory (Průša 2001). Ellenberg and Leuschner (2010) label the presence of beech under the *EQ* = 10 (Table 1) as a subalpine beech forest. The intervals' values, set in the autochthonic stands with the presence of beech in both Hercynicum and Carpaticum, are generally higher and do not fall under the *EQ* = 10. A disproportion can be caused by the different ecological *Fagus* niche in the Alps (Ellenberg, Leuschner 2010). Mellert et al. (2016) list *EQ* = 9.5 as the minimal value of the intermediate value range, in which beech is consecutively present. However, the value for beech marginal occurrence is 7.7. Mikeska and Prausová (2013) state the values in the range of 21–10 for both FVZs, with the 8th FVZ's *EQ* < 10. According to this study, the growth of beech on zonal sites can only be reliably defined for the 6th FVZ in Carpaticum. The occurrence of higher FVZs is only marginal in Carpaticum, and only azonal sites with other than a production/commercial purpose are carefully mapped (Holuša, Holuša st. 2011). In Hercynicum, however, the occurrence of close-to-natural

https://doi.org/10.17221/133/2022-JFS

communities with beech has been monitored even in the 7th FVZ, which is generally caused by higher mountains (e.g. Jeseníky Mts., the Giant Mts., the Bohemian Forest).

Although beech can sporadically occur in the 8th FVZ as well (Průša 2001), in a field mapping practice, the presence of beech is used as a determinator for differentiating between the 7th and 8th FVZs.

The calculated intervals of the *EQ* values do, in our opinion, better correspond to the reality than the values listed in the work published by Mikeska and Prausová (2013), based on Hruban (2010). The value misalliance probably does not stem from a different nature of the climate data (the climatic normal of 1961–1990) as much as from an uncritical interpretation of the calculated values as well as a missing method for the *EQ* calculation. It is necessary to stress that the comparisons of the calculated FVZ values with those by Ellenberg and Leuschner (2010) are tentative, based on differently defined communities of two different classification systems. Therefore, we list them for the completeness of information but make no effort to evaluate the relevance of both classifications in relation to the study area.

The Ellenberg quotient could also be used for predicting the composition of communities with *Fagus* in connection to rapidly changing climate conditions, as was done in Serbia (Stojanović et al. 2013), Denmark (Jensen et al. 2004), Hungary (Mátyás et al. 2010), or southern Germany (Mellert, Šeho 2022).

CONCLUSION

The Ellenberg quotient is one of the currently applied climate indices with the potential of assessing possibly suitable climate conditions for the occurrence of European beech in forest communities. In the CZ, beech is utilized as an indicator in a vertical zonation of forests. Although attempts were made to apply this concept in forestry-typological mapping, their previous results are only informative.

This study presents intervals of the *EQ* values for vertical vegetation frames of the Czech (forest) vegetation which were calculated using objective data of the National Forest Inventory and which represented relatively intact forest communities with *Fagus sylvatica*. For the verification process of the analysis, we selected plots from the 'zonal sites' category, for which macroclimate is a significant gradient of tree vegetation growth and occurrence. The statistical comparisons showed not only disagreements in the FVZs' values but also differences in how the *EQ* climate index behaved within Hercynicum and Carpaticum.

Comparing the calculated *EQ* intervals with the results of the NFI field survey also pointed to the inconsistency between the sites' climatic potential and the FVZs' definitions. The results show that in the case of Carpaticum, the *EQ* values better correspond to the results of the NFI field survey. For Hercynicum, however, the results highlight the need for a more profound revision. The Ellenberg quotient seems to be a significant factor able to crucially contribute to the optimisation of the vertical vegetation zonality of the Czech Republic and similar spatial-functional patterns elsewhere. Aside from the possibility of revising the concept of vertical vegetation zonation, the *EQ* can also be an appropriate indicator for verifying prediction models of potential vegetation migration affected by climate change.

Acknowledgement: This article was curated as a part of a dissertation thesis (Evaluation of Superstructural Units of the Czech Forest Ecosystem Classification based on the National Forest Inventory Data) on the grounds of legally provided data (Contract No. 20200010-ISAT) from the Forest Management Institute, Brandýs nad Labem.

REFERENCES

Ambros Z. (1993): Kombinovaná metoda na určování vegetačního stupně a ekologických řad. Lesnictví, 39: 71–474. (in Czech)

Beck H.E., Zimmermann N.E., McVicar T.R., Vergopolan N., Berg A., Wood E.F. (2018): Present and future Köppen-Geiger climate classification maps at 1-km resolution. Scientific Data, 5: 180214.

Bína J., Demek J. (2012): Z nížin do hor: Geomorfologické jednotky České republiky. Praha, Academia: 344. (in Czech)

Buček A., Lacina J. (2007): Geobiocenologie II. Brno, Mendelova zemědělská a lesnická univerzita: 251. (in Czech)

Chytrý M. (2012): Vegetation of the Czech Republic: Diversity, ecology, history and dynamics. Preslia, 84: 427–504.

Chytrý M. (2013): Vegetation of the Czech Republic. 4. Forest and Scrub Vegetation. Praha, Academia: 551. (in Czech)

Chytrý M., Tichý L., Dřevojan P., Sádlo J., Zelený D. (2018): Ellenberg-type indicator values for the Czech flora. Preslia, 90: 83–103.

https://doi.org/10.17221/133/2022-JFS

Culek M., Buček A., Grulich V., Hartl P., Hrabica A., Kocián J., Kyjovský Š., Lacina J. (2005): Biogeografické členění ČR II. díl (Biochory). Praha, Agentura ochrany přírody a krajiny ČR: 589. (in Czech)

Czúcz B., Gálhidy L., Mátyás C. (2011): Present and forecasted xeric climatic limits of beech and sessile oak distribution at low altitudes in Central Europe. Annals of Forest Science, 68: 99–108.

De'ath G. (2007): Boosted trees for ecological modeling and prediction. Ecology, 88: 243–251.

Dujka P., Kusbach A. (2022): Zonal concept in vegetation classification: Review. Zprávy lesnického výzkumu, 67: 236–245. (in Czech)

Ellenberg H. (2009): Vegetation Ecology of Central Europe. 4th Ed. Cambridge, Cambridge University Press: 756.

Ellenberg H., Leuschner C. (2010): Vegetation Mitteleuropas mit den Alpen: In ökologischer, dynamischer und historischer Sicht. 6th Ed. Stuttgart, UTB: 1357. (in German)

Fang J., Lechowicz M.J. (2006): Climatic limits for the present distribution of beech (*Fagus* L.) species in the world. Journal of Biogeography, 33: 1804–1819.

Fick S.E., Hijmans R.J. (2017): WorldClim 2: New 1-km spatial resolution climate surfaces for global land areas. International Journal of Climatology, 37: 4302–4315.

Frey U.J. (2020): Putting machine learning to use in natural resource management – Improving model performance. Ecology and Society, 25: 45.

Führer E., Horváth L., Jagodics A., Machon A., Szabados I. (2011): Application of a new aridity index in Hungarian forestry practice. Quarterly Journal of the Hungarian Meteorological Service, 115: 205–216.

Funder D.C., Ozer D.J. (2019): Evaluating effect size in psychological research: Sense and nonsense. Advances in Methods and Practices in Psychological Science, 2: 156–168.

Garamszegi B., Kern Z. (2014): Climate influence on radial growth of *Fagus sylvatica* growing near the edge of its distribution in Bükk Mts., Hungary. Dendrobiology, 72: 93–102.

Hastie T., Tibshirani R., Friedman J. (2009): Boosting and additive trees. In: Hastie T., Tibshirani R., Friedman J. (eds.): The Elements of Statistical Learning: Data Mining, Inference, and Prediction. 2nd Ed. New York, Springer: 337–387.

Hintze J.L., Nelson R.D. (1998): Violin plots: A box plot-density trace synergism. The American Statistician, 52: 181–184.

Hohnwald S., Indreica A., Walentowski H., Leuschner C. (2020): Microclimatic tipping points at the beech–oak ecotone in the western Romanian Carpathians. Forests, 11: 1–17.

Holuša O., Holuša st. J. (2011). Characteristics of the 7th (Fageti-piceeta s.lat.), 8th (Piceeta s.lat.) and 9th (Pineta mugo s.lat.) vegetation tiers of the northeastern Moravia and Silesia (Czech Republic). Acta Musei Beskidensis, 3: 1–15.

Houston Durrant T., de Rigo D., Caudullo G. (2016): *Fagus sylvatica* and other beeches in Europe: Distribution, habitat, usage and threats. In: San-Miguel-Ayanz J., de Rigo D., Caudullo G., Houston Durrant T., Mauri A. (eds.): European Atlas of Forest Tree Species. Luxembourg, Publications Office of the EU: 94–95.

Hradecký J., Brázdil R. (2016): Climate in the past and present in the Czech lands in the central European context. In: Pánek T., Hradecký J. (eds.): Landscapes and Landforms of the Czech Republic. Cham, Springer: 19–28.

Hruban R. (2010): Vyhodnocení makroklimatických charakteristik LVS. Kroměříž, Ústav pro hospodářskou úpravu lesů Brandýs nad Labem, Branch Kroměříž: 103. (in Czech)

Jensen L.U., Lawesson E.J., Balslev H., Forchhammer M.C. (2003): Predicting the distribution of *Carpinus betulus* in Denmark with Ellenberg's Climate Quotient. Nordic Journal of Botany, 23: 57–67.

Kubošová K., Komprda J., Bednářová Z., Hájek O., Sáňka M., Jarkovský J., Matoušková P., Kalábová T. (2011): Vyhodnocení dat Databáze lesnické typologie a úpravy typologického systému ÚHÚL: Závěrečná zpráva – 2. část. Brno, CETOCOEN, Masarykova univerzita: 129. (in Czech)

Kučera M., Adolt R. (2019): Národní inventarizace lesů v České republice – výsledky druhého cyklu 2011–2015. Brandýs nad Labem, Ústav pro hospodářskou úpravu lesů Brandýs nad Labem: 439. (in Czech)

Kusbach A., Friedl M., Zouhar V., Mikita T. (2017): Assessing forest classification in a landscape-level framework: An example from Central European forests. Forests, 8: 461.

Kusbach A., Šebesta J., Friedl M., Zouhar V., Mikita T. (2018): 60 years of concept of forest vegetation zonation in Czechia. In: Hrubá V., Friedl M. (eds.): Geobiocenologie a lesnická typologie a jejich aplikace v lesnictví a krajinářství. Brno, Ústav lesnické botaniky, dendrologie a geobiocenologie, Lesnická a dřevařská fakulta Mendelovy univerzity v Brně: 81–96. (in Czech)

Macků J. (2012): Methodology for establishing the degree of naturalness of forest stands. Acta Universitatis Agriculturae et Silviculturae Mendelianae Brunensis, 60: 161–166.

Macků J. (2014): Climatic characteristics of Forest Vegetation Zones of the Czech Republic. Journal of Landscape Ecology, 7: 39–48.

Major J. (1951): A functional, factorial approach to plant ecology. Ecology, 32: 392–412.

Maleki K., Zeller L., Pretzsch H. (2020): Oak often needs to be promoted in mixed beech-oak stands - the structural processes behind competition and silvicultural management in mixed stands of European beech and sessile oak. iForest – Biogeosciences and Forestry, 13: 80–88.

Matějka K. (2013): Climate gradients and modelling of the forest altitudinal zones in the Czech Republic. In: Geo-

https://doi.org/10.17221/133/2022-JFS

biocenologie a její aplikace v lesnictví a krajinářství, Brno, Dec 6–7, 2012: 103–119. Available at: https://www.infodatasys.cz/public/model_lvs_cr_2012.pdf (in Czech)

Mátyás C., Berki I., Czúcz B., Gálos B., Móricz N., Rasztovitis E. (2010): Future of beech in southeast Europe from the perspective of evolutionary ecology. Acta Silvatica et Lignaria Hungarica, 6: 91–100.

Mellert K.H., Ewald J., Hornstein D., Dorado-Liñán I., Jantsch M., Taeger S., Zang C., Menzel A., Kölling C. (2016): Climatic marginality: A new metric for the susceptibility of tree species to warming exemplified by *Fagus sylvatica* (L.) and Ellenberg's quotient. European Journal of Forest Research, 135: 137–152.

Mellert K.H., Šeho M. (2022): Suitability of *Fagus orientalis* Lipsky at marginal *Fagus sylvatica* L. forest sites in southern Germany. iForest – Biogeosciences and Forestry, 15: 417–423.

Mikeska M., Prausová R. (2013): Peat adler woods – A new category in forest typological classification. Zprávy lesnického výzkumu, 58: 294–306. (in Czech)

Miletić B., Orlović S., Lalić B., Đurđević V., Mandić M.V., Vuković A., Gutalj M., Stjepanović S., Matović B., Stojanović D.B. (2021): The potential impact of climate change on the distribution of key tree species in Serbia under RCP4.5 and RCP 8.5 scenarios. Austrian Journal of Forest Science, 138: 183–208.

Neniu A.I., Vlăduț A.Ș. (2020): The influence of climatic conditions on the forest vegetation within the Getic Subcarpatians – Oltenia sector. University of Craiova, 21: 5–18.

Novák J., Dušek D. (2021): Thinning of silver fir stands – Review. Zprávy lesnického výzkumu, 66: 176–187. (in Czech)

Pánek T., Kapustová V. (2016): Long-term geomorphological history of the Czech Republic. In: Pánek T., Hradecký J. (eds.): Landscapes and Landforms of the Czech Republic. Cham, Springer: 29–39.

Patil I. (2021): Visualizations with statistical details: The 'ggstatsplot' approach. Journal of Open Source Software, 6: 3167.

Plíva K. (1971): Typologický systém ÚHÚL. Brandýs nad Labem, Ústav pro hospodářskou úpravu lesů: 90. (in Czech)

Plíva K., Žlábek I. (1986): Přírodní lesní oblasti ČSR. Praha, Státní zemědělské nakladatelství: 313. (in Czech)

Průša E. (2001): Pěstování lesů na typologických základech. Kostelec nad Černými lesy, Lesnická práce: 593. (in Czech)

QGIS Development Team (2023): QGIS Geographic Information System. Open Source Geospatial Foundation. Available at: https://qgis.org/en/site/ (accessed Jan 6, 2023).

Randuška D., Vorel J., Plíva K. (1986): Fytocenológia a lesnická typológia. Bratislava, Príroda: 339. (in Slovak)

Remeš J. (2022): Perspektivy pěstování jedle bělokoré v době klimatické změny. In: Pěstování jedle bělokoré v podmínkách klimatické změny. Praha, Česká lesnická společnost, z. s.: 7–17. (in Czech)

Salamon-Albert É., Lőrincz P., Pauler G., Bartha D., Horváth F. (2016): Drought stress distribution responses of continental beech forests at their xeric edge in Central Europe. Forests, 7: 298.

Šamonil P., Viewegh J. (2005): Forest site classification of forest ecosystems in Bohemian Karst (Czech Republic). Journal of Forest Science, 51: 508–518.

Šamonil P., Polesná K., Unar P. (2009): Plant community variability within potential natural vegetation units: A case study from the Bohemian Karst. Journal of Forest Science, 55: 485–501.

Stojanović D.B., Kržič A., Matović B., Orlović S., Duputie A., Djurdjević V., Calić Z., Stojnić S. (2013): Prediction of the European beech (*Fagus sylvatica* L.) xeric limit using a regional climate model: An example from southeast Europe. Agricultural and Forest Meteorology, 176: 91–103.

Ústav pro hospodářskou úpravu lesů (ÚHÚL) (2023): Přehled lesních typů a souborů lesních typů v ČR. Available at: https://www.uhul.cz/wp-content/uploads/tabulka-LT_2023_web.pdf (in Czech)

Vacek S., Simon J. (2009): Zakládání a stabilizace lesních porostů na bývalých zemědělských a degradovaných půdách. Kostelec nad Černými lesy, Lesnická práce: 792. (in Czech)

Wilcoxon F. (1945): Individual comparisons by ranking methods. Biometrics Bulletin, 1: 80–83.

Zlatník A. (1955): Zdůvodnění komplexního typologického výzkumu a průzkumu lesů a přehled skupin lesních typů ČSR. In: Sborník Československé akademie zemědělských věd: řada Lesnictví. Praha, Ústav vědeckotechnických informací pro zemědělství: 219–248. (in Czech)

Zlatník A. (1961): Grossgliederung der slowakischen Wälder in waldtypologischer und pflanzensoziologischer Auffassung. Veröffentlichungen des Geobotanischen Institutes der Eidg. Tech. Hochschule, Stiftung Rübel, 36: 52–90. (in German)

Zlatník A. (1963): Die Vegetationsstufen und deren Indikation durch Pflanzenarten an Beispiel der Wälder der ČSSR. Preslia, 35: 31–51. (in German)

Zlatník A. (1976): Přehled skuptypů geobiocénů původně lesních a křovinných. Zprávy Geografického ústavu ČSAV, 13: 55–64. (in Czech)

Zouhar V. (2012): Database of Czech Forest Classification System. Biodiversity and Ecology, 4: 346.

Received: September 15, 2022
Accepted: May 25, 2023
Published online: July 20, 2023

https://doi.org/10.17221/44/2023-JFS

A pilot study of continuous cover forestry in boreal forests: Do remaining trees affect forwarder productivity?

Jussi Manner[1], Back Tomas Ersson[2]*

[1]*Skogforsk, Uppsala, Sweden*

[2]*School of Forest Management, Swedish University of Agricultural Sciences, Skinnskatteberg, Sweden*

**Corresponding author: jussi.manner@skogforsk.se*

Citation: Manner J., Ersson B.T. (2023): A pilot study of continuous cover forestry in boreal forests: Do remaining trees affect forwarder productivity? J. For. Sci., 69: 317–323.

Abstract: According to the literature, forwarding productivity depends chiefly on log concentration, the number of assortments, mean log volume, load-size, slope, and extraction distance. However, there is not much scientific knowledge available on forwarding in continuous cover forestry (CCF) in boreal forests, nor whether the presence of remaining trees actually affects forwarding productivity. Thus, the objective of our study was to isolate the effect of remaining trees (i.e. stand density) on forwarding productivity during CCF, specifically selection cutting. The results showed that productivity was explained mainly by the log concentration, while other factors had at most minor effects. Most importantly, stand density did not significantly affect forwarding productivity, *ceteris paribus*. Thus, we conclude that remaining trees do not affect forwarding productivity in boreal forests. Although the study results from this CCF operation must only be cautiously applied to even-aged forestry, our results raise a general question: do we need separate productivity models for thinning and clearcut operations in boreal forests if remaining trees (stand density) do not affect forwarding productivity? Because of the small dataset, we consider our paper to be a pilot study whose findings need to be verified by studies based on larger datasets including several operators and stands.

Keywords: cut-to-length logging; time study; forest operation; partial cutting; single-tree selection; extraction

According to modern forwarding literature, log concentration, expressed as e.g. roundwood volume m^3 per 100 m of strip-road [$m^3\cdot(100\ m)^{-1}$], is clearly the most important factor influencing forwarding productivity (Grönlund, Eliasson 2019; Hildt et al. 2020). Moreover, assortment type, the number of assortments, mean log volume, mean stem volume, number of logs per load, load-size, ground slope (if steep), and extraction distance have also been found to affect forwarding productivity (Nurminen et al. 2006; Eriksson, Lindroos 2014; Strandgard et al. 2017; Cadei et al. 2020; Hildt et al. 2020). The unit of observation in forwarding studies is typically a load (Strandgard et al. 2017; Cadei et al. 2020; Hildt et al. 2020), but it can also be a stand (Eriksson, Lindroos 2014).

Usually, forwarding productivity during thinning and clearcutting is modelled separately, both in boreal forests and beyond (Nurminen et al. 2006; Eriksson, Lindroos 2014; Proto et al. 2018). That said, unlike harvester work during typical boreal thinning operations, forwarding does not require tree-selection decisions from the operator. Thus, given that the above-mentioned factors affecting

Supported by Svea Janssons Skogsfond.

© The authors. This work is licensed under a Creative Commons Attribution-NonCommercial 4.0 International (CC BY-NC 4.0).

https://doi.org/10.17221/44/2023-JFS

forwarding productivity are kept equal, the presence of remaining trees during thinning is the main difference between thinning and clearcutting.

Objectives. Today, there is not much scientific knowledge available on whether the remaining trees affect forwarding productivity, *ceteris paribus* (other things equal). This shortcoming might be because of the difficulty in isolating the effect of remaining trees during ordinary boreal logging operations. However, isolating the effect of remaining trees on forwarding productivity might be easier during selection cutting, which indeed is the novelty and objective of our study. To address this knowledge gap, we analysed the effect of stand density (i.e. the number of remaining trees) on forwarding productivity during selection cutting in boreal forests. We hypothesized that forwarding productivity decreases with increasing stand density, *ceteris paribus*.

MATERIAL AND METHODS

Study setup. The field study was carried out in central Sweden in spring 2022 using a John Deere 1110G forwarder (load capacity: 12 t, John Deere Forestry, Finland). The forwarder was equipped with a rotating and levelling cabin, a CF7 crane (reach: 8.5 m, Waratah, Finland), and a HSP 035 Duo grapple (grapple area: 0.35 m^2, Hassela Skogsprodukter Aktiebolag, Sweden).

To accommodate the field study, three homogeneous plots were demarcated in a mature conifer-dominated stand (Figure 1). The size of each plot was 1 ha. The demarcated plots were then thinned from above prior to the forwarding operation, and the target number of remaining trees after the thinning was set either to 170 trees·ha^{-1} or 340 trees·ha^{-1}, hereafter named 'Sparse' and 'Dense', respectively. To ensure approximately equal roundwood volume between the treatments and hence approximately equal number of forwarder loads, prior to the harvesting two of the plots were randomly assigned to stand density 'Dense', whereas one plot was assigned to 'Sparse'. According to control measurements, the actualized stand densities after thinning were 182 trees·ha^{-1} (Sparse) and 321 trees·ha^{-1} (Dense), respectively.

The plots' terrain conditions were classified according to the Swedish Terrain Classification System (Berg 1992) as follows: bearing capacity: 1; ground roughness: 2; slope: 1. The soil type was mesic, sandy-loam till (moraine) with a field layer consisting mainly of *Vaccinium myrtillus*. The pre-harvest growing stock was circa 230 $m^3 \cdot ha^{-1}$. The overstory of the study stand was relatively sparse because the stand is in a transformation stage; i.e. a previously even-aged stand is gradually being converted into an uneven one. The forwarder operator had nearly 40 years of experience in forwarder work, of which one year was in selection cutting, i.e. thinning from above.

Indata, work elements and time observations. We divided the 'loading stage' into two separate work elements: 'crane work' and 'driving'. Crane work was always the first time interval, and hence the first work element, of a new forwarding cycle. Time intervals for a crane work event commenced as the crane started to move, and the time intervals ended when the crane stopped moving. In this paper 'a crane' comprises the whole boom system, including the grapple. Driving events (i.e. time intervals) between the crane work intervals were defined as driving, given that no crane work occurred simultaneously. Thus, crane work was prioritized over driving, i.e. simultaneous driving and crane work was determined as crane work (Tiernan et al. 2004; Cadei et al. 2020). We did not separate crane work and driving during the unloading stage; there, all work was collectively categorized as 'Unloading'.

All driving between the work elements unloading and the crane work during loading stage was defined as either 'driving empty' or 'driving loaded'. Driving empty and driving loaded were outright excluded from the dataset. Time consumption for these purely driving work elements can be reliably calculated as the relationship between distance driven and speed. Variations in driving speeds and distances have been thoroughly analysed and documented, e.g. in the large follow-up study of Berg et al. (2019).

After each accomplished forwarding cycle (a load), time intervals were summarized work-element-wise. Hence, the unit of observation was a forwarder load. The results are given as productive machine time (PMh). As is customary, we defined PMh as delay-free machine hours (Eriksson, Lindroos 2014), which includes only effective work time. Inactivity longer than 20 s was categorized as pauses (i.e. ineffective time) and excluded from the dataset. If inactivity shorter than 20 s occurred between separate work elements, the inactivity

https://doi.org/10.17221/44/2023-JFS

Figure 1. Forwarding in central Sweden during the field study in the 'Sparse' treatment, i.e. 182 remaining trees·ha^{-1} after the harvesting operation (thinning from above); the overstory was pine (*Pinus sylvestris*) dominated and circa 85 years old, the understory was spruce dominated (*Picea abies*)

Photo: Max Hedlund

in question was incorporated into the initial work element rather than the later one.

All wood volumes in the present study include the bark (solid on bark). Load volumes were approximated based on the forwarder's load-area, the average length of the logs (retrieved plot-wise from the harvester's hpr-file), and a solid volume conversion factor (Biometria 2020). Because total volumes measured by the harvester were available plot-wise via hpr-files, we could compare the sum of the approximated load volumes against the plot-specific total volume. The sums of approximated load volumes differed plot-wise by less than 1 m^3 from the harvester-measured volumes. This indicates that the approximated load volumes were sufficiently accurate.

Analysis of covariance (ANCOVA). When modelling time consumption (min·m^{-3}) during the loading stage, stand density (either 182 trees·ha^{-1} or 321 trees·ha^{-1}) was entered as a categorical variable in the statistical model. Forwarded log concentration, a quotient of load-size (m^3) and loading distance (m), was entered as a continuous variable in the statistical model. Loading distance is the distance driven from the load's first to last loaded pile. Hereafter, forwarded log concentration is simply termed as 'log concentration'. Moreover, we multiplied log concentration with 100 to reduce deci-

https://doi.org/10.17221/44/2023-JFS

mals and provide the variable log concentration per 100 m distance [$m^3 \cdot (100\ m)^{-1}$]. It varied from 2.07 $m^3 \cdot (100\ m)^{-1}$ to 10.26 $m^3 \cdot (100\ m)^{-1}$ during the field study. Loading distances were determined using the forwarders' trip meter readings. Mean log volume, a quotient of load-size (m^3) and the number of logs, was entered as a continuous variable in the statistical model. Mean log volume varied from 0.081 m^3 to 0.283 m^3. The logs were counted after the field study based on photos of the loads (Figure 2).

Unloading was modelled solely based on the mean log volume being a continuous variable. Moreover, the number of assortments in a load was two with two exceptions: one load comprised only a single assortment, and one load comprised three assortments. And because of the uniform conditions at the roadside landing, only minor, practically non-existent, machine repositioning was required during the unloading, irrespective of the number of assortments unloaded (Figure 2). Therefore, including the number of assortments in a load in the analysis was not meaningful.

A general linear model was used to analyse the ANCOVA models. The significance level was set to 5%. ANCOVA assumptions were checked according to Barrett (2011) and Johnson (2016). SAS software (Version 9.4, 2020) was used for all statistical analyses. Prior to the actual statistical analysis, the stand density was also temporarily included in the unloading model to control whether the loads unexpectedly differed between the stand densities. As expected, the loads did not significantly differ between the study plots (P = 0.5015).

Figure 2. The study's roadside landing provided uniform conditions between loads; the operator could easily unload up to three assortments with very minimal machine movements

Photo: Anton Jernberg

https://doi.org/10.17221/44/2023-JFS

RESULTS AND DISCUSSION

ANCOVA, linear regression and post hoc. Dividing the loading stage into crane work and driving did not work out. Large proportions of the driving occurred simultaneously with crane work; and because of the hierarchy applied, we identified this simultaneous work solely as crane work. Consequently, the statistical results were poor especially for driving; meanwhile, thanks to its higher hierarchy, the crane work's statistical results were somewhat better (Table 1).

Combining crane work and driving into a single work element solved the hierarchy-related problem and resulted in relatively good statistical results (Table 1, Loading in total). Loading time, in line with a current literature (Grönlund, Eliasson 2019; Hildt et al. 2020), decreased with increasing log concentration (Table 1; $P = 0.012$). Moreover, loading time decreased with increasing mean log volume, similarly to Hildt et al. (2020), but in our study, the decrease fell just outside of the set significance level (Table 1; $P = 0.098$). That said, the inclusion of mean log volume slightly harmonized residual behaviour (no data shown).

Stand density did not have a significant effect on the loading time consumption, *ceteris paribus* (Table 1; $P = 0.901$). For instance, when entering the study's mean log concentration [4.64 $m^3 \cdot (100\ m)^{-1}$] and mean log volume (0.162 m^3) into the linear regression model, it gives practically equal time consumption irrespective of stand density: 0.94 $min \cdot m^{-3}$ for Sparse, and 0.96 $min \cdot m^{-3}$ for Dense, respectively (Table 1).

Non-linear regression. In addition to combining crane work and driving, the ANCOVA results suggest to us that further simplifications are possible. Because the great majority of the loading time was solely explained by the log concentration (Table 1, Loading in total), we simplified the linear

Table 1. Analysis of covariance (ANCOVA). The dependent variable is effective time ($min \cdot m^{-3}$) per work element; categorical variable is stand density, either Sparse (182 $trees \cdot ha^{-1}$) or Dense (321 $trees \cdot ha^{-1}$); continuous variables are mean log volume (*MLV*, m^3) and log concentration* [*LC*, $m^3 \cdot (100\ m)^{-1}$]; *MLV* varied from 0.081 m^3 to 0.283 m^3, and *LC* from 2.07 $m^3 \cdot (100\ m)^{-1}$ to 10.26 $m^3 \cdot (100\ m)^{-1}$, respectively; these ranges can also be considered as feasible domains for the linear regression models; five loads were forwarded during the stand density Sparse and six during the Dense, respectively; the unit of observation is a load ($n = 11$)

Dependent variable ($min \cdot m^{-3}$)	ANCOVA		Linear regression analysis					Adjusted R-square
	parameter	F	parameter	estimate	standard error	t-value	P-value	
Crane work during loading stage	stand density	0.19	Dense	0.050	0.115	0.440	0.674	0.647
			Sparse	0.000	–	–	–	
	MLV	1.53	*MLV*	–1.003	0.812	–1.240	0.257	
	LC^{-1}	6.36	LC^{-1}	1.796	0.712	2.520	0.040	
			intercept	0.375	0.256	1.470	0.186	
Driving during loading stage	stand density	0.17	Dense	–0.033	0.080	–0.410	0.695	0.519
			Sparse	0.000	–	–	–	
	MLV	2.05	*MLV*	–0.815	0.569	–1.430	0.195	
	LC^{-1}	4.05	LC^{-1}	1.005	0.500	2.010	0.084	
			intercept	0.261	0.180	1.450	0.190	
Loading in total	stand density	0.02	Dense	0.017	0.135	0.130	0.901	0.774
			Sparse	0.000	–	–	–	
	MLV	3.64	*MLV*	–1.818	0.953	–1.910	0.098	
	LC^{-1}	11.23	LC^{-1}	2.801	0.836	3.350	0.012	
			intercept	0.636	0.301	2.120	0.072	
Unloading			*MLV*	–0.532	0.109	–4.90	0.001	0.697
			intercept	0.360	0.021	17.17	< 0.0001	

*roundwood volume m^3 per 100 m's distance on the strip-road, formula: 100 × load volume (m^3) / loading distance (m)

https://doi.org/10.17221/44/2023-JFS

regression into non-linear regression and modelled loading time solely based on the log concentration (Figure 3A). To summarize, the stand density might seemingly affect forwarding productivity, but in reality, the log concentration is the affecting factor.

Unloading. Time consumption decreased mildly, but statistically significantly, with increasing mean log volume (Table 1, Unloading; $P = 0.001$). Because of equal unloading conditions, the time consumption did not vary meaningfully between the loads, and the time consumption was mainly determined by the intercept.

Trees along the haul trail. Because some parts of pure driving work (i.e. driving empty and driving loaded) typically occur on the strip-road (Hansson et al. 2022), the remaining trees might also affect pure driving. That said, we knowingly excluded pure driving from our study because the major part of this work occurs on the haul trail and even at the landing. Trees standing along the haul trail or at the landing do not meet the criteria of remaining trees because they are not directly linked to the type of logging operation (e.g. thinning, clearcutting, etc.); for instance, a haul trail from a thinning stand might go through a clearcut and *vice versa*. Moreover, it is unlikely that the remaining trees would impact pure driving more than they impact loading work. Furthermore, pure driving comprises a lesser proportion of forwarding time than loading does (Figure 3B). Therefore, moderate variations in pure driving time would have a very mild impact on forwarding productivity anyways.

Recommendations for application of results and further research. Although the novelty of our study was to isolate the effect of remaining trees (i.e. stand density) on forwarding productivity during continuous cover forestry (more accurate selection cutting), the results can also be cautiously used to compare productivity during clearcut and thinning operations. Thus, the results raise a question: Do we really need separate forwarder productivity models for

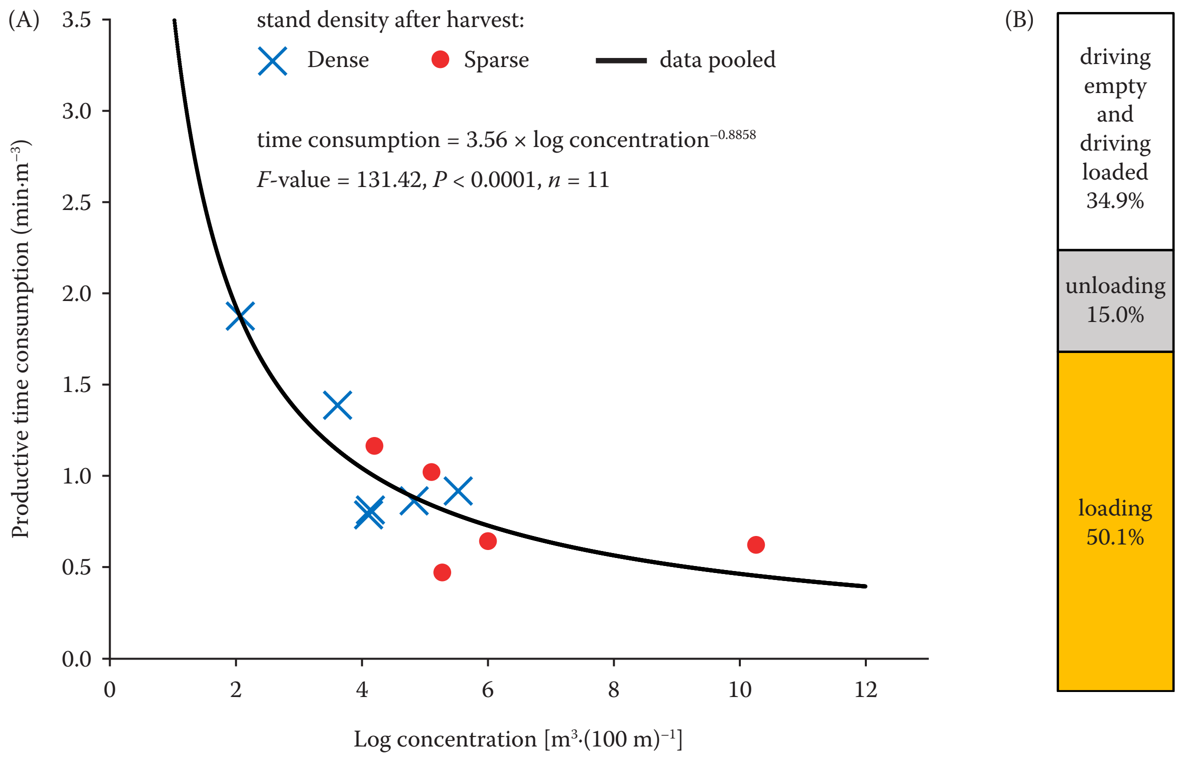

Figure 3. (A) Effective time consumption (min·m^{-3}) for loading (incl. crane work and driving) as a function of log concentration [m^3·(100 m)$^{-1}$] during the study; in the nonlinear regression analysis, we used data pooled across stand density after harvest (Dense: 321 trees·ha^{-1}, and Sparse: 182 trees·ha^{-1}); (B) the distribution of forwarding time consumption during the study; loading time is according to the non-linear regression of Figure 3A at the present study's mean log concentration of 4.64 m^3·(100 m)$^{-1}$; unloading time is according to Table 1 at the present study's mean log volume of 0.162 m^3; driving empty and driving loaded times are calculated based on the medians of the follow-up dataset of Berg et al. (2019): driving empty time = 240 m × (54.8 m·min^{-1})$^{-1}$, and driving loaded time = 189 m × (45.7 m·min^{-1})$^{-1}$; driving empty and driving loaded times are divided by the present study's mean load-size (13.4 m^3) to give a time consumption per m^3

https://doi.org/10.17221/44/2023-JFS

thinning and clearcut operations if remaining trees (stand density) do not affect forwarding productivity?

That said, even the highest stand density in our study was relatively sparse, and consequently the difference between Sparse and Dense was not as drastic as the difference between Nordic thinning and clearcut operations. In fact, the number of remaining trees varies radically when forwarding during even-aged forestry; from dense (first thinning) to practically no trees at all (clearcut). Therefore, our study results from this selection cutting operation must only be cautiously applied to even-aged forestry.

Although there are some international field studies with manually collected datasets that are large and representative (e.g. Hildt et al. 2020), Nordic field studies are typically based on a very small number of loads or only one operator (Nurminen et al. 2006; Manner et al. 2013; Grönlund, Eliasson 2019). Our study is not an exception: our small dataset and the fact that the study included only one operator decrease the representativeness of our study. That said, our field study was well-controlled and produced logical results in line with current literature. Nevertheless, our findings need to be verified by studies based on larger datasets that include several operators and stands. Therefore, we consider our study to be a novel pilot study that raises relevant questions for further investigation.

CONCLUSION

The ANCOVA did not support our hypothesis, which was that forwarding productivity decreases with increasing stand density. Instead, forwarding productivity did not decrease with increasing stand density, i.e. the number of remaining trees did not affect forwarding productivity during selection cutting, *ceteris paribus*. That said, our study was a pilot study, and more research is needed on this topic before definitive conclusions can be made.

Acknowledgement: We graciously thank Max Hedlund and Anton Jernberg for the data gathering.

REFERENCES

Barrett T.J. (2011): Computations using analysis of covariance. Wiley Interdisciplinary Reviews: Computational Statistics, 3: 260–268.

Berg S. (1992): Terrain Classification System for Forestry Work. Stockholm, Forest Operations Institute: 28.

Berg S., Ersson B.T., Manner J. (2019): Distance driven and driving speed when forwarding during final felling in Central Sweden. Journal of Forest Science, 65: 183–194.

Biometria (2020): Measurement of roundwood stacks. Swedish regulations for timber measurement. Version 2020-10-01. Available at: https://www.biometria.se/media/a5xchk3j/measurement-of-roundwood-stacks-2020-10-01.pdf

Cadei A., Mologni O., Röser D., Cavalli R., Grigolato S. (2020): Forwarder productivity in salvage logging operations in difficult terrain. Forests, 11: 341.

Eriksson M., Lindroos O. (2014): Productivity of harvesters and forwarders in CTL operations in northern Sweden based on large follow-up datasets. International Journal of Forest Engineering, 25: 179–200.

Grönlund Ö., Eliasson L. (2019): Birch shelterwood removal – Harvester and forwarder time consumption, damage to understory spruce and net revenues. International Journal of Forest Engineering, 30: 26–34.

Hansson L.J., Forsmark V., Flisberg P., Rönnqvist M., Mörk A., Jönsson P. (2022): A decision support tool for forwarding operations with sequence-dependent loading. Canadian Journal of Forest Research, 52: 1513–1526.

Hildt E., Leszczuk A., Mac Donagh P., Schlichter T. (2020): Time consumption analysis of forwarder activities in thinning. Croatian Journal of Forest Engineering, 41: 13–24.

Johnson T.R. (2016): Violation of the homogeneity of regression slopes assumption in ANCOVA for two-group pre-post designs: Tutorial on a modified Johnson-Neyman procedure. The Quantitative Methods for Psychology, 12: 253–263.

Manner J., Nordfjell T., Lindroos O. (2013): Effects of the number of assortments and log concentration on time consumption for forwarding. Silva Fennica, 47: 1030.

Nurminen T., Korpunen H., Uusitalo J. (2006): Time consumption analysis of the mechanized cut-to-length harvesting system. Silva Fennica, 40: 335–363.

Proto A.R., Macrì G., Visser R., Harrill H., Russo D., Zimbalatti G. (2018): Factors affecting forwarder productivity. European Journal of Forest Research, 137: 143–151.

Strandgard M., Mitchell R., Acuna M. (2017): Time consumption and productivity of a forwarder operating on a slope in a cut-to-length harvest system in a *Pinus radiata* D. Don pine plantation. Journal of Forest Science, 63: 324–330.

Tiernan D., Zeleke G., Owende P.M.O., Kanali C.L., Lyons J., Ward S.M. (2004): Effect of working conditions on forwarder productivity in cut-to-length timber harvesting on sensitive forest sites in Ireland. Biosystems Engineering, 87: 167–177.

Received: April 20, 2023
Accepted: May 30, 2023

CZECH ACADEMY OF AGRICULTURAL SCIENCES

CAAS Agricultural Journals subscription 2023

Unique collection of 11 peer-reviewed agricultural scientific journals published by the Czech Academy of Agricultural Sciences

Journal	Number of issues per year	Annual subscription (EUR)
Agricultural Economics (Zemědělská ekonomika)	12	620
Czech Journal of Animal Science	12	620
Journal of Forest Science	12	510
Plant, Soil and Environment	12	620
Veterinární medicína (Veterinary Medicine – Czech)	12	620
Czech Journal of Food Sciences	6	540
Czech Journal of Genetics and Plant Breeding	4	150
Horticultural Science	4	170
Plant Protection Science	4	150
Research in Agricultural Engineering	4	130
Soil and Water Research	4	170

Prices are without VAT

Please direct any subscription enquiries to: redakce@cazv.cz
https://agriculturejournals.cz

Czech Academy of Agricultural Sciences
Agricultural Journals
Slezská 7, 120 00 Prague 2
Czech Republic

CAAS CZECH ACADEMY OF AGRICULTURAL SCIENCES

AGRICULTURAL JOURNALS

published by the Czech Academy of Agricultural Sciences

Unique collection of 11 peer reviewed international agricultural journals

- indexed in: Web of Science (10), Scopus (11), CrossRef, Google Scholar, DOAJ, ...
- international Editorial Boards
- published in English
- double-blind peer-review
- open access

Agricultural Economics
IF (2021): 2.567
agricultural economics, management, informatics, ecology, social economy and sociology

Czech Journal of Animal Science
IF (2021): 1.349
genetics and breeding, physiology, reproduction, nutrition and feeds, technology, ethology and economics of cattle, pig, sheep, poultry and fish

Czech Journal of Food Sciences
IF (2021): 1.300
chemistry, biochemistry, microbiology, analyse, technology, engineering, and nutrition

Czech Journal of Genetics and Plant Breeding
IF (2021): 1.304
theoretical and applied plant genetics, plant biotechnology and plant breeding

Horticultural Science
IF (2021): 1.192
fruit growing, vegetable growing, viticulture, floriculture, medicinal plants, ornamentals, mashrooms growing

Journal of Forest Science
forestry related to European forest ecosystems and their functions including those in the landscape and wood production

Plant Protection Science
IF (2021): 1.414
diseases and pests of plants, weeds and plant protection

Plant, Soil and Environment
IF (2021): 2.328
experimental biology, agronomy, natural resources, and the environment, plant development, growth and productivity, breeding and seed production

Soil and Water Research
IF (2021): 2.685
soil and water and their interactions in natural and man-modified landscapes

Research in Agricultural Engineering
agricultural engineering and technology, processing of agricultural products

Veterinární Medicína
IF (2021): 0.746
all fields of veterinary and biomedical sciences

www.agriculturejournals.cz

JOURNAL OF FOREST SCIENCE
VOLUME 69
2023

Journal of Forest Science
Published by the Czech Academy of Agricultural Sciences

Editorial Office: Slezská 7, 120 00 Prague 2, Czech Republic
E-mail: jfs@cazv.cz **Distribution:** redakce@cazv.cz

© 2023 Czech Academy of Agricultural Sciences